

# The origin of potency and mutant-selective inhibition by bivalent ATP-allosteric EGFR inhibitors

Florian Wittlinger<sup>[a]</sup>, Surbhi P. Chitnis<sup>[b]</sup>, Calvin D. Pham<sup>[b]</sup>, Tahereh Damghani<sup>[b]</sup>, Ilse K. Schaeffner<sup>[c,d]</sup>, Matthew Q. Deng<sup>[b]</sup>, Blessing C. Ogboo<sup>[b]</sup>, Alexander Rasch<sup>[a]</sup>, Tyler S. Beyett<sup>[c,d,e]</sup>, Brian Buckley<sup>[f]</sup>, Frederic Feru<sup>[c,d]</sup>, Tatiana Shaurova<sup>[g]</sup>, Cornelius Knappe<sup>[h]</sup>, Michael J. Eck<sup>[c,d]</sup>, Pamela A. Hershberger<sup>[g]</sup>, David A. Scott<sup>[c,d]</sup>, Stefan A. Laufer<sup>[a,i,j]</sup>\*, David E. Heppner<sup>[b,g,k]</sup>\*

[a] Department of Pharmaceutical and Medicinal Chemistry, Institute of Pharmaceutical Sciences, Eberhard Karls Universität Tübingen, Auf der Morgenstelle 8, 72076 Tübingen, Germany

[b] Department of Chemistry, University at Buffalo, The State University of New York, Buffalo, NY, 14260, USA

[c] Department of Cancer Biology, Dana-Farber Cancer Institute, Boston, MA, 02215 USA

[d] Department of Biological Chemistry and Molecular Pharmacology, Harvard Medical School, Boston, MA, 02115 USA

[e] Present Address: Department of Pharmacology and Chemical Biology, Emory University School of Medicine, 5119 Rollins Research Center, 1510 Clifton Rd, Atlanta, GA 30322, USA

[f] Department of Cell Stress Biology, Roswell Park Comprehensive Cancer Center, Buffalo, NY, 14203, USA

[g] Department of Pharmacology and Therapeutics, Roswell Park Comprehensive Cancer Center, Buffalo, NY, 14203, USA

[h] Institute of Pharmaceutical Sciences, Pharmaceutical (Bio-)Analysis, University of Tübingen, Auf der Morgenstelle 8, 72076 Tübingen, Germany

[i] Cluster of Excellence iFIT (EXC 2180) “Image-Guided and Functionally Instructed Tumor Therapies” Eberhard Karls Universität Tübingen, 72076 Tübingen, Germany.

[j] Tübingen Center for Academic Drug Discovery & Development (TüCAD2), 72076 Tübingen, Germany

[k] Department of Structural Biology, University at Buffalo, The State University of New York, Buffalo, NY, 14260, USA

\*Corresponding authors

To whom correspondence may be addressed:

David E. Heppner      [davidhep@buffalo.edu](mailto:davidhep@buffalo.edu)

Stefan A. Laufer      [stefan.laufer@uni-tuebingen.de](mailto:stefan.laufer@uni-tuebingen.de)

Supporting information of this article is given via a link at the end of the document.

## Abstract

Targeted small-molecule therapies in mutant epidermal growth factor receptor (EGFR) non-small cell lung cancer (NSCLC) have undergone several generations of development in response to acquired drug resistance. With the emergence of the highly prevalent T790M and C797S drug-resistant mutations, a diverse arsenal of ATP-competitive molecules has led to the front-line drug AZD9291 (osimertinib) and several in clinical development. Several allosteric inhibitors bind a site adjacent to the ATP-binding site and exhibit synergy when dosed in combination with certain ATP-competitive inhibitors. Structure-guided design of molecules that anchor to both sites simultaneously, namely ATP-allosteric bivalent inhibitors, have been reported as proof-of-concept EGFR mutant-selective compounds, however their properties are underexplored and currently exhibit modest activity in human cancer cell lines. To better understand the structural and functional properties of such molecules, we have carried out structure-activity relationships (SAR) defining the groups of the allosteric pocket that are responsible for enabling mutant selectivity and potency of this series. We find that the back pocket phenol ring enables stronger binding while the methylisoindolinone is responsible for enabling selectivity for the oncogenic mutations. An optimized allosteric site-binding group and a C797-targeting ATP-site scaffold exhibit inhibitory effects in a variety of EGFR mutant cell lines, which is improved over earlier examples. Additionally, a closely related reversible-binding analogue exhibits mutant-selective activity and ~1 nM biochemical potency against L858R/T790M/C797S and promising antiproliferative effects in human cancer cells indicating that ATP-allosteric bivalent kinase inhibitors may serve as tool compounds in understanding overcoming these important resistance mechanisms. These results highlight the utility of bivalent ATP-allosteric compounds in understanding the impact certain functional groups have in the potency and mutant-selectivity enabled by allosteric pocket binding. The results of this study incentivize further investigations of compounds that bind within an exit

vector made accessible in the inactive  $\alpha$ C-helix “out” conformation as a novel approach for kinase inhibitors.

### **Keywords**

Kinase inhibitors, non-small cell lung cancer, allosteric inhibitors, mutant selectivity, structure-based design, drug discovery, epidermal growth factor receptor.

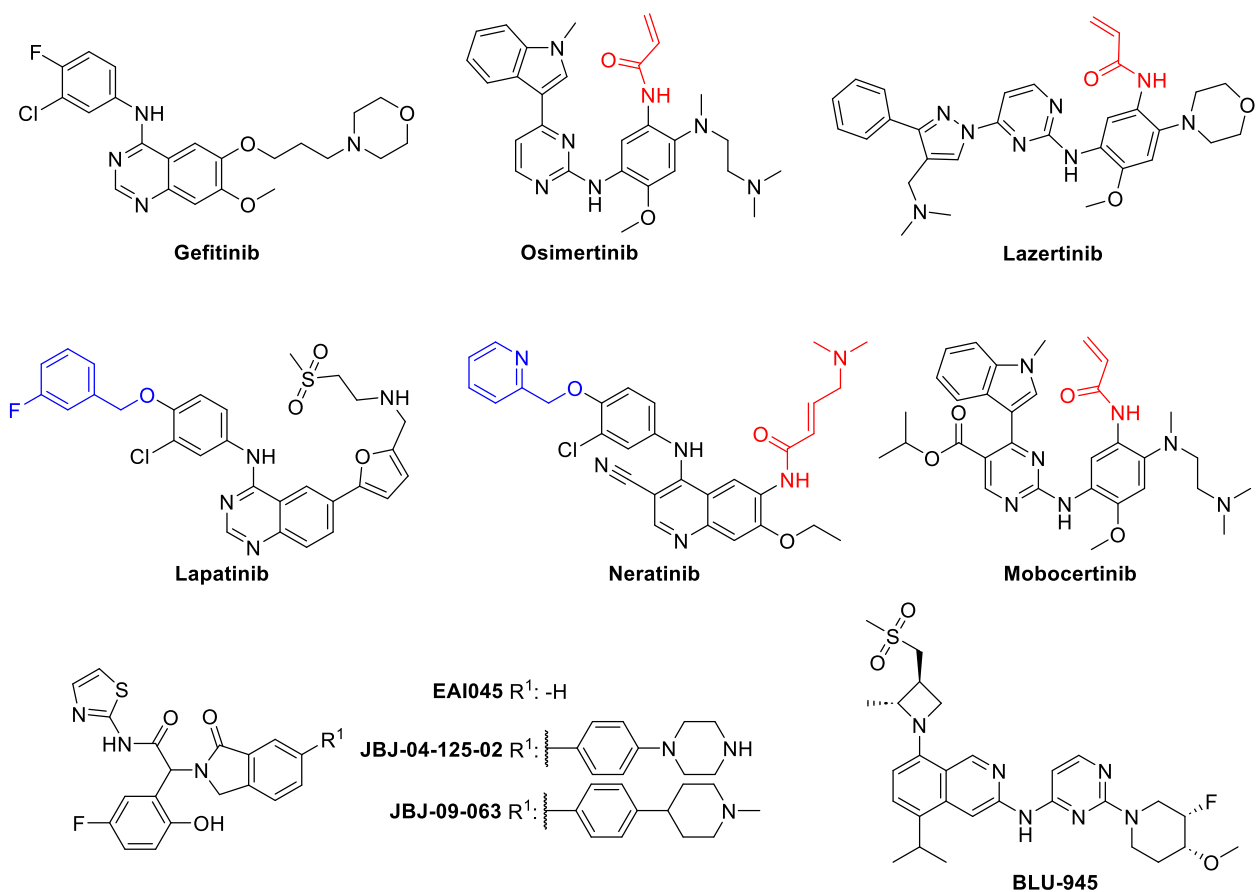
## Introduction

Non-small-cell lung cancer (NSCLC) is commonly driven by activating mutations in the kinase domain of the epidermal growth factor receptor (EGFR) and most prominently the single-point mutation L858R (LR) and the in-frame exon-19-deletion (ex19del).<sup>1,2</sup> Small-molecule therapies are rendered successful by these compounds exhibiting selective inhibition of the mutant EGFR kinase and limited activity on wildtype thereby establishing a viable therapeutic window. Initial generations of quinazoline-based first (e.g., **gefitinib**, **lapatinib** (pan-ErbB-inhibitor)) and second generation (e.g., **neratinib** (pan-ErbB-inhibitor)) small-molecule EGFR tyrosine kinase inhibitors (TKIs) (Figure 1) are eventually rendered ineffective through well appreciated drug resistance mechanisms,<sup>3,4</sup> e.g., by acquisition of a secondary T790M gatekeeper mutation (TM) that is found in approximately 50% of patients.<sup>5-7</sup> While most of these TKIs bind merely to the ATP-site, type 1.5 inhibitors **lapatinib** and irreversible binding **neratinib** partially bind within an allosteric pocket with a fluorophenyl or pyridine moiety, respectively, made accessible due to the outward rotation of the  $\alpha$ C-helix in the inactive conformation.<sup>8,9</sup> The advanced third-generation EGFR TKIs are based on a mutant-selective anilinopyrimidine scaffold that is selective for the TM-containing kinase and is equipped with a Michael acceptor functionality poised to covalently react with residue C797 for maximal efficacy (e.g., **osimertinib**, **lazertinib** (Figure 1)).<sup>10-13</sup> However, despite their initial efficacy, patients eventually develop resistance, in some cases due to a tertiary C797S mutation (CS) that annuls the utility of these covalent warheads, due to the decreased nucleophilicity of the serine residue.<sup>12,14,15</sup>

Development efforts for alternative EGFR inhibitors capable of treating tumors harboring resistant mutations resulted in the discovery of ATP non-competitive phenylglycine-based inhibitors, e.g., **EAI045** and subsequently optimized inhibitors **JBj-04-125-02** and **JBj-09-063**

(Figure 1).<sup>16–18</sup> These compounds all bind to the allosteric pocket adjacent to the ATP-binding site in the kinase “ $\alpha$ C-helix out” inactive conformation with mutant-selective targeting of TM and CS-containing kinase domains, and show encouraging efficacy in *in vitro* assays and *in vivo* xenograft models.<sup>16–18</sup> Importantly, first examples allosteric inhibitors (i.e., **EAI045**) are rendered less effective in biological settings due to dimerization-dependent effects that can be blocked if co-administered with the dimerization blocking antibody cetuximab.<sup>16–18</sup> Recently, combinations of third generation TKIs and allosteric inhibitors have shown synergistic tumor regression and cocrystal structures of EGFR with inhibitors bound simultaneously to both sites suggested a cooperative binding mode with supportive efficacy outcomes.<sup>17,19,20</sup>

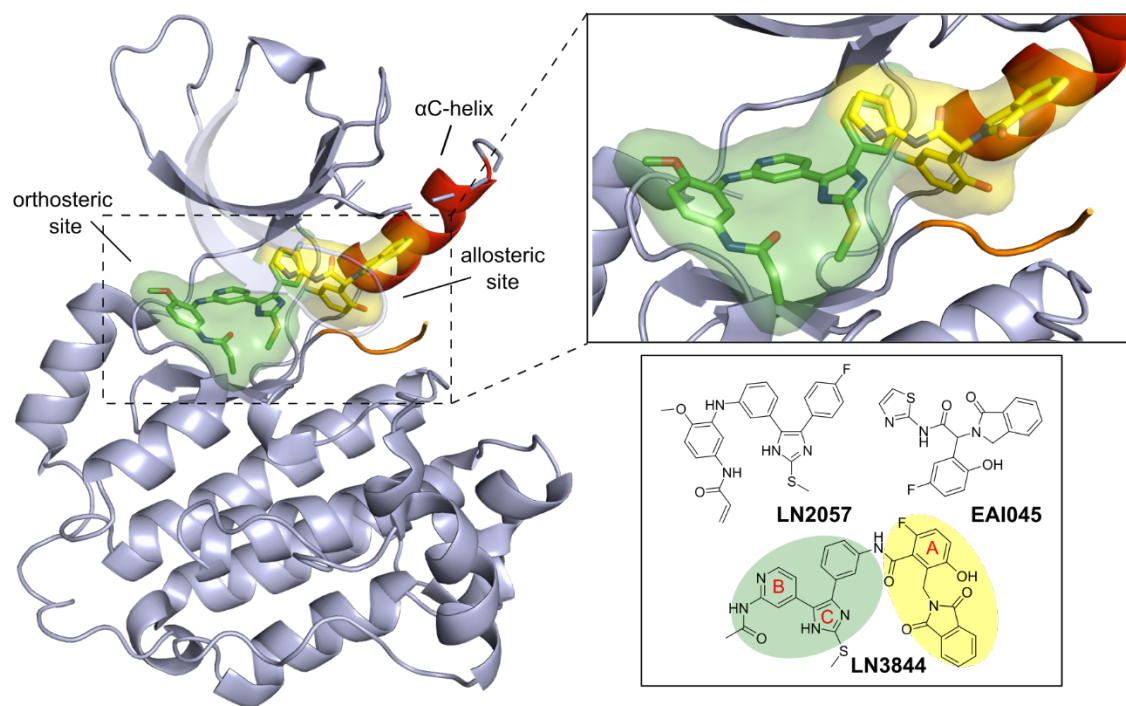
In addition to allosteric inhibitors, several ATP-competitive compounds have been reported and show promising inhibition of CS-containing tumors where no current drugs are approved.<sup>15,21</sup> Our earlier work reported a series of trisubstituted imidazole-based EGFR inhibitors with reversible and irreversible properties as a promising basis with high activity on LR/TM- and LR/TM/CS mutant EGFR.<sup>22–24</sup> We characterized several compounds biochemically and structurally and demonstrated that one of the responsible reversible bindings for overcoming CS mutations is influenced by an imidazole-dependent H-bond with the catalytic lysine (K745).<sup>25</sup> Other advanced inhibitors from industrial research programs feature analogous interactions with a variety of functionalities,<sup>26–29</sup> e.g., the wild-type sparing, isoquinoline-based inhibitor **BLU-945** that positions a methoxy group towards K745 (Figure 1) and is currently evaluated in a phase 1/2 clinical trial in combination with osimertinib against progressed NSCLC.<sup>30,31</sup>



**Figure 1: Chemical structures of representative EGFR inhibitors of 1<sup>st</sup>-4<sup>th</sup> generation.** Warheads of covalent inhibitors are colored in red. Allosteric pocket binding moieties are colored in green.

Inspired by these previous studies, efforts have been directed toward producing and studying ATP-allosteric spanning bivalent compounds that comprise structural elements from ATP and allosteric site inhibitors.<sup>32,33</sup> Our groups recently reported the structure-guided design of ATP and allosteric sites-spanning inhibitors by merging a trisubstituted imidazole with **EAI045** (Figure 2). A small subset of compounds was shown to be biochemically active exhibiting mutant selectivity based on the inclusion of a significant allosteric pocket binding group. A covalent analogue **LN4234** potentially inhibited the enzymatic activity of the LR/TM/CS mutation, exhibited modest cellular efficacies on LR and LR/TM in Ba/F3 cell line models, and this cellular activity was invariant of added cetuximab indicating that bivalent scaffolds do not suffer this liability which was observed in allosteric inhibitor **EAI045**.<sup>32</sup>

To further understand the structural and functional properties of spanning ATP-allosteric inhibitors, we herein present insights into the structure-activity relationships (SAR) of benzylisoindoline-derived trisubstituted imidazole EGFR inhibitors. Optimization of the groups that bind within the allosteric pocket result in improved enzymatic and cellular potency compared to previous lead molecules and provide key insights into how allosteric inhibitors acquire their unique mutant selective properties and motivate drug development to exploit this pocket in other protein kinases.

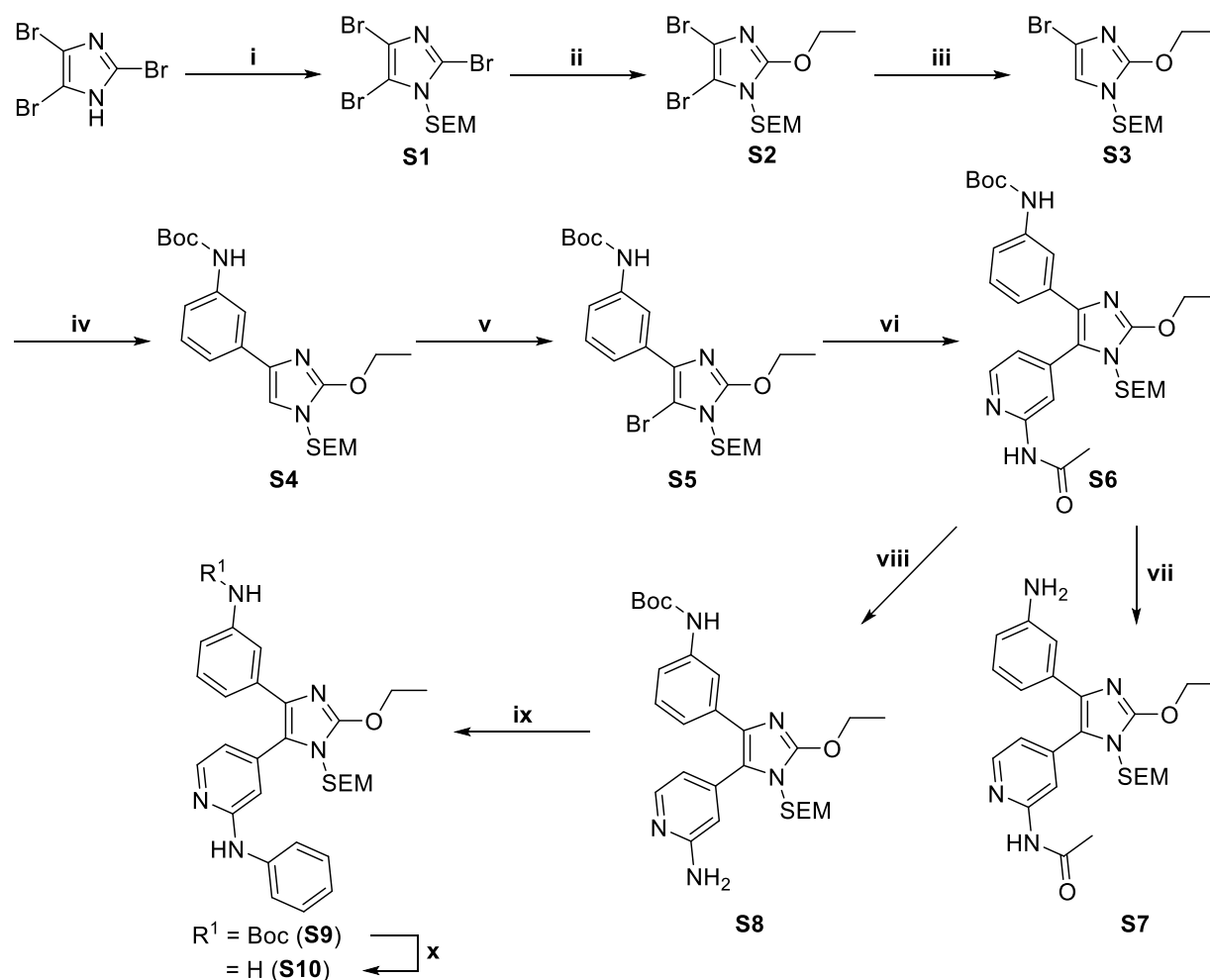


**Figure 2: Overview of the EGFR kinase domain and superimposed cocrystal structures of orthosteric binding imidazole-based inhibitor LN2057 (green, PDB code 6V6K) and allosteric inhibitor EAI045 (yellow, PDB code 6P1L). The isoindolinone motif of EAI045 occupies a hydrophobic region in proximity to the  $\alpha$ C-helix, which renders mutant-selectivity for bivalent inhibitors. Chemical structures of LN2057, EAI045 and the bivalent inhibitor LN3844 are shown and relevant aromatic rings for the SAR study are designated as A, B and C in the merged inhibitor LN3844.**

## Results

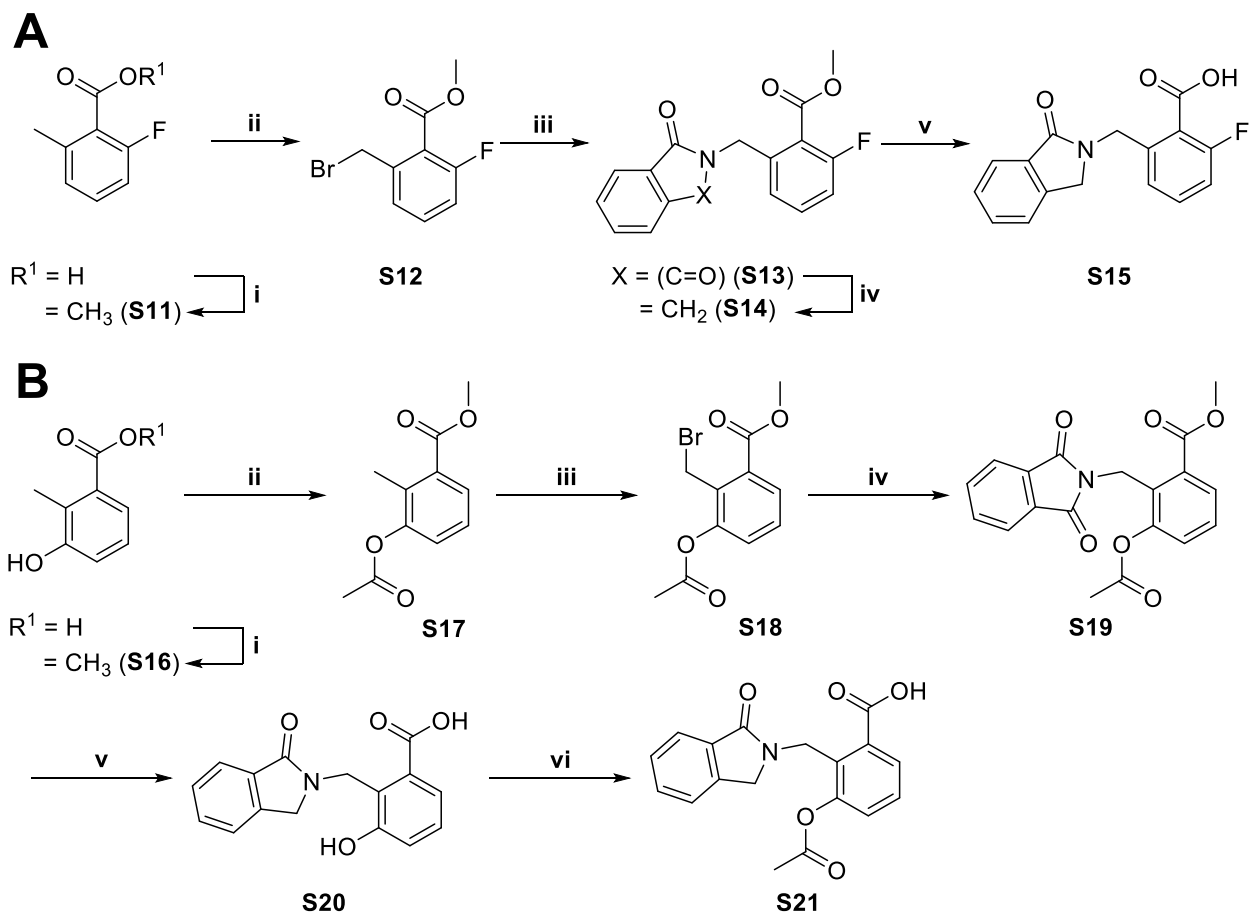
To characterize the SAR of trisubstituted imidazole-based bivalent EGFR inhibitors, we focused our design efforts on moieties that bind inside the allosteric pocket and prepared derivatives by a modular synthetic strategy. Synthesis of the trisubstituted imidazole scaffold

followed our previously described conditions with slight adjustments (Scheme 1,3).<sup>32</sup> Newly prepared carboxylic acids of the allosteric-motifs (Scheme 2) were combined with amines of the pyridinyl-imidazole scaffolds via amide coupling, followed by acidic deprotection (Scheme 4) like previously described.<sup>32</sup>

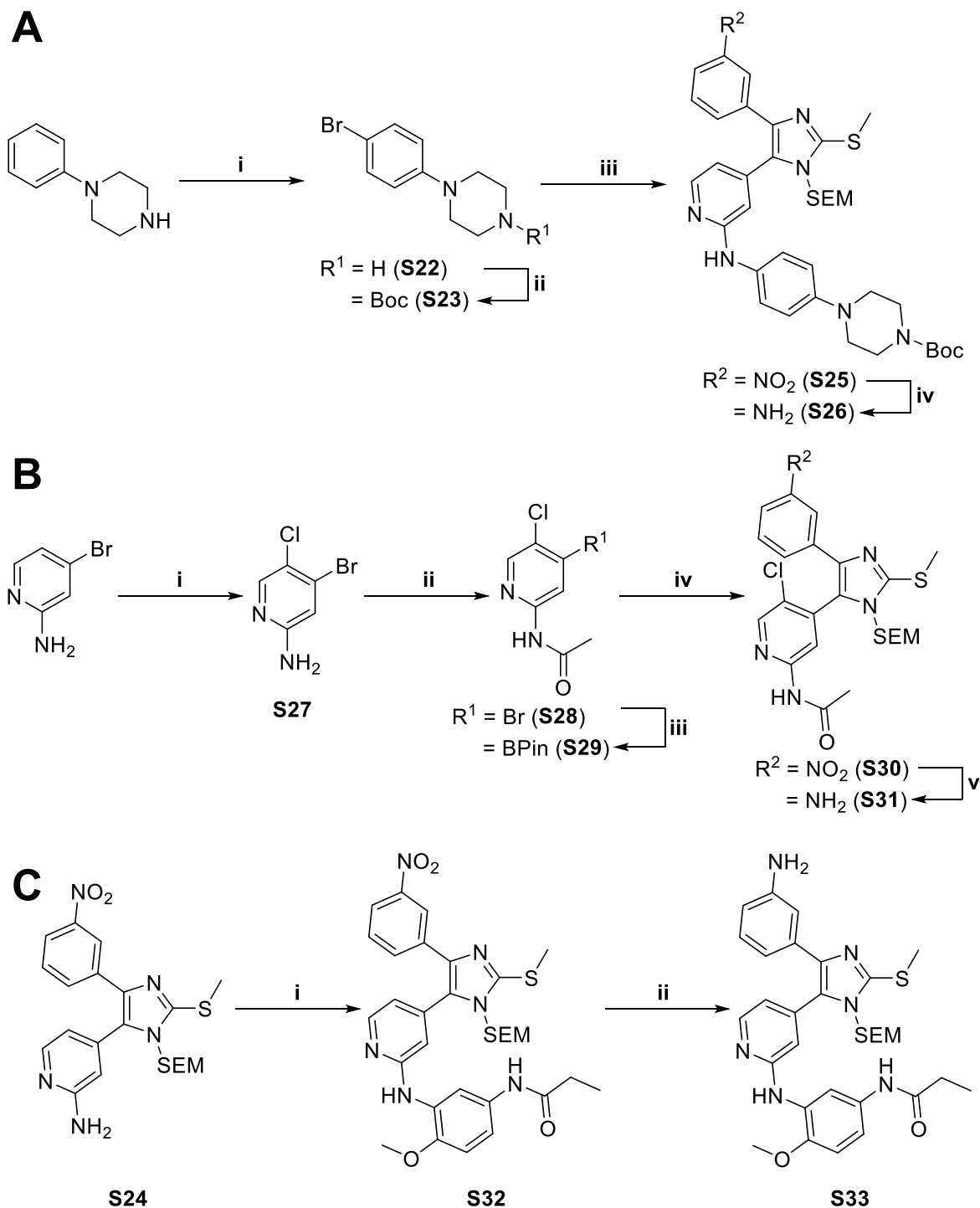


**Scheme 1** Synthesis of the ATP-binding orthosteric motifs - Reagents and conditions are as follows: i) SEM-Cl, NaH (60% dispersion in mineral oil), THF, 0 °C, quant.; ii) *t*-BuOK, EtOH, rf, 96%; iii) *n*-BuLi, THF, - 80 °C, quant.; iv) 3-(*N*-Boc-amino)phenylboronic acid,  $K_3PO_4$  trihydrate,  $P(t\text{-Bu})_3$  Pd G3, 1,4-dioxane/ $H_2O$ , 50 °C, 85%; v) NBS, ACN, - 35 °C, 77%; vi) *N*-(3-(4,4,5,5-tetramethyl-1,3,2-dioxaborolan-2-yl)phenyl)acetamide,  $K_3PO_4$  trihydrate,  $P(t\text{-Bu})_3$  Pd G3, 1,4-dioxane/ $H_2O$ , 55 °C, 64%; vii) 5 % TFA in DCM, rt, 68%; viii) 3 M NaOH (aq), MeOH, 55 °C, 94%; ix) Bromobenzene,  $Cs_2CO_3$ , BrettPhos Pd G3, 1,4-dioxane/*t*-BuOH, rf, 79-87%; x) 10% TFA in DCM, rt, 57-67%. With adjustments to our previously described conditions.<sup>32,34</sup>

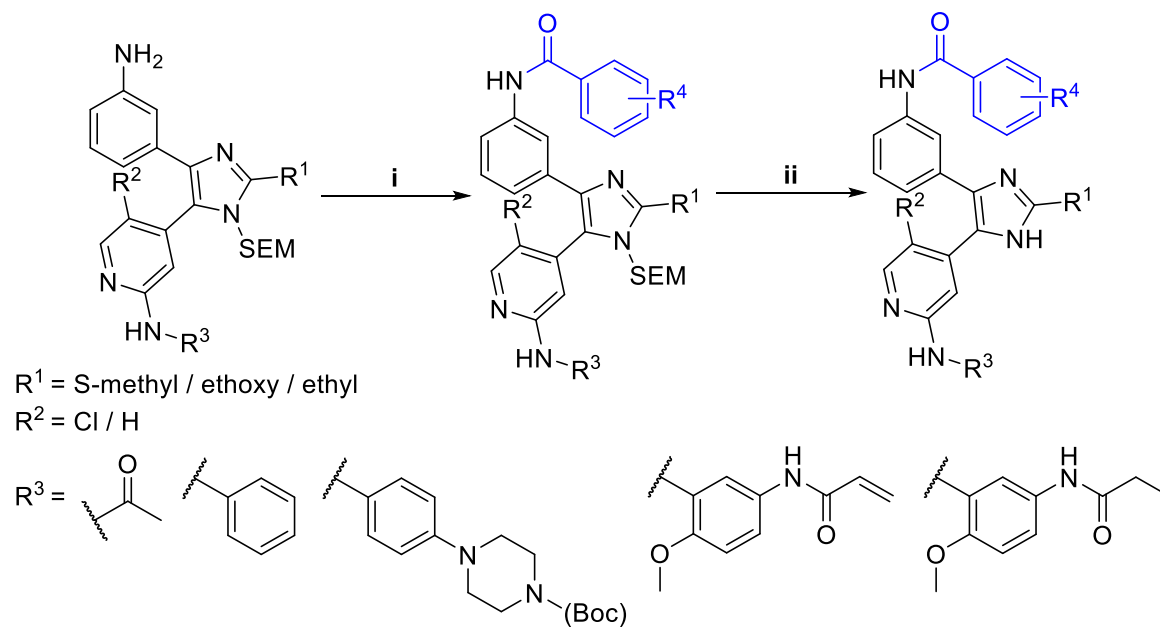




**Scheme 2 Synthesis of allosteric motifs.** Reagents and conditions are as follows: A) i) MeOH, cat. H<sub>2</sub>SO<sub>4</sub>, rf, 77%; ii) NBS, cat. AIBN, CCl<sub>4</sub>, rf, 75%; iii) K-phthalimide, DMF, rt, 72%; iv) conc. HCl/AcOH (1+1), Sn, 40 °C, 95%; v) 3 N NaOH, THF, 50 °C, 72 %. B) i) MeOH, cat. H<sub>2</sub>SO<sub>4</sub>, rf, 93%; ii) Ac<sub>2</sub>O, cat. 4-DMAP, TEA, THF, rt, 93%; iii) NBS, cat. AIBN, CCl<sub>4</sub>, rf, quant.; iii) K-phthalimide, DMF, rt, 94%; iv) conc. HCl/AcOH (1+1), Sn, 40 °C, 73%; v) Ac<sub>2</sub>O, cat. 4-DMAP, TEA, THF, rt, 96%.



**Scheme 3: Preparation of orthosteric motifs.** Reagents and conditions are as follows: A) i) HBr (48%), DMSO, 60 °C, 87%; ii)  $\text{Boc}_2\text{O}$ , TEA, DCM, rt, 88%; iii) **S24**,  $\text{Cs}_2\text{CO}_3$ , BrettPhos Pd G3, 1,4-dioxane/*t*-BuOH, rf, 86%; iv) Fe,  $\text{NH}_4\text{Cl}$ , THF/MeOH/ $\text{H}_2\text{O}$ , 50 °C, 84%. B) i) NCS, ACN, -30°C, 97%; ii)  $\text{Ac}_2\text{O}$ , 4-DMAP, ACN, 80°C, 30%; iii) Bis(pinacolato)diboron, KOAc, Pd(dppf) $\text{Cl}_2$ , 1,4-dioxane, 100 °C, 60%; iv) 5-Bromo-2-(methylthio)-4-(3-nitrophenyl)-1-((2-(trimethylsilyl)ethoxy)methyl)-1H-imidazole,  $\text{K}_3\text{PO}_4$  trihydrate, P(*t*-Bu) $_3$  Pd G3, 1,4-dioxane/ $\text{H}_2\text{O}$ , 55 °C, 81%; v) Zn,  $\text{NH}_4\text{COO}$ , MeOH, rt, 58%. C) i) *N*-(3-bromo-4-methoxyphenyl)propionamide,  $\text{Cs}_2\text{CO}_3$ , BrettPhos Pd G3, 1,4-dioxane/*t*-BuOH, rf, 96%; ii) Zn,  $\text{NH}_4\text{COO}$ , MeOH, rt, 40%.



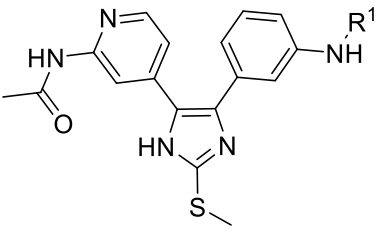
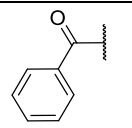
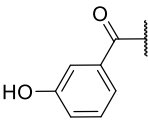
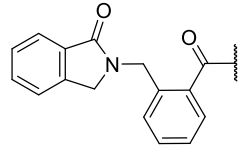
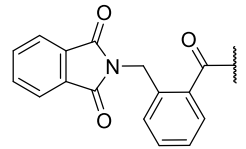
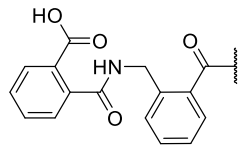
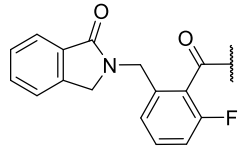
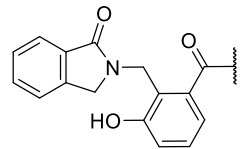
**Scheme 4** General preparation of biologically evaluated compounds. i) amide coupling of aniline reactants and varying benzoic acids of the allosteric motifs (blue); ii) appropriate deprotection conditions via previously described synthetic procedures.<sup>32</sup>

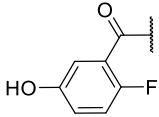
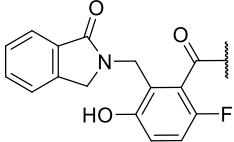
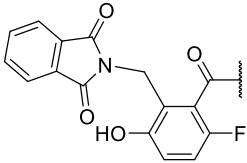
### Structure-activity relationships

We first set out to evaluate reversible binding compounds **1-7** comprising a variety of functional groups within the allosteric-site in HTRF-based biochemical activity assays with purified wild-type (WT) and EGFR mutants (Table 1).<sup>18</sup> Building on our earlier study,<sup>32</sup> we prepared compounds **1** and **2**, which consist of a relatively simple benzoic acid and a 3-hydroxybenzoic acid in the position that would bind the allosteric pocket, respectively and are found to be most potent against WT and LR and to a lesser extent against LR/TM and LR/TM/CS. Introduction of the hydroxy group (**2** and **LN3753**) showed a 10-fold higher activity on all enzymes, consistent with potency improvements influenced by phenyl substitution patterns as seen in allosteric inhibitors **EAI001** and **EAI045** (Table 1, Table S1).<sup>18</sup> Further elaborations into this group include methylene-linked isoindolinone- (**3**) or phthalimide-motifs (**4**) that negatively impact potency compared to **1**. Additionally, a hydrolyzed phthalimide-motif **5** showed no appreciable

improvements to potency as well. We then examined the effects of the -F and -OH phenyl substitutions **6** and **7** (Ring A, Figure 2), as inspired by earlier allosteric inhibitors and our previously reported complexes.<sup>18,32</sup> **7** was found to be the most potent analogue consisting of a phenolic hydroxy group and an isoindolinone, which is notably simpler compared to our earlier **LN3844**.<sup>32</sup> An important comparison to these newer molecules is the clinically-approved type 1.5 TKI **lapatinib**, which similarly anchors a phenyl ring within the allosteric pocket and is highly potent against WT and LR but practically inactive against TM (Table 1).<sup>35</sup> Our spanning ATP-allosteric inhibitors are unique from **lapatinib** in that they are potent against TM-containing EGFR kinase domains with IC<sub>50</sub> values below 1 nM. Additionally, changes to overall potency are generally accomplished through changes to the phenol while the methylisoindolinone allows for mutant-selective inhibition as seen for **1** versus **3**. These biochemical SAR showcase the regions of inhibitor where structure-based optimization enables for overall inhibitor potency (phenyl) and mutant selectivity (methylisoindolinone) all located in regions of the inhibitor that bind within the allosteric pocket.

**Table 1:** Biochemical Activities against WT and Mutant EGFR of Inhibitors with Variance of the Allosteric Motif.

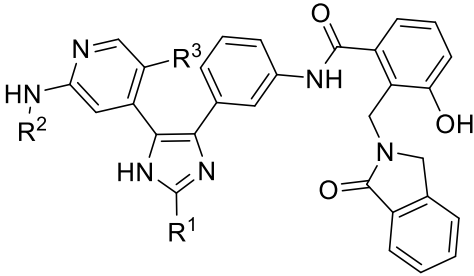
					
Compound	R <sup>1</sup>	EGFR IC <sub>50</sub> [nM] <sup>[b]</sup>			
		WT	LR	LR/TM	LR/TM/CS
1		< 10	45 ± 4	590 ± 30	560 ± 40
2		< 10	5.2 ± 0.3	51 ± 4	54 ± 4
3		> 1000	120 ± 5	460 ± 30	450 ± 30
4		290 ± 50	77 ± 5	870 ± 70	> 1000
5		n.d.	730 ± 400	n.d.	n.d.
6		> 1000	190 ± 8	930 ± 70	> 1000
7		< 10	0.22 ± 0.04	0.20 ± 0.03	0.16 ± 0.02

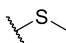
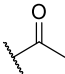
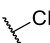

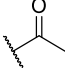
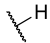
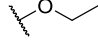
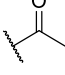
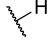
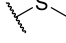
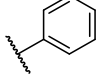
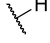

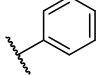
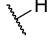
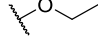
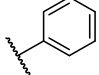
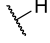
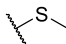
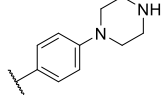
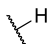
<b>LN3753</b>		$6.2 \pm 1$ [a]	$5.5 \pm 0.3$ [a]	$32 \pm 3$ [a]	$8.0 \pm 1$ [a]
<b>LN3843</b>		> 1000 [a]	$280 \pm 22$ [a]	> 1000 [a]	> 1000 [a]
<b>LN3844</b>		$5.8 \pm 1.0$ [a]	$1.2 \pm 0.4$ [a]	$51 \pm 3$ [a]	$32 \pm 6$ [a]
<b>Lapatinib</b>	-	< 10	< 0.1	> 1000	> 1000

[a] Data from Wittlinger and Heppner et al.<sup>32</sup> [b] IC<sub>50</sub> values were measured from a single experiment in triplicate. The ATP concentration was 100 μM. Errors are reported as ± the standard error.

Having arrived at an optimal structure of the allosteric-site moiety, we next prepared an advanced series of derivatives to explore the SAR at the ATP-binding site (Table 2). Based on our earlier studies, we concentrated on the derivatization of position 2 of the imidazole (R<sup>1</sup>, Table 2) and the amine of the hinge-binding motif (R<sup>2</sup>, Table 2).<sup>23,25,32</sup> We first evaluated the effect of a chlorine substituent on the pyridine ring (R<sup>3</sup>, Table 2) to correlate with other EGFR TKIs with similar substitutions [e.g., **mobocertinib** and **neratinib** (Figure 1)],<sup>36–39</sup> however no improvements to potency were observed in resulting compound **8** (Table 2). Derivatives **9** and **10** showed IC<sub>50</sub> values in a similar range compared to **7** consistent with the apparent tolerance of substitutions at R<sup>2</sup>.<sup>23,24</sup> Phenyl rings at the HR-II instead of *N*-acetyl amides (**11–13**, R<sup>2</sup>, Table 2) showed ~10-fold reduction in potency on all enzymes, which could in turn be restored by the introduction of a piperazine at the para position of the HR-II occupying phenyl (**14**). These observations show that the biochemical potencies of the optimal allosteric site group are generally unchanged with respect to groups bound at the ATP site and may be the ideal positions for future property-structure optimizations.<sup>40,41</sup>

**Table 2:** Biochemical Activities against WT and Mutant EGFR of Inhibitors with an Optimized Allosteric Motif and Derivatized Pyridinyl-imidazole Moieties.



Compound	R <sup>1</sup>	R <sup>2</sup>	R <sup>3</sup>	EGFR IC <sub>50</sub> [nM] <sup>[a]</sup>			
				WT	LR	LR/TM	LR/TM/CS
8				> 1000	500 ± 80	>1000	>1000
9				< 10	0.33 ± 0.03	0.35 ± 0.07	0.09 ± 0.01
10				< 10	0.26 ± 0.02	0.28 ± 0.04	0.12 ± 0.01
11				30 ± 3	6.1 ± 0.8	28 ± 4	5.7 ± 1
12				36 ± 3	2.2 ± 0.3	22 ± 4	3.4 ± 1
13				81 ± 10	2.6 ± 0.2	5.3 ± 0.4	2.1 ± 0.2
14				16 ± 2	1.0 ± 0.1	0.6 ± 0.1	0.58 ± 0.06

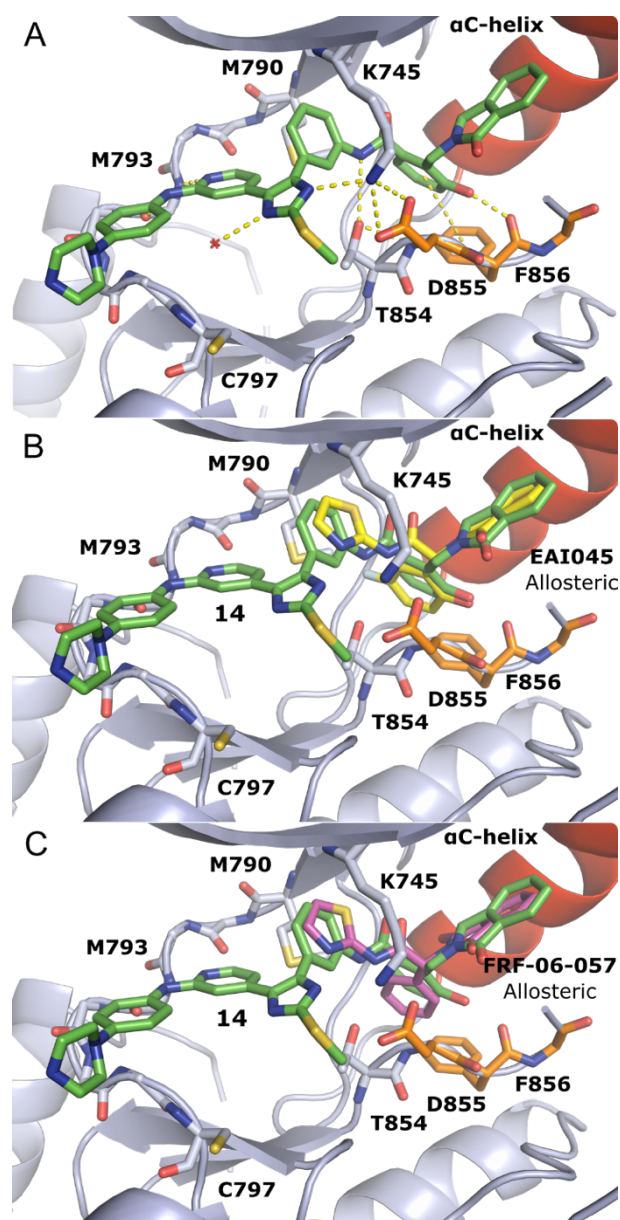
[a] IC<sub>50</sub> values were measured from a single experiment in triplicate. The ATP concentration was 100 μM. Errors are reported as ± the standard error.

To gain structural insights into the binding of our optimized bivalent inhibitor **14**, we carried out compound soaking with EGFR(TM/V948R) crystals as performed previously.<sup>25,32,42</sup>

The V948R (VR) mutation is located within the kinase domain and enables crystallization of the

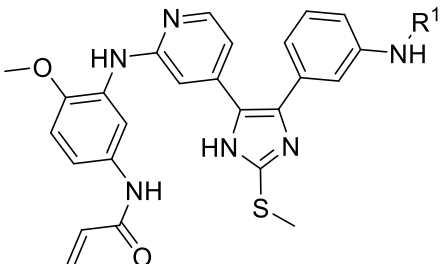
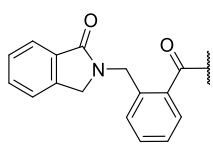
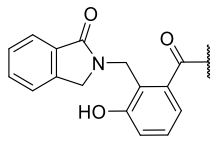
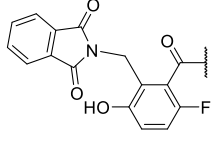
inactive  $\alpha$ C-helix out conformation as this substitution prevents the formation of active asymmetric dimers in the crystal lattice. We succeeded in determining a cocrystal structure of derivative **14** bound to the inactive conformation of EGFR at 2.49 Å-resolution, which shows the binding of this compound as desired within ATP and allosteric pockets (Figure 3A, Figure S1, Table S2). The 2-aminopyridine H-bonds to hinge residue M793 and the imidazole is acting as an H-bond acceptor for the catalytic lysine (K745) as observed in earlier structures (Figure S3).<sup>12,32</sup> The 4-phenylpiperazine is positioned towards the solvent and occupies the HR-II region, and a water molecule is found H-bonding with the imidazole nitrogen opposite from K745. The allosteric site motif is anchored in this site by an H-bond to T854 while the D855 of the DFG-motif interacts through bidentate H-bonding with K745. The phenol interacts with F856 of the DFG-motif through an H-bond to the backbone and  $\pi$ -stacking interactions with the sidechain. Importantly, the mutant selectivity-enabling isoindolinone moiety is located along the  $\alpha$ C-helix with its ketone directed away from the  $\alpha$ C-helix. We found that the overall binding mode of the bivalent ATP-allosteric inhibitor **14** is consistent with the binding mode of our earlier cocrystal structures of **LN3844** (Figure S3B) and the allosteric inhibitor **EAI045** (Figure 3B).<sup>21,34</sup> Additionally, we determined a cocrystal structure of a phthalimide-containing derivative of **EAI001 (FRF-06-057)** soaked into identical TM/VR crystals and show this molecule bound within the allosteric pocket (Figure 3C, Table S1, Scheme S1). Biochemical assays (Table 1, Table S1) indicate that the dual-ketone structure **FRF-06-057** does not make additional electrostatic interactions within the allosteric site as consistent with the binding of **LN3844**. Importantly, the cocrystal structure of **14** confirms the binding mode of our optimized ATP-allosteric bivalent compound showcasing the expected orientation of the phenol and isoindolinone within the allosteric pocket.





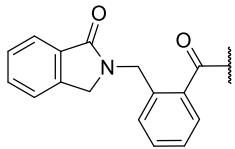
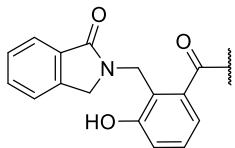
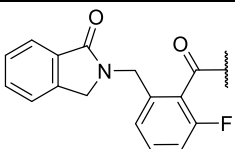
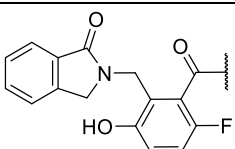
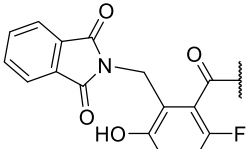
**Figure 3: X-ray crystallographic definition of the binding mode of ATP-allosteric sites spanning inhibitor 14 and structural superposition with allosteric EGFR inhibitors.** A) Binding mode of 14 in complex with EGFR(TM/VR). B) Superposition of crystal structures of 14 (green) and EAI045 (yellow, PDB code 6PIL). C) Superposition of crystal structures of 14 (green) and FRF-06-057 (magenta). The VR mutation allows for the crystallization of the EGFR kinase domain in the inactive conformation. P-loop of kinase domain hidden for better view on the binding site.

**Table 3** Time-dependent kinetic parameters of WT and Mutant EGFR for 15, 16 and LN4234.

					
Compound	R <sup>1</sup>		WT	LR	LR/TM
15		Apparent $k_{inact}/K_I$ [1/M*s]	1350 ± 20	24500 ± 300	2930 ± 100
		$k_{inact}$ [1/s]	0.0011 ± 0.00001	0.00573 ± 0.00009	0.00091 ± 0.00001
		$K_I$ [μM]	0.814 ± 0.021	0.234 ± 0.006	0.31 ± 0.013
16		Apparent $k_{inact}/K_I$ [1/M*s]	753 ± 13	14900 ± 200	2190 ± 60
		$k_{inact}$ [1/s]	0.00099 ± 0.00002	0.00411 ± 0.00006	0.00117 ± 0.00002
		$K_I$ [μM]	1.32 ± 0.04	0.276 ± 0.007	0.543 ± 0.02
LN4234		Apparent $k_{inact}/K_I$ [1/M*s]	1340 ± 20	24200 ± 400	2450 ± 70
		$k_{inact}$ [1/s]	0.00089 ± 0.00001	0.0055 ± 0.00009	0.00107 ± 0.00001
		$K_I$ [μM]	0.662 ± 0.016	0.227 ± 0.006	0.438 ± 0.016

Total enzyme concentration WT EGFR, LR and LR/TM at 4 nM.

**Table 4:** Biochemical Activities against LR/TM/CS Mutant EGFR of Covalent Bivalent Inhibitors (15-18).

Compound	R <sup>1</sup>	Reversible EGFR IC <sub>50</sub> [nM] <sup>[a]</sup>
		LR/TM/CS
15		> 1000
16		1.2 ± 0.09
17		340 ± 50
18		1.6 ± 0.1
LN4234		4.9 ± 1.0 [a]
Osimertinib	-	>1000 [a]
Neratinib	-	280 ± 20

[a] IC<sub>50</sub> values were measured from a single experiment in triplicate. The ATP concentration was 100 μM. Errors are reported as ± the standard error.

We next sought to assess the potency of compounds designed as irreversible binding ATP-allosteric bivalent scaffolds by incorporating a Michael acceptor as covalent warhead in the HR-II region to address the C797-residue at the edge of the ATP-site<sup>32</sup> (Tables 3 & 4). A subset of molecules were assayed in time-dependent measurements of inhibitor potency ( $k_{\text{inact}}/K_{\text{I}}^{\text{app}}$ ), which show that these inhibitors exhibit mutant-selective potency against LR and LR/TM kinases mainly due to reversible binding ( $K_{\text{I}}$ ) as the rate of covalent bond formation is largely similar ( $k_{\text{inact}}$ , Table 3). The CS-containing EGFR kinase domain does not form covalent bonds with inhibitors of this type and can be used to assess strength of reversible-binding. Compounds **15-18** have an isoindolinone motif in common but differ in substitution patterns of their phenyl rings that strongly impact the potency of these molecules against LR/TM/CS. The 5-fluoro substituent **17** is less effective compared to 2-hydroxy containing **16** and **18** further supporting the notion that the phenol is important in enabling tighter binding within these bivalent inhibitors. In contrast, clinically approved covalent inhibitors **osimertinib** and **neratinib** showed high activity on WT, LR, and LR/TM enzymes but have limited activity against the CS-containing EGFR kinase indicating that our bivalent compounds are capable of inhibiting this drug resistant mutation due to their stronger reversible binding. For completeness, we have also measured  $\text{IC}_{50}$  values for WT, LR, and LR/TM for these irreversible-binding compounds, but acknowledge that these measurements are not rigorous enough to make strong claims regarding SAR (Table S3).<sup>43</sup> Additionally, we prepared an alkylated imidazole analogue **19** and compound **20**, which harbors a propionamide instead of the acrylamide warhead that is not capable of covalent bond formation and a routinely employed control to assess reversible-binding properties of acrylamide-containing compounds.<sup>44-46</sup> Biochemical evaluation of **19** and **20** showed practically identical  $\text{IC}_{50}$  values against LR/TM/CS with **20** exhibiting strong and mutant-selective potency, which is expected as the Michael acceptor acrylamide likely contributes minimally to reversible binding (Table 5). The functional studies of

covalent bivalent inhibitors show similar trends in SAR further demonstrating the importance of the allosteric site group in enabling potency and selectivity of these compounds.

**Table 5** Biochemical Activities against WT and Mutant EGFR of alkylated analogue **19** and propionamide derivative **20**.

Compound	EGFR IC <sub>50</sub> [nM] <sup>[a]</sup>			
	WT	LR	LR/TM	LR/TM/CS
<b>19</b>	-	-	-	0.91 ± 0.1
<b>20</b>	29 ± 4	2 ± 0.2	0.91 ± 0.1	0.99 ± 0.1

[a] IC<sub>50</sub> values were measured from a single experiment in triplicate. The ATP concentration was 100 μM. Errors are reported as ± the standard error.

To better understand the biological activity of these structurally diverse bivalent compounds, we next evaluated the antiproliferative activity of several compounds in Ba/F3 cell lines expressing a variety of EGFR mutations (Table 6). We also employed Ba/F3 cells expressing the activating EGFRvIII mutation (vIII) to assess WT-related activity as this protein contains a WT kinase domain and is simpler to culture compared to WT EGFR expressing Ba/F3 cells as they require EGF in the culture medium and the mutants do not.<sup>47,48</sup> Generally, our reversible binding compounds (**7**, **9-14**), showed limited antiproliferative activity despite their low nM biochemical IC<sub>50</sub> values (Table 6). Corresponding irreversible derivatives (**15-19**) exhibited antiproliferative activity, with preferential activity against LR and to a lesser extent LR/TM (Table 6) as consistent with our earlier studies indicating the importance of the covalent bond formation process in cellular activity.<sup>22,23,32</sup> Uniquely, these compounds also exhibit modest cellular activity against Ba/F3 cells

expressing exon 19 deletion delE746-A750 (ex19del) with **15** being most potent. This is unexpected since type 1.5 (**lapatinib**) and allosteric (**EAI045**) EGFR inhibitors are limitedly effective against this mutation and instead imply that bivalent ATP-allosteric inhibitors are uniquely capable of targeting this prevalent mutations.<sup>18,47</sup> We also observed that a subset of our molecules **16, 19, 20** were modestly active against the LR/TM/CS variant implying that they are capable of strong reversible binding to EGFR (Table 6). The propionamide derivative **20** that lacks the ability to make a covalent bond to C797 still exhibits antiproliferative activity in several cell lines, although generally to a lesser extent than the corresponding covalent analogue **16** with the notable exception of LR/TM/CS. This is somewhat expected as reversible binding analogues of covalent inhibitors are likely to be less efficacious on account of their lower residence times despite similar reversible binding properties.<sup>43,49</sup> The variable potencies measured in Ba/F3 cell antiproliferation assays indicate that our structurally optimized bivalent compounds effectively target activating EGFR mutations, most potently LR and ~10-fold improved over our earlier molecule **LN4234**.<sup>32</sup>

**Table 6:** Antiproliferative Activities on the Proliferation of Ba/F3 Cell Lines Models of Selected EGFR Mutants.

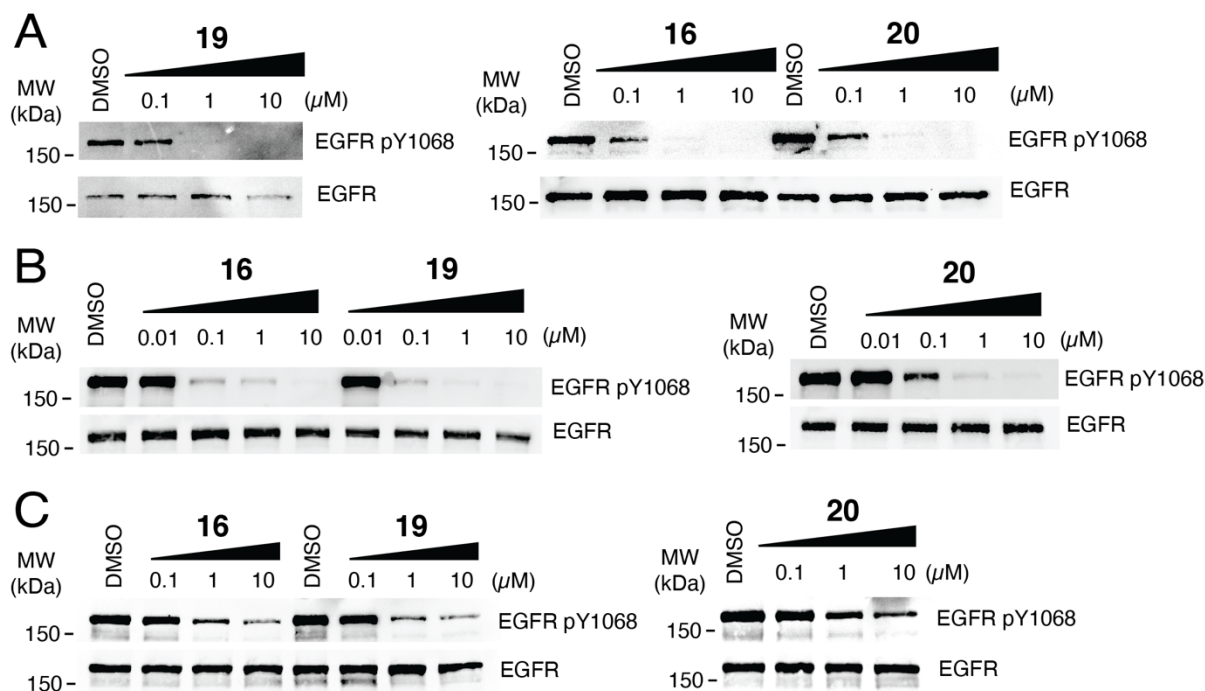
Compound	Ba/F3 Cellular EC <sub>50</sub> [nM] <sup>[b]</sup>				
	LR	LR/TM	LR/TM/CS	ex19del	vIII (WT)
<b>7</b>	> 10,000	> 10,000	n.d.	> 10,000	> 10,000
<b>9</b>	> 10,000	> 10,000	n.d.	> 10,000	> 10,000
<b>10</b>	> 10,000	> 10,000	n.d.	> 10,000	> 10,000
<b>11</b>	3700 ± 1000	> 10,000	n.d.	4000 ± 580	> 10,000
<b>12</b>	3900 ± 200	> 10,000	> 10,000	n.d.	> 10,000
<b>13</b>	2900 ± 1000	> 10,000	n.d.	> 10,000	> 10,000
<b>14</b>	> 10,000	> 10,000	> 10,000	> 10,000	> 10,000
<b>15</b>	170 ± 20	880 ± 100	> 10,000	1400 ± 160	1700 ± 320
<b>16</b>	150 ± 20	430 ± 130	3900 ± 2800	950 ± 190	750 ± 220
<b>17</b>	180 ± 45	1100 ± 400	> 10,000	530 ± 89	720 ± 13
<b>18</b>	370 ± 100	1200 ± 300	> 10,000	1400 ± 140	1100 ± 200
<b>19</b>	220 ± 81	590 ± 400	2100 ± 530	1500 ± 350	1000 ± 96
<b>20</b>	1000 ± 280	> 10,000	1700 ± 410	1800 ± 270	1100 ± 220
<b>LN4234</b>	1200 ± 70 [a]	4400 ± 500 [a]	> 10,000 [a]	n.d.	n.d.
<b>Osimertinib</b>	33 ± 0.6 [a]	8 ± 0 [a]	1200 ± 130 [a]	14 ± 4	n.d.

[a] Data from Wittlinger and Heppner.<sup>32</sup> [b] EC<sub>50</sub> values are averages of at least three independent experiments, with each experiment performed in triplicate. Errors are reported as ± the standard deviation.

Building on these findings from Ba/F3 cells, we proceeded to assess inhibitory properties of our most effective compounds (**16**, **19**, and **20**) against human cancer cell lines driven by diverse EGFR activating mutations. Accordingly, dose-dependent suppression of EGFR phosphorylation (pY1068) in H1975 (LR/TM), H3255 (LR) and HCC827 (delE746-A750, ex19del) cell line models through Western blot is consistent with antiproliferative effects in Ba/F3 cells (Table 6) and further indicate the broad scope of these bivalent inhibitors (Figure 4). Quantitative antiproliferative effects of these compounds against H1975 and HCC827 cells are found to be associated with phosphorylated EGFR suppression with **16** ~15-fold higher EC<sub>50</sub> values compared to **osimertinib** in the H1975 cell assay (Table 7). Strikingly, reversible binding **20** is also active and only slightly

less effective compared to **16** and **19**, which is different from what we observe in Ba/F3 cells. We support the observation that these bivalent inhibitors are active against ex19del in HCC827 cells and further indicate how ATP-allosteric bivalent inhibitors are functionally distinct from their related type 1.5 and allosteric-only analogues. The results of these human cancer cell line experiments demonstrate that these bivalent ATP-allosteric inhibitors are capable of impacting diverse EGFR activating mutations in the context of human cancer cells.





**Figure 4:** Immunoblotting of phosphorylation levels of EGFR in A) H1975 (LR/TM), B) H3255 (LR) and C) HCC827 (ex19del) cells. All experiments performed after 6 hours treatments and western blots are representative of three independent experiments.

**Table 7:** Anti-proliferative potency of compounds **16**, **19** and **20** in cancer cell lines H1975 (LR/TM) and HCC827 (ex19del).

	EC <sub>50</sub> [nM] <sup>[a]</sup>				
	<b>16</b>	<b>19</b>	<b>20</b>	<b>lapatinib</b>	<b>osimertinib</b>
<b>H1975 (LR/TM)</b>	330 ± 200	300 ± 200	420 ± 200	>10,000	22 ± 9
<b>HCC827 (ex19del)</b>	160 ± 100	290 ± 200	270 ± 100	>10,000	2.3 ± 1

[a] EC<sub>50</sub> values are averages of at least three independent experiments, with each experiment performed in triplicate. Errors are reported as ± the standard deviation.

Computer-aided docking has provided a pose for covalent binding **16** in accordance with what is observed in the crystal structure of reversible binding **14** with the expected orientation for covalent bond formation with *C797* and consistent with our earlier structural and functional studies (Figure S4).<sup>25,32</sup> We further measured the metabolic stability for **16** and **19** in human liver microsomes that revealed good stability after 2 hours of incubation. LC-MS analysis of the metabolites revealed a metabolite with a *m/z* + 16 Da only for inhibitor **16**, which can serve as

indicator for the metabolic oxidation of the thioether (Figures S5, S6).<sup>50</sup> A selectivity screening of compound **16** against 468 kinases at 1  $\mu$ M concentration exhibited good selectivity for EGFR mutants with a S(10) of 0.013 (Table S4). Besides EGFR mutants only DMPK2 and MYO3A were inhibited with a POC < 10%. Additionally, we found that none of the kinases that harbor a cysteine at analogous positions to C797 (MKK7, ITK, BTK, BMX, JAK3, TEC, TXK, BLK) outside the ErbB-family were significantly targeted by compound **16** indicating that the bivalent scaffold optimized here is ideally suited for covalent inhibition of EGFR mutations.<sup>49</sup> These results, coupled with our findings in cell lines mentioned previously, indicate that compound **16** showcases early-phase medicinal chemistry characteristics suitable for future property-structure optimizations.

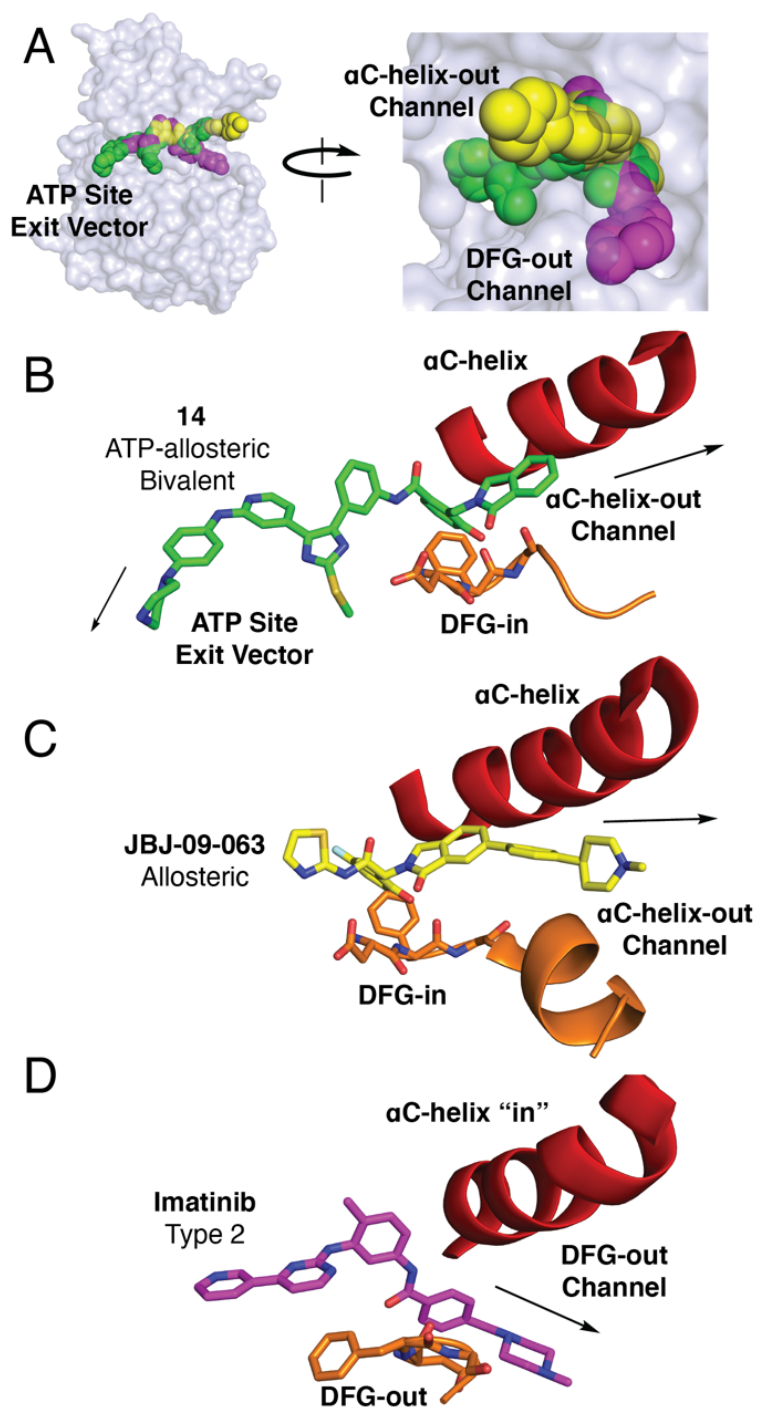
## Discussion

Systematic optimization of small-molecule lead compounds is a proven strategy in medicinal chemistry to understand the impacts of certain functional groups within target binding sites. In this study, we have carried out the optimization of a series of spanning ATP-allosteric bivalent inhibitors based on parent ATP- and allosteric-site motifs to achieve appreciable biological activity in biochemical assays and a series of human cancer cell lines. We have also determined the binding mode of a reversible binding analogue **14** confirming the placement of motifs within the respective pockets and allowing the direct assignment of the sites within in the EGFR kinase domain that afford potency and mutant selectivity. Accordingly, biochemical SAR of reversible and irreversible compounds show that the central phenol binds the allosteric pocket in an identical position of phenyl rings of type 1.5 (**lapatinib**, **neratinib**) and allosteric inhibitors (e.g., **EAI045**), which is responsible for enabling strong reversible binding of the ATP-allosteric bivalent series (Figure S3). Distinctly, the peripheral methylisoindolinone positioned along the  $\alpha$ C-helix in the allosteric pocket enables selectivity for the activating mutations. Uniquely, these bivalent inhibitors

are found to be active against the exon19del mutation (delE746-A750), which is commonly resistant to inhibition by type 1.5 and allosteric TKIs.<sup>17,19,47</sup> While the structural basis for targeting the diverse EGFR deletion mutations is known for certain inhibitors,<sup>51,52</sup> the precise rationale for how bivalent inhibitors bind to and inhibit this mutation is presently unknown and counterintuitive given the requirement for the kinase to adopt the inactive  $\alpha$ C-helix “out” conformation while this deletion mutation likely constrains the inward conformation. Nevertheless, the work detailed here supports the notion that the binding of the methylisoindolinone along the  $\alpha$ C-helix of the EGFR kinase enables critical mutant selective inhibition of the spanning bivalent inhibitor series.

The compounds presented in this work are structurally unique when compared to all other EGFR TKIs in that they bind extensively across most of the drug-binding pockets of the inactive kinase domain. However, they share a variety of structural elements reminiscent of previous EGFR TKIs. At the ATP site, the imidazole-based scaffold, which extends from the hinge makes H-bonding interactions with K745, which is a common feature of CS-targeting fourth-generation inhibitors such as **BLU-945** (Figure S7).<sup>21</sup> Accordingly, compounds from our earlier study (e.g., **LN3753**) consisting of imidazole heterocycles contain phenyl rings in the pocket occupied by type 1.5 inhibitors **lapatinib**, which is important with respect to binding to the  $\alpha$ C-helix out inactive conformation (Figure S3). Our type 1.5 inhibitors (**LN3753**, **1**, **2**) are similar to **lapatinib** but are capable of inhibiting TM/CS-containing EGFR kinases likely due to binding properties stemming from the imidazole ATP-site scaffold. The bivalent molecules, by virtue of their design, share much in common with the phenyl glycine mutant-selective allosteric inhibitors.<sup>16–19,32</sup> The mutant-selectivity of the allosteric pocket is a key feature of the isoindolinone-containing ATP-allosteric bivalent compounds indicating that inhibitors that bind this pocket are unique and enable mutant selective EGFR inhibition. The bivalent inhibitors do not extend as far along the  $\alpha$ C-helix as the most potent **JBj-09-063** or **JBj-04-125-02**, which exit the kinase domain into solvent. It is possible

given our biochemical SAR to conclude that mutant selectivity of the ATP-allosteric bivalent compounds is due to the methylisoindolinone binding of the allosteric site and offer key evidence that the binding of groups in this region of the  $\alpha$ C-helix “out” kinase are capable of enabling mutant selective binding. Earlier studies indicated that mutant selectivity for EGFR inhibitors was due to ATP affinity changes that could be thwarted upon acquisition of the T790M mutation.<sup>5</sup> The binding to this region of the inactive EGFR kinase is another region where one can engineer mutant selective targeting that, in this case, allows for more effective inhibition in the cases of contemporary drug resistance through TM and CS. Importantly, our SAR also indicates that the phenyl ring that is shared with **lapatinib** and **neratinib** is not a location for mutant selective binding, at least in absence of the methylisoindolinone. The ability to draw a direct parallel between the binding site in the allosteric pocket that does and does not enable mutant selective inhibition is only possible in our bivalent ATP-allosteric scaffolds since, we presume, similar SAR is inaccessible in allosteric only compounds such as **EAI045** and **JBj-09-063** where the triblade phenyl glycine structure is absolutely necessary for binding in a general sense.<sup>17-19</sup>



**Figure 5.** The divergent drug-binding channels and exit vectors in protein kinases. Overlay of the regions of the EGFR kinase occupied by an ATP-allosteric bivalent (**14** green, PDB code 8TO3), allosteric **BJJ-09-063** (yellow, PDB code 7JXQ), and type 2 inhibitor **imatinib** (magenta, PDB code 2OIQ) with compounds indicated with space filling spheres. Protein surface (PDB ID) indicated with a transparent surface highlighting the binding channels dependent on the  $\alpha$ C-helix out and DFG-out channels. Binding modes of B) **14**, C) **BJJ-09-063**, and D) **imatinib** from structure in A) highlighting the group bound within the respective allosteric pockets and the direction of the exit vector along the respective drug binding.

Given the ability to determine the pocket within the  $\alpha$ C-helix “out” kinase that allows for mutant selective inhibition by our ATP-allosteric molecules, it is especially interesting to consider how this site is related to kinase inhibitors more broadly. The outward rotation of the  $\alpha$ C-helix is a key feature of the inactive kinase and cocrystal structures of bivalent inhibitors along with allosteric inhibitors show that this site is actually a solvent accessible channel, which we denote this channel in the inactive  $\alpha$ C-helix out kinase as the “ $\alpha$ C-helix-out channel” (Figure 5). The residues along this pocket are mainly hydrophobic until the *N*-terminus of the  $\alpha$ C-helix where the channel terminates into hydrophilic residues at the solvent interface (green and yellow, Figure 5A-C). It is interesting to juxtapose this channel in the context of the distinct and alternative allosteric pocket made accessible in type 2 TKIs where the DFG-motif outward conformation leads to a completely different exit vector, which we denote as the “DFG-out channel” (**imatinib** in magenta, Figure 5A and D). These two channels are never present at the same time as they are made accessible to drug binding by structural changes of either the  $\alpha$ C-helix or DFG-motif and correspondingly the orientation of the activation loop (Figure S8). The  $\alpha$ C-helix “out” conformation has to this point been considered only relevant for type 1.5 inhibitors, but our SAR would suggest that further elaborative binding from allosteric-site binding molecules along the  $\alpha$ C-helix is likely to enable beneficial and desired drug properties as has been done previously with Type 2 inhibitors. A search of kinase inhibitors in available structural databases reveals very few kinases have been studied with compounds that bind the  $\alpha$ C-helix channel (Table S5). The results of this study would strongly suggest that more attention should be paid to molecules that can anchor into this  $\alpha$ C-helix-out channel in an analogous fashion to the compounds studied in the present work.

## Conclusion

We have carried out the structure-based optimization of a series of ATP-allosteric EGFR inhibitors to maximize potency in cells and establish mutant-selective inhibition. We achieve broad inhibition of EGFR mutants that are highly prevalent in NSCLC and show marked improvements in cellular efficacy. Biochemical SAR and cocrystal structures indicate the desired selectivity for EGFR mutations is enabled by anchoring of a methylisoindolinone group within a channel made accessible by the outward rotation of the  $\alpha$ C-helix in the inactive kinase domain. These ATP-allosteric EGFR inhibitors represent novel examples of mutant-targeting agents that offer a platform for the development of unique inhibitors that bind the  $\alpha$ C-helix-out channel in other kinases that may enable selectivity and potency needed for drug development.

## Contributions

F.W., S.P.C., C.D.P., T.D., I.K.S., M.Q.D., B.C.O., A.R., T.S.B., B.B., F.F., T.S., C.K., M.J.E., P.A.H., D.A.S., S.A.L., D.E.H. conceived and designed the experiments; F.W. and F.F. performed synthesis; S.P.C., T.D., C.D.P., I.K.S., T.S.B., T.S. and B.B. performed biological assays; B.C.O., T.S.B. and D.E.H. performed X-ray crystallography; S.C. performed molecular docking; A.R. performed metabolic stability experiments; C.K. performed MS experiments; F.W., S.A.L. and D.E.H. interpreted the data; F.W., S.A.L. and D.E.H. wrote the paper. The manuscript was written through the contributions of all authors. All authors have given approval to the final version of the manuscript.

## Acknowledgments

We acknowledge support from startup funds from The State University of New York (DEH) and support by the National Center for Advancing Translational Sciences of the National Institutes of Health under award Number UL1TR001412-08 (BTC K Scholar Award to DEH). S.A.L. and iFIT are funded by the Deutsche Forschungsgemeinschaft (DFG, German Research Foundation) under Germany's Excellence Strategy (EXC 2180-390900677). TüCAD2 is funded by the Federal Ministry of Education and Research (BMBF) and the Baden-Württemberg Ministry of Science as part of the Excellence Strategy of the German Federal and State Governments. National Institutes of Health Grants R01CA201049, R01CA116020, and R35CA242461 (to M.J.E), Roswell Park Alliance Foundation (PAH). The content is solely the responsibility of the authors and does not necessarily represent the official views of the NIH. T.S.B is supported by a Ruth L. Kirschstein National Research Service Award (5F32CA247198-02). This work was partially done in the Drug



Discovery Core Facility of Roswell Park Comprehensive Cancer Center supported by National Cancer Institute (R01CA197967 to K.V. Gurova and P30CA016056 to Roswell Park Cancer Center). Kinetics of irreversible inhibitors was obtained by contact with AssayQuant Technology, Inc. This work is based on research utilizing resources of the Frontier Microfocusing Macromolecular Crystallography (17-ID-2, FMX) beamline at National Synchrotron Light Source II at Brookhaven National Laboratory to Block Allocation Group 308246. We thank Dr. Michael Malkowski and Dr. Liang Dong for SF21 cells and access to their tissue culture lab. We also acknowledge Dr. Diana Monteiro and Dr. Edward Snell for access to laboratory space and equipment for protein purification and crystallization resources.

## Experimental

### Protein expression and purification

The EGFR kinase domain (residues 696-1022) was cloned into pTriEx with an N-terminal 6xHis-glutathione S-transferase (GST) fusion tag followed by a TEV protease cleavage site. EGFR WT, L858R, L858R/T790M, L858R/T790M/C797S was expressed after baculoviral infection in SF9 cells and EGFR(T790M/V948R) was expressed in SF21 cells. Briefly, cells were pelleted and resuspended in lysis buffer composed of 50 mM Tris pH 8.0, 500 mM NaCl, 1 mM tris(2-carboxyethyl) phosphine (TCEP), and 5% glycerol. Cells were lysed via sonication prior to ultracentrifugation at >200,000 g for 1 h. Imidazole pH 8.0 was added to the supernatant for a final concentration of 40 mM and flowed through a column containing Ni-NTA agarose beads. The resin was washed with lysis buffer supplemented with 40 mM imidazole and eluted with lysis buffer containing 200 mM imidazole. Eluted EGFR kinase domain was dialyzed overnight in the presence of 5% (w/w) TEV protease against dialysis buffer containing 50 mM Tris pH 8.0, 500 mM NaCl, 1 mM TCEP, and 5% glycerol. The cleaved protein was passed through Ni-NTA resin to remove the 6xHis-GST fusion protein and TEV prior to size exclusion chromatography on a prep-grade Superdex S200 column in 50 mM Tris pH 8.0, 500 mM NaCl, 1 mM TCEP, and 5% glycerol. Fractions containing EGFR kinase of  $\geq 95\%$  purity as assessed by Coomassie-stained SDS-PAGE were concentrated to approximately 4 mg/mL as determined by Bradford assay or absorbance.

### Crystallization and structure determination

EGFR(T790M/V948R) pre-incubated with 1 mM AMP-PNP and 10 mM MgCl<sub>2</sub> on ice was prepared by hanging-drop vapor diffusion over a reservoir solution containing 0.1 M Bis-Tris (pH = 5.5), 25% PEG-3350, and 5 mM TCEP (buffer A for crystals soaked with compound 1) or 0.1 M Bis-Tris (pH = 5.7), 30% PEG-3350 TCEP (buffer B for crystals soaked with compound 2). Drops containing crystals in buffer A and B were exchanged with solutions of both buffers containing  $\sim 1.0$  mM **14** and **FRF-06-057** were exchanged three times for an hour and then left to soak overnight. Crystals were flash frozen after rapid immersion in a cryoprotectant solution with buffer A or BA containing 25% ethylene glycol. X-ray diffraction data on soaked T790M/V948R crystals were collected at 100K at the National Synchrotron Light Source II 17-ID-2<sup>58</sup>. Diffraction data was processed and merged in Xia2 using aimless and dials. The structure was determined by molecular replacement with the program PHASER using the inactive kinase domain EGFR(T790M/V948R) kinase from our previous work excluding the **LN3844** ligand (PDB 6WXN). Repeated rounds of manual refitting and crystallographic refinement were performed using COOT and Phenix. The inhibitor was modeled into the closely fitting positive  $F_o - F_c$  electron density and then included



in following refinement cycles. Statistics for diffraction data processing and structure refinement are shown in Table S1.

### **Time-dependent Kinase Inhibition Assays**

Biochemical assays were performed with commercially available EGFR WT, cytoplasmic domain (669-1210), GST-tagged, Carna (Cat#/Lot#: 08-115/21CBS-0127H), EGFR [T790M/L858R] and EGFR [L858R], cytoplasmic domain (669-1210), GST-tagged, Carna (Cat#/Lot#: 08-510/12CBS-0765M). Reactions were performed with kinase domain enzyme concentrations of 4 nM in final solutions of 52 mM HEPES pH 7.5, 1 mM ATP, 0.5 mM TCEP, 0.011% Brij-35, 0.25% glycerol, 0.1 mg/ml BSA, 0.52 mM EGTA, 10 mM MgCl<sub>2</sub>, 15 μM Sox-based substrate (AQT0734). BSA was not included in this experiment to prevent interference with irreversible inhibitor characterization via off-target binding. All reactions were run for 240 minutes at 30 °C. Time-dependent fluorescence from the Sox-based substrate was monitored in PerkinElmer ProxiPlate-384 Plus, white shallow well microplates (Cat. #6008280) Biotek Synergy Neo 2 microplate reader with excitation (360 nm) and emission (485 nm) wavelengths. **15**, **18** and **LN4234** was dosed between 0 and 10 μM in 24-point curves with 1.5-fold dilutions. Fluorescence, determined with identical reactions but lacking purified enzyme or crude cell lysate was subtracted from the total fluorescence signal for each time point, with both determined in duplicate, to obtain corrected relative fluorescence units (RFU). Corrected RFU values then were plotted vs. time and the reaction velocity for the first ~40 min (initial reaction rates) were determined from the slope using GraphPad Prism (La Jolla, CA) with units of RFU/min.

### **HTRF Assays**

Biochemical assays for EGFR domains were carried out using a homogeneous time-resolved fluorescence (HTRF) KinEASE-TK (Cisbio) assay, as described previously.<sup>59</sup> Assays were optimized for ATP concentration of 100 μM with enzyme concentrations WT EGFR 10 nM, L858R 0.1 nM, L858R/T790M at 0.02 nM and L858R/T790M/C797S at 0.02 nM. Inhibitor compounds in DMSO were dispensed directly in 384-well plates with the D300 digital dispenser (Hewlett Packard) followed immediately by the addition of aqueous buffered solutions using the Multidrop Combi Reagent Dispenser (Thermo Fischer). Compound IC<sub>50</sub> values were determined by 11-point inhibition curves (from 1.0 to 0.00130 μM) in triplicate. The data was graphically displayed using GraphPad Prism version 7.0, (GraphPad software). The curves were fitted using a non-linear regression model with a sigmoidal dose response.

### **Ba/F3 Cellular Antiproliferative Experiments**

The parental Ba/F3 cells was a generous gift from the laboratory of Dr. David Weinstock (in 2014), Dr. Pasi Jänne (2020) and was used to generate the L858R (LR), L858R/T790M (LR/TM), L858R/T790M/C797S (LR/TM/CS), exon19del and vIII EGFR mutant Ba/F3 cells. These cells were previously characterized as described.<sup>38 60</sup> All Ba/F3 cells were cultured in RPMI1640 media with 10% fetal bovine serum and 1% penicillin and streptomycin. All cell lines were tested negative for *Mycoplasma* using Mycoplasma Plus PCR Primer Set (Agilent) and were passaged and/or used for no longer than 4 weeks for all experiments. Assay reagents were purchased from MilliporeSigma (Cat# R7017-5G). Ba/F3 cells were plated and treated with increasing concentrations of inhibitors in triplicate for 72 hours. Compounds were dispensed using the Tecan D300e Digital Dispenser. Cellular growth or the inhibition of growth was assessed by resazurin

viability assay. All experiments were repeated at least 3 times and values were reported as an average with standard deviation.

### **Western blotting**

H1975 cells were treated for 6 hours with concentrations and inhibitors indicated in the figure legend. Cells were collected and lysed with lysis buffer (5M NaCl, 1M TRIS pH 8.0, 10% SDS, 10% Triton X-100 and a tablet of protease inhibitors) and processed for Western blotting analysis. Primary antibodies used; phospho-EGFR (Tyr1068; #2234, 1:1,000), EGFR (#4267; 1:1,000 or 1:2000), phospho-AKT (Ser473; #4060, 1:1,000), AKT (#9272, 1:1,000), phospho-ERK1/2 (Thr202/Tyr204; #4370, 1:1,000), and ERK1/2 (#4695, 1:1,000) antibodies; were purchased from Cell Signaling Technology. Secondary Goat anti-rabbit IgG starbright blue 700 and Anti-tubulin hFAB Rhodamine Tubulin were purchased from Bio-rad.

### **MTT Antiproliferative Assay**

Cells were seeded at a density of  $6 \times 10^4$  cells/ml or  $8 \times 10^4$  cells/ml in a clear 96-well plate and incubated for 24 hours at 37 °C. Cells were treated with different concentrations of desired drugs for 72 hours. Media was sucked out and 1X MTT working solution was added to each well. The plates were incubated for 4 hours, and the converted dye was dissolved using MTT solubilization solution. The absorbance was measured at 570 nm and reference wavelength at 650 nm using a microplate reader. MTT cell proliferation Assay Kit was purchased from OZ Biosciences.

### **Metabolic stability in Human Liver Microsomes (HLM)**

Pooled liver microsomes from humans (male) were purchased from *Sekisui XenoTech, LLC*, Kansas City, KS, USA. Metabolic stability assays were performed in the presence of an NADPH-regenerating system consisting of 5 mM glucose-6-phosphate, 5 U/mL glucose-6-phosphate dehydrogenase, and 1 mM NADP<sup>+</sup>. Liver microsomes (20 mg/mL), NADPH-regenerating system, and 4 mM MgCl<sub>2</sub>·6 H<sub>2</sub>O in 0.1 M TRIS-HCl-buffer (pH 7.4) were preincubated for 5 min at 37 °C and 750 rpm on a shaker. The reaction was started by adding the preheated compound at 10 mM resulting in a final concentration of 0.1 mM. The reaction was quenched at selected time points (0, 10, 20, 30, 60, and 120 min) by pipetting 100 µL of internal standard (ketoprofen) at a concentration of 150 µM in acetonitrile. The samples were vortexed for 30 s and centrifuged (21910 relative centrifugal force, 4 °C, 20 min). The supernatant was used directly for LC-MS analysis. All compound incubations were conducted at least in triplicates. Additionally, a negative control containing BSA (20 mg/mL) instead of liver microsomes and a positive control using verapamil instead of compound were performed. A limit of 1% organic solvent during incubation was not exceeded. Sample separation and detection were performed on an *Alliance 2695 Separations Module* HPLC system (*Waters Corporation*, Milford, MA, USA) equipped with a *Phenomenex Kinetex 2.6 µm XB-C18 100 Å 50 x 3 mm* column (*Phenomenex Inc.*, Torrance, CA, USA) coupled to an *Alliance 2996 Photodiode Array Detector* and a *MICROMASS QUATTRO micro API* mass spectrometer (both *Waters Corporation*, Milford, MA, USA) using electrospray ionization in positive mode. Mobile phase A: 90% water, 10% acetonitrile and additionally 0.1% formic acid (v/v), mobile phase B: 100% acetonitrile with additionally 0.1% formic acid (v/v). The gradient was set to: 0-2.5 min 0% B, 2.5-10 min from 0 to 40% B, 10-12 min 40% B, 12.01-15 min from 40 to 0% B at a flow rate of 0.7 mL/min. Samples were maintained at 10 °C, the column temperature was set to 20 °C with an injection volume of 5 µL. Spray, cone, extractor, and RF lens voltages were at 4 kV, 30 V, 8 V and 2 V, respectively. The source and desolvation temperatures

were set to 120 °C and 350 °C, respectively, and the desolvation gas flow was set to 750 L/h. Data analysis was conducted using *MassLynx 4.1* software (*Waters Corporation*, Milford, MA, USA).

## Chemistry

### General Information

All starting materials, reagents, and (anhydrous) solvents were commercially available and were used as received without any further purification or drying procedures unless otherwise noted. All NMR spectra were obtained with Bruker Avance 200 MHz / 400 MHz spectrometers, Bruker Ascend 400 MHz or with a Bruker Avance 600 MHz spectrometer (NMR Department, Institute of Organic Chemistry, Eberhard-Karls-Universität Tübingen). Solvents for NMR are noted in the experimental procedures for each compound. Residual solvent peaks were used to calibrate the chemical shifts. Chemical shifts ( $\delta$ ) are reported in parts per million. Mass spectra were obtained by Advion TLC-MS (ESI), from the MASS Spectrometry Department (ESI-HRMS), Institute of Organic Chemistry, Eberhard-Karls-Universität Tübingen or by TripleTOF 5600+ MS, Institute of Pharmaceutical Sciences, Pharmaceutical (Bio-)Analysis, University of Tübingen (see below for specifications). The purity of the tested compounds was determined via HPLC analysis on an Agilent 1100 Series LC with a Phenomenex Luna C8 column (150 × 4.6 mm, 5  $\mu$ m), and detection was performed with a UV diode array detector (DAD) at 254 and 230 nm wavelengths and was >95%. Elution was carried out with the following gradient: 0.01 M KH<sub>2</sub>PO<sub>4</sub>, pH 2.30 (solvent A), and MeOH (solvent B), 40% B to 85% B in 8 min, 85% B for 5 min, 85% to 40% B in 1 min, 40% B for 2 min, stop time of 16 min, 5  $\mu$ L injection volume, flow rate of 1.5 mL/min, and 25 °C oven temperature. Thin-layer chromatography (TLC) analyses were performed on fluorescent silica gel 60 F254 plates (Merck) and visualized via UV illumination at 254 and 366 nm. Column chromatography was performed either on DAVISIL LC60A 20–45  $\mu$ m silica from Grace Davison or on LiChroprep RP-18 40–63  $\mu$ m from Merck as the stationary phase and Geduran Si60 63–200  $\mu$ m silica from Merck for the precolumn. using an Interchim PuriFlash XS 420 automated flash chromatography system. Chromatographic purification was performed via gradient flash chromatography, if not stated otherwise, and the final mixture of the mobile phase is stated in the procedures.

### HRMS

An Agilent (Waldbronn, Germany) 1290 UHPLC system was used comprising of a binary pump (G4220A), a thermostated column compartment (G1316C) and a PAL HTC-xt Autosampler (CTC Analytics, Zwingen, Switzerland) coupled to a TripleTOF 5600+ MS-instrument (Sciex, Ontario, Canada) with a DuoSpray Ion Source operated in positive electrospray ionization mode. Data was acquired in Sequential Window Acquisition of all Theoretical Mass Spectra (SWATH-MS) mode, consisting of a MS1 full scan and various SWATH experiments (MS2). For full scan an accumulation time of 50 ms, collision energy of 10 V and a scan range of 50–1000 m/z were used. Twelve SWATH windows, each 25 Da wide, starting from 500 m/z spanned the area 500–800 m/z for precursor selection. The MS/MS experiments utilized an accumulation time of 50 ms and rolling collision energy with a collision energy spread (CES) of 15 V. For all MS experiments a declustering potential (DP) of 80 V, curtain gas (CUR) 30 psi, nebulizing gas (GS1) 50 psi, heater gas (GS2) 40 psi, a source temperature of 550 °C and an ion spray voltage floating (ISVF) of 4500 V were used. A Kinetex C8 column (50 × 3.0 mm, 2.6  $\mu$ m) from Phenomenex (Torrance, USA) was used. Mobile phase A consisted of water with 0.1% (v/v) formic acid and mobile phase B of

acetonitrile with 0.1% (v/v) formic acid. The column temperature was kept at 40 °C and flow rate was set to 0.5 mL/min. Gradient profile was 10-100 % mobile phase B in 13 min followed by six column volumes wash and eight column volumes re-equilibration. Samples were diluted to a concentration of 0.1 mg/mL with water/ACN (9:1, v/v) and 2.5 µL were injected.

#### **2,4,5-Tribromo-1-((2-(trimethylsilyl)ethoxy)methyl)-1*H*-imidazole (S1)**

To begin, 21.4 g (70.2 mmol) of 2,4,5-tribromoimidazole was dissolved in 110 mL of THF under a nitrogen atmosphere, and the solution was cooled to 0 °C. To the solution was added 3.09 g (77.2 mmol, 60% dispersion in oil) sodium hydride portion wise while maintaining the temperature under 0 °C. To the stirred reaction mixture was added 13.2 mL (74.4 mmol) of SEM-Cl dropwise via syringe while the temperature was maintained at 0 °C. After full addition, the mixture was warmed up to ambient temperature and stirred for 2 h. To the mixture was added demineralized water and the aqueous layer was extracted several times with EtOAc. The combined organic layers were dried over Na<sub>2</sub>SO<sub>4</sub>, filtered, and solvents were removed in vacuo. The brownish yellow crude was obtained in quantitative yield (30.8 g, 70.2 mmol) and used in the next step without further purification. <sup>1</sup>H NMR (400 MHz, DMSO) δ 5.32 (s, 2H), 3.58 (t, *J* = 7.9 Hz, 2H), 0.86 (t, *J* = 7.9 Hz, 2H), -0.04 (s, 9H). <sup>13</sup>C NMR (101 MHz, DMSO) δ 119.7, 116.4, 106.3, 75.7, 66.3, 17.1, -1.5.

#### **4,5-Dibromo-2-ethoxy-1-((2-(trimethylsilyl)ethoxy)methyl)-1*H*-imidazole (S2)**

To begin, 2.00 g (4.60 mmol) **S1** was dissolved in 10 mL EtOH and 1.55 g (13.8 mmol) of KO<sup>*t*</sup>Bu was added to the solution and the mixture was stirred overnight at reflux temperature. The reaction mixture was cooled down to ambient temperature and the solvent was removed in vacuo. The residue was dissolved in EtOAc, and the organic layer was washed several times with aqueous NaHCO<sub>3</sub>. The organic phase was dried over Na<sub>2</sub>SO<sub>4</sub> and evaporated. The crude product was obtained as light-yellow oil in 96% yield (1.77 g, 4.42 mmol) and was used without further purification in the next step. <sup>1</sup>H NMR (400 MHz, CDCl<sub>3</sub>) δ 5.11 (s, 2H), 4.41 (q, *J* = 7.1 Hz, 2H), 3.57 – 3.52 (m, 2H), 1.38 (t, *J* = 7.1 Hz, 3H), 0.92 – 0.88 (m, 2H), -0.02 (s, 9H). <sup>13</sup>C NMR (101 MHz, CDCl<sub>3</sub>) δ 152.1, 111.9, 97.6, 72.2, 66.7, 66.3, 17.8, 14.7, -1.3.

#### **4-Bromo-2-ethoxy-1-((2-(trimethylsilyl)ethoxy)methyl)-1*H*-imidazole (S3)**

To begin, 1.74 g (4.35 mmol) of **S2** was dissolved in 10 mL of THF under an argon atmosphere, and the solution was cooled to -80 °C. To the solution was added 1.74 mL (4.35 mmol) of *n*-BuLi (2.5 M in *n*-hexane solution) dropwise via syringe while the temperature was maintained at -80 °C. After full addition, the reaction mixture was stirred for 15 minutes, whereupon MeOH was added, and the mixture was warmed up to ambient temperature. To the mixture was added brine, and the organic layer was separated. The aqueous layer was extracted several times with EtOAc. The combined organic layers were dried over Na<sub>2</sub>SO<sub>4</sub>, filtered and volatiles were removed in vacuo. The product was obtained as a yellow oil in quantitative yield (1.40 g, 4.35 mmol) and was used without further purification in the next step. <sup>1</sup>H NMR (400 MHz, CDCl<sub>3</sub>) δ 6.60 (s, 1H), 5.03 (s, 2H), 4.41 (q, *J* = 7.1 Hz, 2H), 3.53 – 3.47 (m, 2H), 1.37 (t, *J* = 7.1 Hz, 3H), 0.92 – 0.86 (m, 2H), -0.01 – -0.03 (m, 9H). <sup>13</sup>C NMR (101 MHz, CDCl<sub>3</sub>) δ 151.7, 113.8, 110.2, 72.7, 66.44, 66.36, 17.8, 14.7, -1.3.

***tert*-Butyl (3-(2-ethoxy-1-((2-(trimethylsilyl)ethoxy)methyl)-1*H*-imidazol-4-yl)phenyl)carbamate (S4)**

To begin, 1.00 g (3.11 mmol) of **S3**, 0.81 g (3.42 mmol) of 3-(*N*-Boc-amino)phenylboronic acid, and 3.32 g (12.5 mmol) of K<sub>3</sub>PO<sub>4</sub> trihydrate were dissolved in 32 mL of 1,4-dioxane and 8 mL of demineralized water. The solution was degassed with three cycles of evacuation and backfilling with argon. To the solution was added 36 mg (2 mol%) of P(*t*-Bu)<sub>3</sub> Pd G3, and another three cycles of evacuation and argon backfilling were carried out. The reaction mixture was warmed to 50 °C and stirred overnight. After cooling to ambient temperature, brine was added, and the aqueous layer was extracted several times with EtOAc. The combined organic layers were dried over Na<sub>2</sub>SO<sub>4</sub>, filtered, and evaporated to dryness. The crude product was purified via flash chromatography (SiO<sub>2</sub>; *n*-hexane/EtOAc 75:25) to obtain a yellowish oil in 85% yield (1.15 g, 2.65 mmol). <sup>1</sup>H NMR (400 MHz, DMSO) δ 9.28 (s, 1H), 7.88 – 7.82 (m, 1H), 7.29 – 7.25 (m, 2H), 7.24 – 7.20 (m, 1H), 7.20 – 7.17 (m, 1H), 5.10 (s, 2H), 4.41 (q, *J* = 7.0 Hz, 2H), 3.56 – 3.50 (m, 2H), 1.49 – 1.47 (m, 9H), 1.36 (t, *J* = 7.0 Hz, 3H), 0.88 – 0.83 (m, 2H), -0.04 (s, 9H). <sup>13</sup>C NMR (101 MHz, DMSO) δ 152.8, 152.0, 139.7, 134.8, 134.7, 128.5, 117.9, 116.2, 113.8, 111.9, 78.8, 72.3, 65.30, 65.27, 28.1, 17.1, 14.6, -1.4. TLC-MS (ESI<sup>+</sup>): calcd. *m/z* 433.24 for C<sub>22</sub>H<sub>35</sub>N<sub>3</sub>O<sub>4</sub>Si, found 456.5 [M + Na]<sup>+</sup>.

***tert*-Butyl (3-(5-bromo-2-ethoxy-1-((2-(trimethylsilyl)ethoxy)methyl)-1*H*-imidazol-4-yl)phenyl)carbamate (S5)**

To begin, 1.00 g (2.31 mmol) of **S4** was dissolved in 25 mL of ACN under an argon atmosphere and the solution was cooled to -30 °C. Then, 0.39 g (2.19 mmol) of *N*-bromosuccinimide dissolved in 10 mL of ACN was added dropwise to the solution, while the temperature was maintained at -30 °C. The reaction mixture was stirred for 1 h at -30 °C and then slowly warmed up to ambient temperature. To the reaction mixture was added an aqueous saturated Na<sub>2</sub>SO<sub>3</sub> solution, and the aqueous layer was extracted several times with EtOAc. The organic layers were dried over Na<sub>2</sub>SO<sub>4</sub>, filtered, and evaporated to dryness. The crude product was purified via flash chromatography (SiO<sub>2</sub>; *n*-hexane/EtOAc 70:30) to obtain a colorless oil in 77% yield (912 mg, 1.78 mmol). <sup>1</sup>H NMR (400 MHz, DMSO) δ 9.38 (s, 1H), 7.99 (s, 1H), 7.46 (d, *J* = 7.7 Hz, 1H), 7.37 (d, *J* = 7.7 Hz, 1H), 7.26 (t, *J* = 7.9 Hz, 1H), 5.15 (s, 2H), 4.43 (q, *J* = 7.0 Hz, 2H), 3.56 (t, *J* = 7.9 Hz, 2H), 1.48 (s, 9H), 1.37 (t, *J* = 7.0 Hz, 3H), 0.87 (t, *J* = 7.9 Hz, 2H), -0.03 (s, 9H). <sup>13</sup>C NMR (101 MHz, DMSO) δ 152.8, 152.1, 139.5, 133.4, 132.5, 128.4, 119.9, 116.9, 116.1, 93.9, 78.9, 71.2, 65.6, 65.4, 28.1, 17.1, 14.4, -1.4. TLC-MS (ESI<sup>+</sup>): calcd. *m/z* 511.15 for C<sub>22</sub>H<sub>34</sub>BrN<sub>3</sub>O<sub>4</sub>Si, found 533.7/535.9 [M + Na]<sup>+</sup>.

***tert*-Butyl (3-(5-(2-acetamidopyridin-4-yl)-2-ethoxy-1-((2-(trimethyl silyl)ethoxy )methyl)-1*H*-imidazol-4-yl)phenyl)carbamate (S6)**

To begin, 850 mg (1.66 mmol) of **S5**, 565 mg (2.16 mmol) of *N*-(4-(4,4,5,5-tetramethyl-1,3,2-dioxaborolan-2-yl)pyridin-2-yl)acetamide and 1.41 g (6.63 mmol) of K<sub>3</sub>PO<sub>4</sub> trihydrate were dissolved in 33 mL of 1,4-dioxane and 4.5 mL of demineralized water. The solution was degassed with three cycles of evacuation and backfilling with argon. To the solution was added 24 mg (2.5 mol%) of P(*t*-Bu)<sub>3</sub> Pd G3, and another three cycles of evacuation and argon backfilling were carried out. The reaction mixture was warmed to 55 °C and stirred overnight. After cooling to ambient temperature, brine was added, and the aqueous layer was extracted several times with EtOAc. The combined organic layers were dried over Na<sub>2</sub>SO<sub>4</sub>, filtered, and evaporated to dryness. The crude



product was purified via flash chromatography (SiO<sub>2</sub>; *n*-hexane/EtOAc 40:60) to obtain a yellowish solid in 64% yield (600 mg, 1.06 mmol). <sup>1</sup>H NMR (400 MHz, DMSO) δ 10.55 (s, 1H), 9.24 (s, 1H), 8.34 – 8.29 (m, 1H), 8.10 (s, 1H), 7.65 – 7.59 (m, 1H), 7.27 (d, *J* = 7.7 Hz, 1H), 7.06 (t, *J* = 7.9 Hz, 1H), 7.03 – 6.99 (m, 1H), 6.88 (d, *J* = 7.8 Hz, 1H), 4.99 (s, 2H), 4.47 (q, *J* = 7.0 Hz, 2H), 3.43 – 3.38 (m, 2H), 2.06 (s, 3H), 1.44 (s, 9H), 1.40 (t, *J* = 7.0 Hz, 3H), 0.83 – 0.77 (m, 2H), -0.08 (s, 9H). <sup>13</sup>C NMR (101 MHz, DMSO) δ 169.2, 152.8, 152.70, 152.67, 148.3, 139.8, 139.5, 134.4, 133.2, 128.2, 121.8, 120.7, 120.5, 116.9, 116.6, 114.4, 78.9, 70.5, 65.6, 65.4, 28.1, 23.9, 17.2, 14.6, -1.5. TLC-MS (ESI+): calcd. *m/z* 567.29 for C<sub>29</sub>H<sub>41</sub>N<sub>5</sub>O<sub>5</sub>Si, found 590.9 [M + Na]<sup>+</sup>.

***N*-(4-(4-(3-Aminophenyl)-2-ethoxy-1-((2-(trimethylsilyl)ethoxy)methyl)-1*H*-imidazol-5-yl)pyridin-2-yl)acetamide (S7)**

180 mg (0.32 mmol) of **S6** was dissolved in 13 mL of a mixture of TFA/DCM 5% v/v. The solution was stirred overnight at ambient temperature. The reaction mixture was concentrated in vacuo and to the residue was added a saturated aqueous NaHCO<sub>3</sub> solution, whereupon the aqueous layer was extracted several times with EtOAc. The combined organic layers were dried over Na<sub>2</sub>SO<sub>4</sub>, filtered, and the solvents removed in vacuo. The crude product was purified via flash chromatography (SiO<sub>2</sub>; *n*-hexane/EtOAc/MeOH 10:80:10) to give the pure product as an off-white solid in a 67% yield (100 mg, 0.21 mmol). <sup>1</sup>H NMR (400 MHz, DMSO) δ 10.54 (s, 1H), 8.35 – 8.27 (m, 1H), 8.10 (s, 1H), 7.06 – 6.98 (m, 1H), 6.87 – 6.80 (m, 1H), 6.80 – 6.77 (m, 1H), 6.46 – 6.32 (m, 2H), 5.08 – 4.86 (m, 4H), 4.46 (q, *J* = 6.9 Hz, 2H), 3.45 – 3.36 (m, 2H), 2.07 (s, 3H), 1.39 (t, *J* = 7.0 Hz, 3H), 0.83 – 0.76 (m, 2H), -0.07 (s, 9H). <sup>13</sup>C NMR (101 MHz, DMSO) δ 169.2, 152.64, 152.55, 148.5, 148.1, 140.2, 134.5, 133.9, 128.4, 121.2, 120.6, 114.8, 114.4, 112.64, 112.56, 70.4, 65.4, 65.3, 23.9, 17.2, 14.6, -1.5. TLC-MS (ESI+): calcd. *m/z* 467.24 for C<sub>24</sub>H<sub>33</sub>N<sub>5</sub>O<sub>3</sub>Si, found 489.8 [M + Na]<sup>+</sup>.

***tert*-Butyl (3-(5-(2-aminopyridin-4-yl)-2-ethoxy-1-((2-(trimethylsilyl) ethoxy) methyl)-1*H*-imidazol-4-yl)phenyl)carbamate (S8)**

To begin, 380 mg (0.67 mmol) of **S6** was dissolved in 15 mL of MeOH and aqueous 3 N NaOH solution was added. The reaction mixture was stirred at 55 °C for 5 h. After cooling down to ambient temperature, solvents were concentrated in vacuo. The oily residue was dissolved in small amounts of MeOH and the slow addition of iced water precipitated a white solid, which was collected by filtration and dried in the oven to obtain the product in 94% yield (330 mg, 0.63 mmol). <sup>1</sup>H NMR (400 MHz, DMSO) δ 9.27 (s, 1H), 7.94 (d, *J* = 5.2 Hz, 1H), 7.66 (t, *J* = 1.7 Hz, 1H), 7.28 (d, *J* = 7.7 Hz, 1H), 7.06 (t, *J* = 7.9 Hz, 1H), 6.88 – 6.84 (m, 1H), 6.46 (dd, *J* = 5.2, 1.4 Hz, 1H), 6.38 (s, 1H), 5.97 (s, 2H), 4.97 (s, 2H), 4.45 (q, *J* = 7.0 Hz, 2H), 3.46 – 3.41 (m, 2H), 1.46 (s, 9H), 1.39 (t, *J* = 7.0 Hz, 3H), 0.84 – 0.79 (m, 2H), -0.05 (s, 9H). <sup>13</sup>C NMR (101 MHz, DMSO) δ 160.2, 152.8, 152.5, 148.3, 139.4, 138.7, 134.8, 132.2, 128.1, 122.5, 120.7, 117.1, 116.5, 113.1, 109.0, 78.8, 70.4, 65.5, 65.4, 28.1, 17.3, 14.6, -1.5. TLC-MS (ESI+): calcd. *m/z* 525.28 for C<sub>27</sub>H<sub>39</sub>N<sub>5</sub>O<sub>4</sub>Si, found 548.3 [M + Na]<sup>+</sup>.

***tert*-Butyl (3-(2-ethoxy-5-(2-(phenylamino)pyridin-4-yl)-1-((2-(trimethylsilyl) ethoxy)methyl)-1*H*-imidazol-4-yl)phenyl)carbamate (S9)**

To begin, 300 mg (0.57 mmol) of **S8**, 179 mg (1.14 mmol) of bromobenzene, and 279 mg (0.86 mmol) Cs<sub>2</sub>CO<sub>3</sub> in 6 mL of a mixture of 1,4-dioxane/*t*-BuOH (4 + 1) was degassed three times by

evacuating and backfilling with argon under stirring. To the mixture was added 26 mg of BrettPhos Pd G3 (5 mol%), and another three cycles of evacuation and argon backfilling were carried out. The solution was stirred under reflux for 5 h. After cooling to ambient temperature, Celite was added to the mixture, and solvents were removed in vacuo. Purification via flash chromatography (SiO<sub>2</sub>; *n*-hexane/EtOAc 60:40) yielded 79% (270 mg, 0.45 mmol) of an off-white solid. <sup>1</sup>H NMR (400 MHz, DMSO) δ 9.29 (s, 1H), 9.02 (s, 1H), 8.20 (d, *J* = 5.1 Hz, 1H), 7.67 – 7.65 (m, 1H), 7.56 (s, 1H), 7.54 (s, 1H), 7.31 (d, *J* = 7.8 Hz, 1H), 7.23 – 7.18 (m, 2H), 7.12 (t, *J* = 7.9 Hz, 1H), 6.96 – 6.92 (m, 1H), 6.88 – 6.83 (m, 1H), 6.78 – 6.75 (m, 2H), 5.02 (s, 2H), 4.47 (q, *J* = 7.0 Hz, 2H), 3.48 – 3.42 (m, 2H), 1.44 – 1.38 (m, 12H), 0.83 – 0.79 (m, 2H), -0.07 (s, 9H). <sup>13</sup>C NMR (101 MHz, DMSO) δ 156.3, 152.73, 152.67, 147.9, 141.5, 139.5, 138.8, 134.6, 132.9, 128.5, 128.3, 122.1, 120.8, 120.5, 118.1, 117.1, 116.6, 115.2, 111.4, 78.9, 70.5, 65.52, 65.50, 28.1, 17.3, 14.6, -1.5. TLC-MS (ESI<sup>+</sup>): calcd. *m/z* 601.31 for C<sub>33</sub>H<sub>43</sub>N<sub>5</sub>O<sub>4</sub>Si, found 624.4 [M + Na]<sup>+</sup>.

#### **4-(4-(3-Aminophenyl)-2-ethoxy-1-((2-(trimethylsilyl)ethoxy)methyl)-1*H*-imidazol-5-yl)-*N*-phenylpyridin-2-amine (S10)**

250 mg (0.42 mmol) of **S9** was dissolved in 20 mL of a mixture of TFA/DCM 10% v/v. The solution was stirred overnight at ambient temperature. The reaction mixture was concentrated in vacuo and to the residue was added a saturated aqueous NaHCO<sub>3</sub> solution, and the aqueous layer was extracted several times with EtOAc. The combined organic layers were dried over Na<sub>2</sub>SO<sub>4</sub>, filtered, and volatiles were removed in vacuo. The crude product was purified via flash chromatography (SiO<sub>2</sub>; *n*-hexane/EtOAc/MeOH 40:55:5) to give the product as an off-white solid in a 67% yield (140 mg, 0.28 mmol). <sup>1</sup>H NMR (400 MHz, DMSO) δ 9.03 (s, 1H), 8.21 – 8.16 (m, 1H), 7.59 – 7.53 (m, 2H), 7.24 – 7.19 (m, 2H), 6.89 – 6.84 (m, 2H), 6.83 – 6.81 (m, 1H), 6.79 (s, 1H), 6.78 – 6.75 (m, 1H), 6.48 – 6.43 (m, 1H), 6.43 – 6.37 (m, 1H), 5.05 – 4.97 (m, 4H), 4.45 (q, *J* = 7.0 Hz, 2H), 3.47 – 3.41 (m, 2H), 1.39 (t, *J* = 7.0 Hz, 3H), 0.83 – 0.79 (m, 2H), -0.07 (s, 9H). <sup>13</sup>C NMR (101 MHz, DMSO) δ 156.2, 152.6, 148.6, 147.8, 141.5, 139.2, 134.7, 133.6, 128.6, 128.5, 121.6, 120.5, 118.1, 115.3, 114.9, 112.7, 112.5, 111.4, 70.4, 65.5, 65.4, 17.3, 14.6, -1.5. TLC-MS (ESI<sup>+</sup>): calcd. *m/z* 501.26 for C<sub>28</sub>H<sub>35</sub>N<sub>5</sub>O<sub>2</sub>Si, found 624.4 [M + Na]<sup>+</sup>.

#### **Methyl 2-fluoro-6-methylbenzoate (S11)**

To begin, 750 mg (4.86 mmol) 2-fluoro-6-methylbenzoic acid was dissolved in 10 mL of MeOH and five drops of conc. H<sub>2</sub>SO<sub>4</sub> was added. Refluxing over 48 h led to complete conversion. After cooling to ambient temperature, saturated aqueous NaHCO<sub>3</sub> was added, and the aqueous layer was extracted with EtOAc. The combined organic layers were dried over Na<sub>2</sub>SO<sub>4</sub>, filtered and volatiles were removed in vacuo to obtain the product in 77% yield (630 mg, 3.74 mmol) as a white amorphous solid. <sup>1</sup>H NMR (200 MHz, DMSO) δ 7.52 – 7.34 (m, 1H), 7.21 – 7.05 (m, 2H), 3.87 (s, 3H), 2.32 (s, 3H). <sup>13</sup>C NMR (50 MHz, DMSO) δ 165.4, 159.1 (d, *J* = 248.0 Hz), 138.2 (d, *J* = 2.5 Hz), 131.8 (d, *J* = 9.0 Hz), 126.4 (d, *J* = 3.0 Hz), 121.1 (d, *J* = 16.0 Hz), 113.2 (d, *J* = 21.4 Hz), 52.5, 19.0 (d, *J* = 2.2 Hz).

#### **Methyl 2-(bromomethyl)-6-fluorobenzoate (S12)**

To begin, 590 mg (3.51 mmol) **S11** was dissolved in 8 mL of CCl<sub>4</sub> and the temperature was set to refluxing conditions. 656 mg (3.68 mmol) *N*-bromosuccinimide and 34 mg (0.35 mmol) of AIBN were added in one portion and the mixture was refluxed overnight. After cooling down to ambient temperature, the solvent was removed in vacuo and the residue was purified via flash chromatography (SiO<sub>2</sub>, *n*-hexane/EtOAc 90:10) to obtain the product in 75% yield (620 mg, 2.63 mmol) as colorless oil. <sup>1</sup>H NMR (200 MHz, DMSO) δ 7.63 – 7.50 (m, 1H), 7.46 – 7.40 (m, 1H), 7.38 – 7.27 (m, 1H), 4.78 (s, 2H), 3.91 (s, 3H). <sup>13</sup>C NMR (50 MHz, DMSO) δ 164.3, 159.3 (d, *J* = 250.5 Hz), 138.4 (d, *J* = 2.5 Hz), 132.8 (d, *J* = 9.3 Hz), 126.8 (d, *J* = 3.1 Hz), 120.6 (d, *J* = 16.2 Hz), 116.5 (d, *J* = 22.0 Hz), 52.8, 30.3 (d, *J* = 2.6 Hz).

### **Methyl 2-((1,3-dioxoisindolin-2-yl)methyl)-6-fluorobenzoate (S13)**

To begin, 580 mg (2.36 mmol) **S12** and 458 mg (2.47 mmol) potassium phthalimide were suspended in 5 mL of DMF and stirred at ambient temperature for 48 h. Thereupon, the solvent was removed in vacuo and the residue was precipitated in *n*-hexane and filtered. The residue was redissolved in EtOAc and brine was added. Layers were separated, and the aqueous phase was extracted several times with EtOAc. The combined organic layers were dried over Na<sub>2</sub>SO<sub>4</sub>, filtered and solvents were removed in vacuo to yield 72% (530 mg, 1.66 mmol) of a crude product as yellow solid that was used without further purification in the next step. <sup>1</sup>H NMR (200 MHz, DMSO) δ 7.94 – 7.80 (m, 4H), 7.57 – 7.44 (m, 1H), 7.34 – 7.15 (m, 2H), 4.88 (s, 2H), 3.86 (s, 3H). <sup>13</sup>C NMR (50 MHz, DMSO) δ 167.5, 164.7, 159.2 (d, *J* = 249.6 Hz), 136.8 (d, *J* = 1.9 Hz), 134.6, 132.6 (d, *J* = 9.2 Hz), 131.5, 124.1 (d, *J* = 3.0 Hz), 123.3, 119.9 (d, *J* = 16.5 Hz), 115.2 (d, *J* = 21.7 Hz), 52.8, 38.5 (d, *J* = 2.4 Hz). TLC-MS (ESI<sup>+</sup>): calcd. *m/z* 313.08 for C<sub>17</sub>H<sub>12</sub>FNO<sub>4</sub>, found 336.1 [M+Na]<sup>+</sup>.

### **Methyl 2-fluoro-6-((1-oxoisindolin-2-yl)methyl)benzoate (S14)**

To begin, 210 mg (0.67 mmol) **S13** was suspended in 3 mL acetic acid and 3 mL concentrated hydrochloric acid and warmed up to 40 °C. 397 mg (3.35 mmol) of tin powder was added portion wise over 4 h under stirring at 40 °C until complete conversion via TLC was indicated. The reaction mixture was cooled down to ambient temperature and the aqueous layer was extracted several times with DCM. The combined organic layers were dried over Na<sub>2</sub>SO<sub>4</sub>, solvents were removed in vacuo and the residue was purified via flash chromatography (SiO<sub>2</sub>; *n*-hexane/EtOAc 60:40). The product was obtained as colorless oil in 95% yield (190 mg, 0.63 mmol). <sup>1</sup>H NMR (200 MHz, CDCl<sub>3</sub>) δ 7.92 – 7.84 (m, 1H), 7.60 – 7.44 (m, 2H), 7.43 – 7.31 (m, 2H), 7.21 – 7.14 (m, 1H), 7.11 – 7.00 (m, 1H), 4.90 (s, 2H), 4.29 (s, 2H), 3.93 (s, 3H). <sup>13</sup>C NMR (50 MHz, CDCl<sub>3</sub>) δ 168.8, 165.7, 160.3 (d, *J* = 252.9 Hz), 141.5, 138.1 (d, *J* = 1.9 Hz), 132.4 (d, *J* = 1.7 Hz), 132.2, 131.7, 128.2, 125.0 (d, *J* = 3.3 Hz), 124.1, 123.0, 121.2 (d, *J* = 16.0 Hz), 115.5 (d, *J* = 22.0 Hz), 52.9, 49.9, 43.7 (d, *J* = 2.4 Hz). TLC-MS (ESI<sup>+</sup>): calcd. *m/z* 299.10 for C<sub>17</sub>H<sub>14</sub>FNO<sub>3</sub>, found 322.3 [M+Na]<sup>+</sup>.

### **2-Fluoro-6-((1-oxoisindolin-2-yl)methyl)benzoic acid (S15)**

To begin, 180 mg (0.60 mmol) of **S14** was dissolved in 3 mL THF and 6 mL of an aqueous 3 N NaOH solution was added. The reaction mixture was stirred for 15 h at 50 °C. After cooling down to ambient temperature, EtOAc was added and the layers were separated. The aqueous layer was acidified with 1 N HCl precipitating a white solid, which was collected by filtration, washed with small amounts of an iced aqueous 0.1 N HCl and dried in the oven. The product was obtained as



white solid in 73% (125 mg, 0.44 mmol) yield.  $^1\text{H}$  NMR (200 MHz, DMSO)  $\delta$  13.71 (s, 1H), 7.82 – 7.38 (m, 5H), 7.34 – 7.18 (m, 1H), 7.16 – 6.99 (m, 1H), 4.82 (s, 2H), 4.36 (s, 2H). TLC-MS (ESI-): calcd.  $m/z$  285.08 for  $\text{C}_{16}\text{H}_{12}\text{FNO}_3$ , found 284.3  $[\text{M}-\text{H}]^-$ .

### Methyl 3-hydroxy-2-methylbenzoate (S16)

To begin, 3.80 g (25.0 mmol) 3-hydroxy-2-methylbenzoic acid was dissolved in 50 mL of MeOH and few drops of conc.  $\text{H}_2\text{SO}_4$  were added. The reaction mixture was refluxed for 48 h until complete conversion. After cooling to ambient temperature, the solvent was evaporated, saturated aqueous  $\text{NaHCO}_3$  was added, and the aqueous layer was extracted several times with EtOAc. The combined organic layers were dried over  $\text{Na}_2\text{SO}_4$ , filtered and volatiles were removed in vacuo. The product was obtained as amorphous solid in 93% (3.84 g, 23.1 mmol) yield.  $^1\text{H}$  NMR (200 MHz,  $\text{CDCl}_3$ )  $\delta$  7.41 (d,  $J = 7.7$  Hz, 1H), 7.10 (t,  $J = 7.7$  Hz, 1H), 6.94 (d,  $J = 7.8$  Hz, 1H), 5.48 (bs, 1H), 3.90 (s, 3H), 2.45 (s, 3H).  $^{13}\text{C}$  NMR (50 MHz,  $\text{CDCl}_3$ )  $\delta$  168.9, 154.6, 131.9, 126.3, 125.7, 122.7, 118.6, 52.2, 12.7.

### Methyl 3-acetoxy-2-methylbenzoate (S17)

To begin, 3.84 g (23.1 mmol) **S16** was dissolved in 45 mL dry THF. 9.66 mL (69.3 mmol) TEA, 2.40 mL (25.4 mmol) acetic anhydride and 282 mg (2.31 mmol) 4-dimethylaminopyridine were added. The mixture was stirred overnight at ambient temperature. Brine was added and the aqueous layer was extracted several times with EtOAc. Combined organic layers were dried over  $\text{Na}_2\text{SO}_4$ , filtered and solvents were removed in vacuo. The product was obtained in 93% (4.48 g, 21.5 mmol) yield as colorless oil.  $^1\text{H}$  NMR (200 MHz,  $\text{CDCl}_3$ )  $\delta$  7.77 (dd,  $J = 7.6, 1.6$  Hz, 1H), 7.25 (t,  $J = 7.8$  Hz, 1H), 7.17 (dd,  $J = 8.0, 1.6$  Hz, 1H), 3.89 (s, 3H), 2.39 (s, 3H), 2.34 (s, 3H).  $^{13}\text{C}$  NMR (50 MHz,  $\text{CDCl}_3$ )  $\delta$  169.2, 167.7, 149.9, 132.3, 131.9, 128.3, 126.3, 125.9, 52.2, 20.9, 13.5. TLC-MS (ESI+): calcd.  $m/z$  208.07 for  $\text{C}_{11}\text{H}_{12}\text{O}_4$ , found 231.3  $[\text{M}+\text{Na}]^+$ .

### Methyl 3-acetoxy-2-(bromomethyl)benzoate (S18)

To begin, 3.45 g (16.6 mmol) **S17** was dissolved in 16 mL of  $\text{CCl}_4$  and the temperature was set to refluxing conditions. 3.00 g (16.9 mmol) *N*-bromosuccinimide and 272 mg (1.66 mmol) of AIBN were added in one portion and the mixture was stirred overnight under refluxing conditions. After cooling down to ambient temperature, the solvent was removed in vacuo and the residue was precipitated in *n*-hexane and collected by filtration. The crude product was obtained in quantitative yield (4.85 g 16.6 mmol) as pale brown solid.  $^1\text{H}$  NMR (400 MHz, DMSO)  $\delta$  7.77 (dd,  $J = 7.8, 1.3$  Hz, 1H), 7.53 (t,  $J = 8.0$  Hz, 1H), 7.45 (dd,  $J = 8.2, 1.3$  Hz, 1H), 4.91 (s, 2H), 3.88 (s, 3H), 2.37 (s, 3H).  $^{13}\text{C}$  NMR (101 MHz, DMSO)  $\delta$  168.6, 166.1, 149.5, 130.7, 130.4, 129.5, 128.0, 127.5, 52.5, 24.3, 20.7. TLC-MS (ESI+): calcd.  $m/z$  285.98 for  $\text{C}_{11}\text{H}_{11}\text{BrO}_4$ , found 309.5/311.4  $[\text{M}+\text{Na}]^+$ .

### Methyl 3-acetoxy-2-((1,3-dioxoisindolin-2-yl)methyl)benzoate (S19)

To begin, 4.05 g (14.1 mmol) **S18** and 2.61 g (14.1 mmol) potassium phthalimide were suspended in 17 mL of DMF and stirred at ambient temperature for 48 h. Iced water was added to the mixture under precipitation of a white solid, which was collected by filtration and dried in the oven. The crude product was obtained as white solid in 94% (4.68 g, 13.3 mmol) yield.  $^1\text{H}$  NMR (400 MHz, DMSO)  $\delta$  7.85 – 7.78 (m, 4H), 7.66 (dd,  $J = 7.8, 1.2$  Hz, 1H), 7.47 (t,  $J = 7.9$  Hz, 1H), 7.32 (dd,  $J$

= 8.1, 1.1 Hz, 1H), 5.11 (s, 2H), 3.88 (s, 3H), 2.25 (s, 3H). <sup>13</sup>C NMR (101 MHz, DMSO) δ 169.7, 167.8, 167.7, 150.5, 135.0, 134.4, 131.8, 129.5, 128.3, 127.5, 127.0, 123.5, 53.0, 33.3, 21.4.

### 3-Hydroxy-2-((1-oxoisindolin-2-yl)methyl)benzoic acid (S20)

To begin, 4.13 g (11.7 mmol) **S19** was suspended in 25 mL acetic acid and 25 mL concentrated hydrochloric acid and warmed up to 80 °C. 5.55 g (46.8 mmol) of tin powder was added in one portion and the mixture was stirred overnight at 80 °C. The reaction mixture was cooled down to ambient temperature, whereupon the addition of cold 0.1 N HCl precipitated a white solid, which was collected by filtration, washed with aq. 0.1 N HCl and dried in the oven. The product was obtained as white solid in 73% (2.41 g, 8.51 mmol) yield. <sup>1</sup>H NMR (400 MHz, DMSO) δ 13.03 (s, 1H), 10.03 (s, 1H), 7.67 (d, *J* = 7.5 Hz, 1H), 7.56 – 7.50 (m, 2H), 7.48 – 7.43 (m, 1H), 7.29 – 7.23 (m, 2H), 7.07 – 7.01 (m, 1H), 4.97 (s, 2H), 4.24 (s, 2H). <sup>13</sup>C NMR (101 MHz, DMSO) δ 169.5, 167.9, 157.2, 142.4, 134.7, 132.7, 131.6, 129.3, 128.2, 123.9, 123.0, 122.4, 120.9, 119.2, 49.9, 38.2. TLC-MS (ESI-): calcd. *m/z* 283.08 for C<sub>16</sub>H<sub>13</sub>NO<sub>4</sub>, found 282.4 [M-H]<sup>-</sup>.

### 3-Acetoxy-2-((1-oxoisindolin-2-yl)methyl)benzoic acid (S21)

To begin, 2.18 g (7.70 mmol) **S20** was dissolved in 10 mL dry THF. 3.22 mL (23.1 mmol) TEA, 0.76 mL (8.09 mmol) acetic anhydride and 94 mg (0.77 mmol) 4-dimethylaminopyridine were added. The mixture was stirred overnight at ambient temperature until complete conversion. Iced aqueous 0.1 N HCl was added under precipitation of a white solid, which was collected by filtration and dried in the oven. The product was obtained as white solid in 96% (2.40 g, 7.38 mmol) yield. <sup>1</sup>H NMR (400 MHz, DMSO) δ 13.47 (s, 1H), 7.76 (dd, *J* = 7.8, 1.2 Hz, 1H), 7.70 (d, *J* = 7.5 Hz, 1H), 7.57 – 7.44 (m, 4H), 7.33 (dd, *J* = 8.0, 1.1 Hz, 1H), 5.00 (s, 2H), 4.12 (s, 2H), 2.20 (s, 3H). <sup>13</sup>C NMR (101 MHz, DMSO) δ 169.3, 168.2, 166.8, 150.4, 141.7, 134.2, 131.9, 131.3, 129.1, 128.7, 127.8, 127.5, 126.7, 123.4, 122.7, 48.6, 37.0, 20.8. TLC-MS (ESI+): calcd. *m/z* 325.10 for C<sub>18</sub>H<sub>15</sub>NO<sub>5</sub>, found 348.6 [M+Na]<sup>+</sup>.

### 1-(4-Bromophenyl)piperazine (S22)

(Adapted from procedures described by Cong Liu J.; et al)<sup>53</sup> To begin, 1.60 g (9.86 mmol) of phenylpiperazine was dissolved in 10 mL of DMSO and 10 mL of aqueous HBr (~48%) solution was added. The mixture was stirred for 2 h at 60 °C. The reaction mixture was cooled down to 0 °C and neutralized by the addition of an aqueous 3 N NaOH solution under precipitation of a solid, which was collected by filtration, washed with cold, aqueous 0.1 N NaOH solution and dried in the oven to yield 87% (2.08 g, 8.61 mmol) of the crude product, which was used without further purification in the next step. <sup>1</sup>H NMR (200 MHz, DMSO) δ 7.31 (d, *J* = 6.9 Hz, 2H), 6.85 (d, *J* = 6.7 Hz, 2H), 3.09 – 2.70 (m, 9H). <sup>13</sup>C NMR (50 MHz, DMSO) δ 150.8, 131.4, 117.1, 109.7, 49.0, 45.5.

### *tert*-Butyl 4-(4-bromophenyl)piperazine-1-carboxylate (S23)

To begin, 2.00 g (8.29 mmol) of **S22** was dissolved in DCM and 2.30 mL (16.6 mmol) of TEA was added. 1.90 g (8.71 mmol) of di-*tert*-butyl dicarbonate was added and the mixture was stirred overnight at ambient temperature. The solvent was removed in vacuo and the addition of *n*-hexane and diethylether precipitated a white solid, which was collected by filtration and dried in the oven. The crude product was obtained in 88% (2.50 g, 7.32 mmol) yield and was used without further

purification in the next step.  $^1\text{H}$  NMR (400 MHz, DMSO)  $\delta$  7.35 (d,  $J$  = 8.8 Hz, 2H), 6.90 (d,  $J$  = 8.9 Hz, 2H), 3.49 – 3.40 (m, 4H), 3.12 – 3.04 (m, 4H), 1.41 (s, 9H).  $^{13}\text{C}$  NMR (101 MHz, DMSO)  $\delta$  153.8, 150.0, 131.5, 117.8, 110.4, 79.0, 47.9, 42.9, 28.0.

#### **4-(2-(Methylthio)-4-(3-nitrophenyl)-1-((2-(trimethylsilyl)ethoxy)methyl)-1H-imidazol-5-yl)pyridin-2-amine (S24)**

To begin, 2.75 g (5.50 mmol) of *N*-(4-(2-(methylthio)-4-(3-nitrophenyl)-1-((2-(trimethylsilyl)ethoxy)methyl)-1H-imidazol-5-yl)pyridin-2-yl)acetamide<sup>32</sup> was dissolved in 55 mL of MeOH and 5 mL aqueous 3 N NaOH solution was added. The reaction mixture was stirred at 60 °C for 3 h. After cooling down to ambient temperature, solvents were removed in vacuo. The oily residue was dissolved in small amounts of MeOH and the slow addition of iced water precipitated a yellowish solid, which was collected by filtration and dried in the oven to obtain the product in quantitative yield (2.60 g, 5.50 mmol).  $^1\text{H}$  NMR (400 MHz,  $\text{CDCl}_3$ )  $\delta$  8.51 (t,  $J$  = 1.9 Hz, 1H), 8.13 – 8.10 (m, 1H), 8.02 (ddd,  $J$  = 8.2, 2.2, 0.9 Hz, 1H), 7.71 – 7.68 (m, 1H), 7.35 (t,  $J$  = 8.0 Hz, 1H), 6.64 (dd,  $J$  = 5.3, 1.3 Hz, 1H), 6.56 – 6.54 (m, 1H), 5.13 (s, 2H), 4.70 (s, 2H), 3.58 – 3.54 (m, 2H), 2.74 (s, 3H), 0.94 – 0.89 (m, 2H), -0.01 (s, 9H).  $^{13}\text{C}$  NMR (101 MHz,  $\text{CDCl}_3$ )  $\delta$  159.2, 149.2, 148.7, 146.4, 139.6, 137.2, 135.8, 132.8, 129.6, 129.2, 122.1, 121.7, 115.4, 109.7, 73.1, 66.9, 18.1, 16.2, -1.3. TLC-MS (ESI+): calcd  $m/z$  457.16 for  $\text{C}_{21}\text{H}_{27}\text{N}_5\text{O}_3\text{SSi}$ , found 458.2  $[\text{M}+\text{H}]^+$ .

#### ***tert*-Butyl 4-(4-((4-(2-(methylthio)-4-(3-nitrophenyl)-1-((2-(trimethylsilyl)ethoxy)methyl)-1H-imidazol-5-yl)pyridin-2-yl)amino)phenyl)piperazine-1-carboxylate (S25)**

To begin, 1.00 g (2.19 mmol) of **S24**, 783 mg (2.29 mmol) of **S23**, and 2.49 g (7.65 mmol)  $\text{Cs}_2\text{CO}_3$  in 15 mL of a mixture of 1,4-dioxane/*t*-BuOH (4 + 1) was degassed three times by evacuating and backfilling with argon under stirring. To the mixture was added 99 mg of BrettPhos Pd G3 (5 mol%), and another three cycles of evacuation and argon backfilling were carried out. The solution was stirred under reflux for 3 h. After cooling to ambient temperature, Celite was added to the mixture, and solvents were removed in vacuo. Purification via flash chromatography ( $\text{SiO}_2$ ; *n*-hexane/EtOAc/MeOH 55:40:5) yielded 86% (1.35 g, 2.19 mmol) of a yellow solid.  $^1\text{H}$  NMR (400 MHz, DMSO)  $\delta$  8.90 (s, 1H), 8.33 (s, 1H), 8.25 – 8.21 (m, 1H), 8.07 (dd,  $J$  = 8.1, 1.8 Hz, 1H), 7.80 (d,  $J$  = 7.9 Hz, 1H), 7.59 (t,  $J$  = 8.0 Hz, 1H), 7.42 (d,  $J$  = 8.9 Hz, 2H), 6.87 (d,  $J$  = 8.9 Hz, 2H), 6.74 – 6.69 (m, 2H), 5.15 (s, 2H), 3.48 – 3.39 (m, 6H), 3.03 – 2.95 (m, 4H), 2.70 (s, 3H), 1.42 (s, 9H), 0.82 – 0.75 (m, 2H), -0.08 (s, 9H).  $^{13}\text{C}$  NMR (101 MHz, DMSO)  $\delta$  156.9, 153.8, 148.7, 148.0, 145.9, 145.5, 137.9, 135.5, 135.4, 133.8, 132.3, 130.1, 129.7, 121.4, 120.5, 120.2, 116.9, 114.3, 110.5, 78.9, 72.7, 65.8, 49.3, 28.1, 24.9, 17.2, 15.4, -1.5. TLC-MS (ESI+): calcd.  $m/z$  717.31 for  $\text{C}_{36}\text{H}_{47}\text{N}_7\text{O}_5\text{SSi}$ , found 740.5  $[\text{M}+\text{Na}]^+$ .

#### ***tert*-Butyl 4-(4-((4-(3-aminophenyl)-2-(methylthio)-1-((2-(trimethylsilyl)ethoxy)methyl)-1H-imidazol-5-yl)pyridin-2-yl)amino)phenyl)piperazine-1-carboxylate (S26)**

1.30 g (1.81 mmol) of **S25**, 506 mg (9.05 mmol) iron powder, and 969 mg (18.1 mmol) ammonium chloride were suspended in a mixture of THF/MeOH/ $\text{H}_2\text{O}$  (5:2:1, 18 mL). The mixture was vigorously stirred at 50 °C for 1 h. Then, 1 mL of 0.1 N aqueous HCl was added, and the mixture was stirred for another 1 h at 50 °C. Thereupon, the reaction mixture was cooled to ambient temperature and filtered through a pad of Celite. To the filtrate, 0.1 N aqueous NaOH was added,

and the aqueous layer was extracted several times with EtOAc. The organic layer was dried over Na<sub>2</sub>SO<sub>4</sub>, filtered and concentrated in vacuo. Purification via flash chromatography (SiO<sub>2</sub>; *n*-hexane/EtOAc/MeOH 40:55:5) yielded 84% (1.05 g, 1.53 mmol) of a yellow-brownish solid. <sup>1</sup>H NMR (400 MHz, DMSO) δ 8.81 (s, 1H), 8.17 – 8.13 (m, 1H), 7.41 – 7.36 (m, 2H), 6.90 – 6.83 (m, 4H), 6.68 – 6.65 (m, 2H), 6.52 – 6.41 (m, 2H), 5.15 – 5.01 (m, 4H), 3.46 – 3.43 (m, 4H), 3.41 – 3.37 (m, 2H), 3.00 – 2.96 (m, 4H), 2.64 – 2.62 (m, 3H), 1.42 (s, 9H), 0.80 – 0.75 (m, 2H), -0.08 – -0.10 (m, 9H). <sup>13</sup>C NMR (101 MHz, DMSO) δ 156.6, 153.8, 148.6, 148.1, 145.7, 144.1, 139.1, 138.8, 134.3, 134.0, 128.6, 127.9, 119.9, 116.9, 114.8, 114.6, 112.71, 112.66, 110.7, 78.9, 72.5, 65.6, 49.4, 28.1, 17.2, 15.6, -1.5. TLC-MS (ESI<sup>+</sup>): calcd. *m/z* 687.34 for C<sub>36</sub>H<sub>49</sub>N<sub>7</sub>O<sub>3</sub>SSi, found 688.6 [M+H]<sup>+</sup>.

#### 4-Bromo-5-chloropyridin-2-amine (S27)

(Adapted from Xie, Dongsheng; et al)<sup>54</sup> To begin, 2.20 g (12.7 mmol) of 4-bromopyridin-2-amine was suspended in 40 mL of ACN and the suspension was cooled down to -30 °C. 1.72 g (12.8 mmol) *N*-chlorosuccinimide dissolved via ultrasonication in 20 mL of ACN was added dropwise and the mixture was stirred overnight at ambient temperature. The solvent was removed in vacuo and the residue was dissolved in MeOH. The addition of cold, aqueous 1 N NaOH solution precipitated a brown solid, which was collected by filtration, washed with water and dried in the oven. The crude product was obtained in 97% yield (2.55 g, 12.3 mmol) and used without further purification in the next step. <sup>1</sup>H NMR (400 MHz, DMSO) δ 8.00 (s, 1H), 6.81 (s, 1H), 6.42 (s, 2H). <sup>13</sup>C NMR (101 MHz, DMSO) δ 159.2, 147.3, 131.4, 117.2, 111.4.

#### *N*-(4-Bromo-5-chloropyridin-2-yl)acetamide (S28)

To begin, 2.50 g (12.1 mmol) of **S27** was dissolved in ACN and 1.25 mL (13.26 mmol) of acetic anhydride and 147 mg (1.21 mmol) of 4-dimethylaminopyridine was added. The mixture was stirred overnight at 80 °C. After the reaction mixture was cooled down to ambient temperature, brine was added, and the aqueous layer was extracted several times with EtOAc. Combined organic layers were dried over Na<sub>2</sub>SO<sub>4</sub>, filtered and solvents were removed in vacuo. The crude product was purified via flash chromatography (SiO<sub>2</sub>; *n*-hexane/EtOAc 70:30) to obtain a white solid in 30% (900 mg, 3.61 mmol) yield. <sup>1</sup>H NMR (400 MHz, DMSO) δ 10.86 (s, 1H), 8.48 (s, 2H), 2.10 (s, 3H). <sup>13</sup>C NMR (101 MHz, DMSO) δ 169.8, 151.1, 147.6, 132.8, 125.2, 117.1, 23.9.

#### *N*-(5-Chloro-4-(4,4,5,5-tetramethyl-1,3,2-dioxaborolan-2-yl)pyridin-2-yl)acetamide (S29)

To begin, 830 mg (3.33 mmol) of **S28**, 845 mg (3.33 mmol) bis(pinacolato)diboron and 980 mg (9.98 mmol) KOAc were suspended in 30 mL of 1,4-dioxane under an argon atmosphere. The suspension was degassed with three cycles of evacuation and backfilling with argon, followed by the addition of 122 mg (5 mol%) of Pd(dppf)Cl<sub>2</sub> and another three cycles of degassing. The reaction mixture was heated to 100 °C and stirred overnight. Thereupon, the reaction mixture was cooled down to ambient temperature and filtered through a pad of Celite. The filtrate was concentrated, and the residue was precipitated in *n*-hexane. The crude, brown product was obtained in 60% (596 mg, 2.01 mmol) yield after filtration and used without further purification in the next step. <sup>1</sup>H NMR (400 MHz, DMSO) δ 10.62 (s, 1H), 8.34 (s, 1H), 8.30 (s, 1H), 2.09 (s, 3H), 1.32 (s, 12H). <sup>13</sup>C NMR (101 MHz, DMSO) δ 169.3, 150.2, 146.8, 128.9, 119.1, 84.7, 24.5, 23.9. TLC-MS (ESI<sup>+</sup>): calcd. *m/z* 296.11 for C<sub>13</sub>H<sub>18</sub>BClN<sub>2</sub>O<sub>3</sub>, found 319.0 [M+Na]<sup>+</sup>.

***N*-(5-Chloro-4-(2-(methylthio)-4-(3-nitrophenyl)-1-((2-(trimethylsilyl)ethoxy)methyl)-1*H*-imidazol-5-yl)pyridin-2-yl)acetamide (S30)**

To begin, 400 mg (0.90 mmol) of 5-bromo-2-(methylthio)-4-(3-nitrophenyl)-1-((2-(trimethylsilyl)ethoxy)methyl)-1*H*-imidazo[2-*b*]pyridin-3-yl acetamide<sup>32</sup>, 400 mg (1.35 mmol) of **S29** and 960 mg (3.60 mmol) of K<sub>3</sub>PO<sub>4</sub> trihydrate were dissolved in 10 mL of 1,4-dioxane and 2.5 mL of demineralized water. The solution was degassed with three cycles of evacuation and backfilling with argon. To the solution was added 51 mg (10 mol%) of P(*t*-Bu)<sub>3</sub> Pd G3, and another three cycles of evacuation and argon backfilling were carried out. The reaction mixture was warmed to 45 °C and stirred overnight. After cooling to ambient temperature, brine was added, and the aqueous layer was extracted several times with EtOAc. The combined organic layers were dried over Na<sub>2</sub>SO<sub>4</sub>, filtered, and evaporated to dryness. The crude product was purified via flash chromatography (SiO<sub>2</sub>; *n*-hexane/EtOAc 50:50) to obtain a yellow solid in 81% (390 mg, 0.73 mmol) yield with residues of deborylated **S31** as indicated by HPLC and NMR. The impure product was used in the next step without further purification due to simplification of the chromatographic purification after conversion. <sup>1</sup>H NMR (400 MHz, DMSO) δ 10.92 (s, 1H), 8.62 (s, 1H), 8.26 (s, 1H), 8.25 – 8.21 (m, 1H), 8.06 (dd, *J* = 8.1, 1.5 Hz, 1H), 7.69 (d, *J* = 7.9 Hz, 1H), 7.57 (t, *J* = 8.0 Hz, 1H), 5.17 (d, *J* = 11.5 Hz, 1H), 5.03 (d, *J* = 11.5 Hz, 1H), 3.32 – 3.29 (m, 2H), 2.73 (s, 3H), 2.09 (s, 3H), 0.78 – 0.71 (m, 2H), -0.10 (s, 9H). <sup>13</sup>C NMR (101 MHz, DMSO) δ 169.4, 151.4, 148.2, 148.0, 146.2, 137.9, 136.3, 135.0, 131.2, 130.3, 125.46, 125.45, 121.6, 119.6, 116.3, 73.0, 65.7, 24.9, 17.1, 15.3, -1.5. TLC-MS (ESI+): calcd. *m/z* 533.13 for C<sub>23</sub>H<sub>28</sub>ClN<sub>5</sub>O<sub>4</sub>SSi, found 556.2 [M+Na]<sup>+</sup>.

***N*-(4-(4-(3-Aminophenyl)-2-(methylthio)-1-((2-(trimethylsilyl)ethoxy)methyl)-1*H*-imidazol-5-yl)-5-chloropyridin-2-yl)acetamide (S31)**

To begin, 350 mg (0.66 mmol) of **S30** was dissolved in MeOH, and to the solution was added 214 mg (3.28 mmol) of zinc powder. To the suspension was added 206 mg (3.28 mmol) of ammonium formate portion wise over 15 min. After TLC indicated complete conversion, the crude mixture was filtered over Celite and washed with MeOH. The filtrate was evaporated to dryness and the crude product was purified via flash chromatography (SiO<sub>2</sub>; *n*-hexane/EtOAc 55:45) to obtain a yellow solid in 58% yield (190 mg, 0.38 mmol). <sup>1</sup>H NMR (400 MHz, DMSO) δ 10.83 (s, 1H), 8.53 (s, 1H), 8.17 (s, 1H), 6.86 – 6.78 (m, 2H), 6.39 (dd, *J* = 8.0, 1.1 Hz, 1H), 6.31 (d, *J* = 7.7 Hz, 1H), 5.12 (d, *J* = 11.4 Hz, 1H), 5.01 (s, 2H), 4.94 (d, *J* = 11.4 Hz, 1H), 3.28 – 3.25 (m, 2H), 2.67 (s, 3H), 2.09 (s, 3H), 0.75 – 0.70 (m, 2H), -0.10 (s, 9H). <sup>13</sup>C NMR (101 MHz, DMSO) δ 169.5, 151.1, 148.6, 147.8, 144.5, 139.4, 139.1, 133.9, 128.7, 125.9, 123.7, 116.6, 113.4, 112.9, 111.7, 72.7, 65.5, 23.9, 17.1, 15.5, -1.5. TLC-MS (ESI+): calcd. *m/z* 503.16 for C<sub>23</sub>H<sub>30</sub>ClN<sub>5</sub>O<sub>2</sub>SSi, found 526.3 [M+Na]<sup>+</sup>.

***N*-(4-methoxy-3-((4-(2-(methylthio)-4-(3-nitrophenyl)-1-((2-(trimethylsilyl) ethoxy)methyl)-1*H*-imidazol-5-yl)pyridin-2-yl)amino)phenyl)propionamide (S32)**

To begin, 540 mg (1.18 mmol) of **S24**, 396 mg (1.53 mmol) of *N*-(3-bromo-4-methoxyphenyl) propionamide and 577 mg of Cs<sub>2</sub>CO<sub>3</sub> (1.77 mmol) in 12 mL of a mixture of 1,4-dioxane/*t*-BuOH (4 + 1) was degassed three times by evacuating and backfilling with argon under stirring. To the mixture was added 53 mg of BrettPhos Pd G3 (5 mol%), and another three cycles of evacuation and argon backfilling were carried out. The solution was stirred under reflux for 4 h. After cooling to ambient temperature, cold demineralized water was added under precipitation of a yellow solid,



which was collected by filtration and dried in the oven. The crude product was isolated as yellow solid in 95% yield (715 mg, 1.13 mmol) and used without further purification in the next step with residues of the bromo reactant. <sup>1</sup>H NMR (400 MHz, DMSO) δ 9.68 (s, 1H), 8.36 – 8.32 (m, 1H), 8.31 – 8.24 (m, 3H), 8.05 (ddd, *J* = 8.2, 2.3, 0.8 Hz, 1H), 7.80 (d, *J* = 8.0 Hz, 1H), 7.58 (t, *J* = 8.0 Hz, 1H), 7.32 (dd, *J* = 8.8, 2.5 Hz, 1H), 7.02 (s, 1H), 6.91 (d, *J* = 8.9 Hz, 1H), 6.76 (dd, *J* = 5.2, 1.1 Hz, 1H), 5.17 (s, 2H), 3.75 (s, 3H), 3.42 – 3.36 (m, 2H), 2.70 (s, 3H), 2.28 (q, *J* = 7.5 Hz, 2H), 1.07 (t, *J* = 7.6 Hz, 3H), 0.80 – 0.73 (m, 2H), -0.07 – -0.11 (m, 9H). <sup>13</sup>C NMR (101 MHz, DMSO) δ 171.4, 156.6, 148.3, 148.0, 145.5, 145.3, 138.1, 135.5, 135.4, 132.4, 132.2, 130.0, 129.6, 129.3, 121.4, 120.4, 115.2, 113.2, 112.2, 111.9, 110.9, 72.6, 65.8, 55.8, 29.4, 17.2, 15.4, 9.8, -1.5. TLC-MS (ESI+): calcd. *m/z* 634.24 for C<sub>31</sub>H<sub>38</sub>N<sub>6</sub>O<sub>5</sub>SSi, found 657.1 [M+Na]<sup>+</sup>.

### ***N*-(3-((4-(4-(3-aminophenyl)-2-(methylthio)-1-((2-(trimethylsilyl)ethoxy)methyl)-1*H*-imidazol-5-yl)pyridin-2-yl)amino)-4-methoxyphenyl)propionamide (S33)**

To begin, 650 mg (1.02 mmol) of **S32** was dissolved in MeOH, and to the solution was added 335 mg (5.12 mmol) of zinc powder. To the suspension was added 323 mg (5.12 mmol) of ammonium formate portion wise over 15 min. After TLC indicated complete conversion, the crude mixture was filtered over Celite and washed with MeOH. The filtrate was concentrated and demineralized water was added to the residue under precipitation of a yellowish solid, which was collected by filtration and dried in the oven. The crude product was triturated with a mixture of *n*-hexane/diethylether (9+1) to obtain 40% (250 mg, 0.41 mmol) of the product as yellow solid. <sup>1</sup>H NMR (400 MHz, DMSO) δ 9.67 (s, 1H), 8.28 (d, *J* = 2.5 Hz, 1H), 8.20 – 8.16 (m, 2H), 7.32 (dd, *J* = 8.8, 2.5 Hz, 1H), 6.98 (s, 1H), 6.92 – 6.89 (m, 2H), 6.86 (t, *J* = 7.9 Hz, 1H), 6.67 (dd, *J* = 5.2, 1.2 Hz, 1H), 6.46 – 6.43 (m, 1H), 6.41 (ddd, *J* = 8.0, 2.3, 0.9 Hz, 1H), 5.19 – 5.07 (m, 4H), 3.77 (s, 3H), 3.39 – 3.35 (m, 2H), 2.65 (s, 3H), 2.29 (q, *J* = 7.6 Hz, 2H), 1.07 (t, *J* = 7.5 Hz, 3H), 0.78 – 0.74 (m, 2H), -0.08 (s, 9H). <sup>13</sup>C NMR (101 MHz, DMSO) δ 171.4, 156.3, 148.4, 147.5, 145.1, 144.0, 139.1, 138.8, 134.3, 132.4, 129.5, 128.5, 127.7, 115.8, 114.7, 112.9, 112.8, 112.7, 112.2, 111.9, 110.7, 72.4, 65.6, 55.8, 29.3, 17.2, 15.6, 9.8, -1.5. TLC-MS (ESI+): calcd. *m/z* 604.27 for C<sub>31</sub>H<sub>40</sub>N<sub>6</sub>O<sub>3</sub>SSi, found 627.1 [M+Na]<sup>+</sup>.

### ***tert*-Butyl (3-(2-ethyl-5-(2-(phenylamino)pyridin-4-yl)-1-((2-(trimethylsilyl) ethoxy)methyl)-1*H*-imidazol-4-yl)phenyl)carbamate (S34)**

To begin, 350 mg (0.69 mmol) of *tert*-butyl (3-(5-(2-aminopyridin-4-yl)-2-ethyl-1-((2-(trimethylsilyl)ethoxy)methyl)-1*H*-imidazol-4-yl)phenyl)carbamate<sup>34</sup>, 162 mg (1.03 mmol) of bromobenzene, and 336 mg of Cs<sub>2</sub>CO<sub>3</sub> (1.03 mmol) in 7 mL of a mixture of 1,4-dioxane/*t*-BuOH (4 + 1) was degassed three times by evacuating and backfilling with argon under stirring. The mixture was added 31 mg of BrettPhos Pd G3 (5 mol%), and another three cycles of evacuation and argon backfilling were carried out. The solution was stirred under reflux for 5 h. After cooling to ambient temperature, Celite was added to the mixture, and solvents were removed in vacuo. Purification via flash chromatography (SiO<sub>2</sub>; *n*-hexane/EtOAc 40:60) yielded 87% (350 mg, 0.60 mmol) of a yellow solid. <sup>1</sup>H NMR (400 MHz, DMSO) δ 9.28 (s, 1H), 9.06 (s, 1H), 8.23 (d, *J* = 5.2 Hz, 1H), 7.75 – 7.72 (m, 1H), 7.61 – 7.59 (m, 1H), 7.59 – 7.57 (m, 1H), 7.29 – 7.25 (m, 1H), 7.24 – 7.20 (m, 2H), 7.10 (t, *J* = 7.9 Hz, 1H), 6.93 – 6.90 (m, 1H), 6.89 – 6.85 (m, 1H), 6.74 (s, 1H), 6.73 – 6.70 (m, 1H), 5.14 (s, 2H), 3.35 – 3.31 (m, 2H), 2.80 (q, *J* = 7.5 Hz, 2H), 1.43 (s, 9H), 1.32 (t, *J* = 7.5 Hz, 3H), 0.78 – 0.73 (m, 2H), -0.10 (s, 9H). <sup>13</sup>C NMR (101 MHz, DMSO) δ 156.3, 152.7,

150.4, 148.0, 141.4, 139.5, 139.4, 136.3, 134.8, 128.6, 128.2, 126.4, 120.64, 120.59, 118.1, 117.0, 116.5, 115.5, 111.9, 78.8, 71.7, 65.1, 28.1, 19.8, 17.2, 12.1, -1.5. TLC-MS (ESI+): calcd.  $m/z$  585.31 for  $C_{33}H_{43}N_5O_3Si$ , found 608.3  $[M + Na]^+$ .

#### **4-(4-(3-Aminophenyl)-2-ethyl-1-((2-(trimethylsilyl)ethoxy)methyl)-1H-imidazol-5-yl)-N-phenylpyridin-2-amine (S35)**

320 mg (0.55 mmol) of **S1** was dissolved in 18 mL of a mixture of TFA/DCM 10% v/v. The solution was stirred for 24 h at ambient temperature. The reaction mixture was concentrated in vacuo and to the residue was added a saturated aqueous  $NaHCO_3$  solution, whereupon the aqueous layer was extracted several times with EtOAc. The combined organic layers were dried over  $Na_2SO_4$ , filtered, and the solvents removed in vacuo. The crude product was purified via flash chromatography ( $SiO_2$ ; *n*-hexane/EtOAc/MeOH 30:65:5) to give the product as light yellow solid in 57% yield (150 mg, 0.31 mmol).  $^1H$  NMR (400 MHz, DMSO)  $\delta$  9.07 (s, 1H), 8.23 (d,  $J = 5.1$  Hz, 1H), 7.60 (s, 1H), 7.58 (s, 1H), 7.25 – 7.20 (m, 2H), 6.90 – 6.87 (m, 2H), 6.86 – 6.82 (m, 1H), 6.76 (s, 1H), 6.74 – 6.70 (m, 1H), 6.45 – 6.41 (m, 1H), 6.41 – 6.36 (m, 1H), 5.12 (s, 2H), 4.99 (s, 2H), 3.34 – 3.32 (m, 2H), 2.78 (q,  $J = 7.5$  Hz, 2H), 1.31 (t,  $J = 7.5$  Hz, 3H), 0.78 – 0.72 (m, 2H), -0.10 (s, 9H).  $^{13}C$  NMR (101 MHz, DMSO)  $\delta$  156.2, 150.1, 148.6, 147.9, 141.4, 139.8, 137.0, 134.9, 128.6, 128.4, 125.9, 120.6, 118.1, 115.6, 114.7, 112.7, 112.3, 111.9, 71.7, 65.1, 19.8, 17.2, 12.1, -1.5. TLC-MS (ESI+): calcd.  $m/z$  485.26 for  $C_{28}H_{35}N_5OSi$ , found 508.2  $[M + Na]^+$ .

#### **N-(4-(4-(3-Aminophenyl)-2-(methylthio)-1-((2-(trimethylsilyl)ethoxy)methyl)-1H-imidazol-5-yl)pyridin-2-yl)acetamide (S36)**

Prepared as previously described.<sup>32</sup>

#### **4-(2-(Methylthio)-4-(3-nitrophenyl)-1-((2-(trimethylsilyl)ethoxy)methyl)-1H-imidazol-5-yl)-N-phenylpyridin-2-amine (S37)**

To begin, 410 mg (0.90 mmol) of **S24**, 155 mg (0.99 mmol) of bromobenzene, and 1022 mg of  $Cs_2CO_3$  (3.14 mmol) in 18 mL of a mixture of 1,4-dioxane/*t*-BuOH (4 + 1) was degassed three times by evacuating and backfilling with argon under stirring. To the mixture was added 20 mg of BrettPhos Pd G3 (2.5 mol%), and another three cycles of evacuation and argon backfilling were carried out. The solution was stirred under reflux for 5 h. After cooling to ambient temperature, Celite was added to the mixture, and solvents were removed in vacuo. Purification via flash chromatography ( $SiO_2$ ; *n*-hexane/EtOAc 30:70) afforded 94% (450 mg, 0.84 mmol) of a yellow solid.  $^1H$  NMR (400 MHz, DMSO)  $\delta$  9.14 (s, 1H), 8.37 – 8.33 (m, 1H), 8.31 (d,  $J = 5.6$  Hz, 1H), 8.07 (ddd,  $J = 8.3, 2.4, 0.9$  Hz, 1H), 7.83 – 7.79 (m, 1H), 7.64 – 7.57 (m, 3H), 7.27 – 7.22 (m, 2H), 6.90 (t,  $J = 7.3$  Hz, 1H), 6.84 – 6.79 (m, 2H), 5.17 (s, 2H), 3.45 – 3.39 (m, 2H), 2.71 (s, 3H), 0.81 – 0.76 (m, 2H), -0.08 (s, 9H).  $^{13}C$  NMR (101 MHz, DMSO)  $\delta$  156.5, 148.6, 148.0, 145.6, 141.2, 138.1, 135.6, 135.3, 132.3, 130.1, 129.5, 128.6, 121.4, 120.9, 120.5, 118.3, 115.1, 111.5, 72.7, 65.8, 17.2, 15.4, -1.5. TLC-MS (ESI+): calcd.  $m/z$  533.19 for  $C_{27}H_{31}N_5O_3SSi$ , found 534.2  $[M+H]^+$ .

#### **4-(4-(3-Aminophenyl)-2-(methylthio)-1-((2-(trimethylsilyl)ethoxy)methyl)-1H-imidazol-5-yl)-N-phenylpyridin-2-amine (S38)**

To begin, 450 mg (0.84 mmol) of **S37** was dissolved in MeOH, and to the solution was added 276 mg (4.22 mmol) of zinc powder. To the suspension was added 266 mg (4.22 mmol) of ammonium

formate portion wise over 15 min. After TLC indicated complete conversion, the crude mixture was filtered over Celite and washed with MeOH. The filtrate was evaporated to dryness and the crude product was purified via flash chromatography (SiO<sub>2</sub>; *n*-hexane/EtOAc/MeOH 5%) 65:35) to obtain a yellow solid in 72% yield (305 mg, 0.61 mmol). <sup>1</sup>H NMR (400 MHz, DMSO) δ 9.07 (s, 1H), 8.23 (d, *J* = 5.8 Hz, 1H), 7.58 (d, *J* = 7.7 Hz, 2H), 7.25 – 7.20 (m, 2H), 6.91 – 6.84 (m, 3H), 6.79 – 6.74 (m, 2H), 6.48 – 6.39 (m, 2H), 5.14 (s, 2H), 5.03 (s, 2H), 3.42 – 3.37 (m, 2H), 2.65 (s, 3H), 0.80 – 0.75 (m, 2H), -0.09 (s, 9H). <sup>13</sup>C NMR (101 MHz, DMSO) δ 156.2, 148.6, 148.0, 144.2, 141.4, 139.07, 139.05, 134.2, 128.6, 128.5, 127.7, 120.6, 118.1, 115.4, 114.8, 112.69, 112.67, 111.6, 72.5, 65.6, 17.2, 15.6, -1.5. TLC-MS (ESI+): calcd. *m/z* 503.22 for C<sub>27</sub>H<sub>33</sub>N<sub>5</sub>OSSi, found 526.1 [M+Na]<sup>+</sup>.

***N*-(3-((4-(4-(3-Aminophenyl)-2-(methylthio)-1-((2-(trimethylsilyl)ethoxy)methyl)-1*H*-imidazol-5-yl)pyridin-2-yl)amino)-4-methoxyphenyl)acrylamide (S39)**

Prepared as previously described.<sup>32</sup>

***N*-(4-(4-(3-Aminophenyl)-2-ethyl-1-((2-(trimethylsilyl)ethoxy)methyl)-1*H*-imidazol-5-yl)pyridin-2-yl)acetamide (S40)**

Prepared as previously described.<sup>34</sup>

***N*-(3-((4-(4-(3-Aminophenyl)-2-ethyl-1-((2-(trimethylsilyl)ethoxy)methyl)-1*H*-imidazol-5-yl)pyridin-2-yl)amino)-4-methoxyphenyl)acrylamide (S41)**

Prepared as previously described.<sup>34</sup>

***tert*-Butyl 4-(4-((4-(4-(3-(3-acetoxy-2-((1-oxoisindolin-2-yl)methyl)benzamido) phenyl)-2-(methylthio)-1-((2-(trimethylsilyl)ethoxy)methyl)-1*H*-imidazol-5-yl)pyridin-2-yl)amino)phenyl)piperazine-1-carboxylate (S42)**

To begin, 850 mg (1.24 mmol) **S26** and 563 mg (1.73 mmol) **S21** were suspended in 15 mL toluene and the mixture was cooled down to -5 °C. To the mixture was added 379 mg (1.98 mmol) EDC-HCl and the mixture was slowly warmed up to ambient temperature and stirred overnight. The solvent was removed in vacuo and EtOAc was added to the residue. The organic phase was washed with saturated, aqueous NH<sub>4</sub>Cl and then dried over Na<sub>2</sub>SO<sub>4</sub>. After evaporation of the solvent the crude product was purified via flash chromatography (SiO<sub>2</sub>, *n*-hexane/EtOAc 20:80) to obtain a yellow solid in 73% yield (900 mg, 0.90 mmol). <sup>1</sup>H NMR (400 MHz, DMSO) δ 10.63 (s, 1H), 8.80 (s, 1H), 8.16 (d, *J* = 5.2 Hz, 1H), 8.01 – 7.98 (m, 1H), 7.67 (d, *J* = 7.5 Hz, 1H), 7.64 – 7.60 (m, 1H), 7.56 – 7.49 (m, 2H), 7.49 – 7.42 (m, 3H), 7.35 (d, *J* = 9.0 Hz, 2H), 7.28 – 7.21 (m, 2H), 7.08 (d, *J* = 7.8 Hz, 1H), 6.81 (d, *J* = 9.0 Hz, 2H), 6.71 (dd, *J* = 5.2, 1.1 Hz, 1H), 6.68 (s, 1H), 5.15 (s, 2H), 4.75 (s, 2H), 4.17 (s, 2H), 3.45 – 3.38 (m, 6H), 2.98 – 2.93 (m, 4H), 2.66 (s, 3H), 2.20 (s, 3H), 1.41 (s, 9H), 0.80 – 0.76 (m, 2H), -0.09 (s, 9H). <sup>13</sup>C NMR (101 MHz, DMSO) δ 169.2, 166.8, 166.4, 156.8, 153.8, 150.0, 148.3, 145.7, 144.6, 141.7, 139.7, 139.0, 138.4, 137.9, 134.2, 133.9, 131.9, 131.3, 129.1, 128.6, 128.5, 127.7, 126.7, 125.3, 124.8, 123.3, 122.7, 122.4, 119.9, 118.71, 118.65, 116.9, 114.4, 110.6, 78.9, 72.6, 65.7, 49.3, 49.0, 48.6, 37.7, 28.1, 20.8, 17.2, 15.6, -1.5. TLC-MS (ESI+): calcd. *m/z* 994.42 for C<sub>54</sub>H<sub>62</sub>N<sub>8</sub>O<sub>7</sub>SSi, found 1017.4 [M+Na]<sup>+</sup>.

***N*-(3-(5-(2-Acetamidopyridin-4-yl)-2-(methylthio)-1*H*-imidazol-4-yl)phenyl)benzamide (1)**



Prepared as previously described.<sup>55</sup>

***N*-(3-(5-(2-Acetamidopyridin-4-yl)-2-(methylthio)-1*H*-imidazol-4-yl)phenyl)-3-hydroxybenzamide (2)**

To begin, 60 mg (0.13 mmol) of **S36**, 35 mg (0.19 mmol) of 3-acetoxybenzoic acid, and 82 mg (0.25 mmol) of TBTU were dissolved in 2 mL of DMF, and to the mixture was added 53  $\mu$ L (0.38 mmol) of TEA. The reaction mixture was stirred overnight at ambient temperature. After addition of brine, the aqueous layer was extracted with DCM, the combined organic layers were dried over Na<sub>2</sub>SO<sub>4</sub>, filtered and volatiles were removed in vacuo. The crude product was purified via flash chromatography (SiO<sub>2</sub>; DCM/MeOH 90:10) (identification of the intermediate via TLC-MS (ESI+): calcd. *m/z* 631.23 for C<sub>32</sub>H<sub>37</sub>N<sub>5</sub>O<sub>5</sub>SSi, found 654.1 [M+Na]<sup>+</sup>). The intermediate was then dissolved in a 33% TFA/DCM mixture. After stirring overnight at room temperature, a saturated aqueous NaHCO<sub>3</sub> solution was added to the mixture, and the aqueous layer was extracted with EtOAc. Combined organic layers were dried over Na<sub>2</sub>SO<sub>4</sub>, and solvents were removed in vacuo (identification of the intermediate via TLC-MS (ESI+): calcd. *m/z* 501.15 for C<sub>26</sub>H<sub>23</sub>N<sub>5</sub>O<sub>4</sub>S, found 524.3 [M+Na]<sup>+</sup>) The intermediate was dissolved in MeOH, a saturated aqueous NaHCO<sub>3</sub> solution was added and the mixture was stirred for 1 h. The aqueous layer was extracted with DCM. The combined organic layers were dried over Na<sub>2</sub>SO<sub>4</sub>, and solvents were removed in vacuo. The residue was purified via flash chromatography (SiO<sub>2</sub>; DCM/MeOH 90:10) to obtain the product in 42% yield (27 mg, 0.05 mmol) of a white solid. <sup>1</sup>H NMR (400 MHz, DMSO)  $\delta$  12.81 – 12.63 (m, 1H), 10.50 – 10.30 (m, 1H), 10.27 – 10.12 (m, 1H), 9.80 – 9.68 (m, 1H), 8.39 – 8.05 (m, 2H), 8.00 – 7.89 (m, 1H), 7.86 – 7.74 (m, 1H), 7.44 – 7.32 (m, 2H), 7.32 – 7.23 (m, 2H), 7.15 (d, *J* = 7.2 Hz, 1H), 7.08 – 7.01 (m, 1H), 6.97 (d, *J* = 7.3 Hz, 1H), 2.63 (s, 3H), 2.10 – 2.00 (m, 3H). <sup>13</sup>C NMR (101 MHz, DMSO)  $\delta$  168.9, 165.7, 157.4, 152.4, 147.5, 143.7, 142.1, 139.6, 136.3, 134.3, 131.1, 130.6, 129.4, 129.1, 123.8, 120.1, 120.0, 118.6, 118.2, 116.4, 114.5, 110.5, 23.9, 15.1. HRMS (ESI): exact mass calcd. for C<sub>24</sub>H<sub>21</sub>N<sub>5</sub>O<sub>3</sub>S [M+H]<sup>+</sup>: 460.14379. Found: 460.14445.

***General procedures for synthesis of bivalent EGFR inhibitors:***

An amine, a carboxylic acid, and an appropriate coupling reagent (TBTU, EDC-HCl) were dissolved in DMF or toluene (0.05 M) and TEA or DIPEA was added to the solution in the stated amounts. The reaction mixture was stirred overnight at ambient temperatures. After addition of brine, the aqueous layer was extracted three times with EtOAc, the combined organic layers were dried over Na<sub>2</sub>SO<sub>4</sub>, filtered and volatiles were removed in vacuo. The crude product was purified via gradient silica flash chromatography. The Intermediate was identified via TLC-MS and was then dissolved in 2-5 mL of a mixture of TFA in DCM (20-33% v/v). The mixture was stirred at ambient temperature overnight. After complete consumption of the starting material and identification of the intermediate via TLC-MS, the volatiles were removed by rotary evaporation and the oily residue was resuspended in (A) EtOAc, a saturated aqueous NaHCO<sub>3</sub> solution was added, and the aqueous layer was extracted several times with EtOAc. The combined organic layers were dried over Na<sub>2</sub>SO<sub>4</sub>, filtered and the solvents removed by rotary evaporation. The crude product was purified via flash chromatography. (B) Compounds with phenol acetyl ester protection group: the residue was dissolved in 2-5 mL of MeOH, few drops of an aqueous 0.1 N NaOH were added, and the residue was stirred for 2-5 h at ambient temperature. After the complete consumption of starting material was indicated by HPLC, the aqueous layer was neutralized by the

addition of saturated aqueous NH<sub>4</sub>Cl solution, and the aqueous layer was extracted several times with EtOAc. Organic layers were dried over Na<sub>2</sub>SO<sub>4</sub>, filtered and solvents were removed in vacuo. The crude product was purified via flash chromatography.

Starting materials, mobile phases for chromatographic purification, analytics for characterization and deviations from above-mentioned procedures are given in detail in the following for the tested compounds of this study.

***N*-(3-(5-(2-Acetamidopyridin-4-yl)-2-(methylthio)-1*H*-imidazol-4-yl)phenyl)-2-((1,3-oxoisindolin-2-yl)methyl)benzamide (3)**

Prepared as previously described.<sup>32</sup>

***N*-(3-(5-(2-Acetamidopyridin-4-yl)-2-(methylthio)-1*H*-imidazol-4-yl)phenyl)-2-((1,3-dioxoisindolin-2-yl)methyl)benzamide (4)**

The title compound was synthesized according to *general procedure A*) from 135 mg (0.29 mmol) **S36**, 121 mg (0.43 mmol) of 2-((1,3-dioxoisindolin-2-yl)methyl)benzoic acid,<sup>32</sup> 138 mg (0.43 mmol) TBTU and 120  $\mu$ l (0.86 mmol) TEA dissolved in DMF. Purification via flash chromatography (SiO<sub>2</sub>; *n*-hexane/EtOAc 15:85) [identification of intermediate via TLC-MS (ESI+): calcd. *m/z* 732.26 for C<sub>39</sub>H<sub>40</sub>N<sub>6</sub>O<sub>5</sub>SSi Found 755.6 [M+Na]<sup>+</sup>]. The intermediate was dissolved in a 33% TFA/DCM mixture and purification of the product via flash chromatography (SiO<sub>2</sub>; DCM/MeOH 90:10) afforded 64% (112 mg, 0.19 mmol) of an off-white solid. As mixture of tautomers: <sup>1</sup>H NMR (200 MHz, DMSO)  $\delta$  12.92 – 12.55 (m, 1H), 10.67 – 10.27 (m, 2H), 8.43 – 8.05 (m, 2H), 8.01 – 7.70 (m, 6H), 7.56 (s, 1H), 7.48 – 7.14 (m, 5H), 7.12 – 7.00 (m, 1H), 4.98 (s, 2H), 2.63 (s, 3H), 2.04 (s, 3H). HRMS (ESI): exact mass calcd for C<sub>33</sub>H<sub>26</sub>N<sub>6</sub>O<sub>4</sub>S [M+H]<sup>+</sup>: 603.18090. Found: 603.18165.

**2-((2-((3-(5-(2-Acetamidopyridin-4-yl)-2-(methylthio)-1*H*-imidazol-4-yl)phenyl)carbamoyl)benzyl)carbamoyl)benzoic acid (5)**

To begin, 40 mg (0.06 mmol) of **4** was dissolved in 1.3 mL MeOH, 1.3 mL of a saturated aqueous NaHCO<sub>3</sub> solution was added and the mixture was stirred for 5 h at ambient temperature. Demineralized water was added, and the pH was adjusted to 4-5 with diluted aqueous HCl. The aqueous layer was extracted multiple times with EtOAc. Combined organic layers were dried over Na<sub>2</sub>SO<sub>4</sub>, filtered and volatiles were removed in vacuo. DCM was added to the residue and the mixture was filtered through a syringe filter. Removal of the solvent in vacuo afforded the product in 85% (35 mg, 0.056 mmol) yield as yellow solid. <sup>1</sup>H NMR (200 MHz, DMSO)  $\delta$  12.81 (s, 1H), 10.71 – 10.26 (m, 2H), 8.97 (s, 1H), 8.40 – 8.09 (m, 2H), 7.99 – 7.73 (m, 3H), 7.66 – 7.59 (m, 1H), 7.57 – 7.43 (m, 5H), 7.43 – 7.28 (m, 2H), 7.20 – 7.04 (m, 2H), 4.66 – 4.50 (m, 2H), 2.62 (s, 3H), 2.10 – 1.97 (m, 3H). With missing signal of carboxylic acid. HRMS (ESI): exact mass calcd for C<sub>33</sub>H<sub>28</sub>N<sub>6</sub>O<sub>5</sub>S [M+H]<sup>+</sup>: 621.19147. Found: 621.19205.

***N*-(3-(5-(2-Acetamidopyridin-4-yl)-2-(methylthio)-1*H*-imidazol-4-yl)phenyl)-2-fluoro-6-((1-oxoisindolin-2-yl)methyl)benzamide (6)**

To begin, 30 mg (0.11 mmol) **S15** was dissolved in 3.5 mL THF and 3 drops DMF was added. 14  $\mu$ l (0.16 mmol) oxalyl chloride was added drop wise under gas formation and the mixture was

stirred for 0.5 h at ambient temperature, whereupon the excess of oxalyl chloride was removed in vacuo. 50 mg (0.11 mmol) **S36** was dissolved in 3.5 mL THF, 45  $\mu$ l (0.32 mmol) TEA was added and the mixture was cooled down to 0 °C. The beforehand prepared acid chloride dissolved in 3.5 mL THF was slowly added, whereupon the mixture was warmed up to ambient temperature and stirred for 0.5 h. Volatiles were removed in vacuo and the crude product was purified via flash chromatography (SiO<sub>2</sub>; DCM/MeOH 90:10). [Identification of intermediate via TLC-MS (ESI+): calcd. *m/z* 736.27 for C<sub>39</sub>H<sub>41</sub>FN<sub>6</sub>O<sub>4</sub>SSi Found 760.4 [M+Na]<sup>+</sup>]. The intermediate was dissolved in a 33% TFA/DCM mixture and purification of the product via flash chromatography (SiO<sub>2</sub>; *n*-hexane/EtOAc/MeOH 30:60:10) afforded 25% (16 mg, 0.03 mmol) of an off-white solid (in 94.6% HPLC purity). As mixture of tautomers: <sup>1</sup>H NMR (400 MHz, DMSO)  $\delta$  12.82 – 12.66 (m, 1H), 10.60 – 10.30 (m, 2H), 8.39 – 8.08 (m, 2H), 7.97 – 7.84 (m, 1H), 7.78 – 7.67 (m, 1H), 7.63 – 7.54 (m, 2H), 7.51 – 7.33 (m, 4H), 7.31 – 7.27 (m, 1H), 7.26 – 7.21 (m, 1H), 7.17 (d, *J* = 7.7 Hz, 1H), 7.10 – 7.02 (m, 1H), 4.85 (s, 2H), 4.43 (s, 2H), 2.63 (s, 3H), 2.08 – 1.99 (m, 3H). HRMS (ESI): exact mass calcd for C<sub>33</sub>H<sub>27</sub>FN<sub>6</sub>O<sub>3</sub>S [M+Na]<sup>+</sup>: 629.17460. Found: 629.17416.

***N*-(3-(5-(2-Acetamidopyridin-4-yl)-2-(methylthio)-1*H*-imidazol-4-yl)phenyl)-3-hydroxy-2-((1-oxoisindolin-2-yl)methyl)benzamide (7)**

The title compound was synthesized according to *general procedure B* from 53 mg (0.11 mmol) **S36**, 40 mg (0.12 mmol) **S21**, 47 mg (0.15 mmol) TBTU and 47  $\mu$ l (0.32 mmol) TEA in DMF. Purification via flash chromatography (SiO<sub>2</sub>, *n*-hexane/EtOAc/MeOH 10:85:5). [Identification of intermediate via TLC-MS (ESI+): calcd. *m/z* 776.28 for C<sub>41</sub>H<sub>44</sub>N<sub>6</sub>O<sub>6</sub>SSi Found 799.9 [M+Na]<sup>+</sup>]. The intermediate was dissolved in a 33% TFA/DCM mixture [Identification of intermediate via TLC-MS (ESI+): calcd. *m/z* 646.20 for C<sub>35</sub>H<sub>30</sub>N<sub>6</sub>O<sub>5</sub>S Found 669.7 [M+Na]<sup>+</sup>], followed by deprotection under basic conditions and purification via flash chromatography (SiO<sub>2</sub>, *n*-hexane/EtOAc/MeOH 10:85:5) afforded 77% (50 mg, 0.08 mmol) of a yellow solid. As mixture of tautomers: <sup>1</sup>H NMR (200 MHz, DMSO)  $\delta$  12.84 – 12.64 (m, 1H), 10.85 – 10.55 (m, 1H), 10.50 – 10.25 (m, 1H), 10.15 – 9.92 (m, 1H), 8.39 – 8.04 (m, 2H), 7.90 – 7.66 (m, 2H), 7.65 – 7.50 (m, 3H), 7.48 – 7.22 (m, 3H), 7.20 – 7.02 (m, 2H), 7.02 – 6.89 (m, 2H), 4.77 (s, 2H), 4.38 (s, 2H), 2.69 – 2.58 (m, 3H), 2.03 (s, 3H). HRMS (ESI): exact mass calcd for C<sub>33</sub>H<sub>28</sub>N<sub>6</sub>O<sub>4</sub>S [M+H]<sup>+</sup>: 605.19655. Found: 605.19597.

***N*-(3-(5-(2-Ac-amido-5-chloropyridin-4-yl)-2-(methylthio)-1*H*-imidazol-4-yl)phenyl)-3-hydroxy-2-((1-oxoisindolin-2-yl)methyl)benzamide (8)**

The title compound was synthesized according to *general procedure B* from 170 mg (0.34 mmol) **S31**, 143 mg (0.44 mmol) **S21**, 97 mg (0.51 mmol) EDC-HCl in toluene at 0 °C starting temperature. Flash chromatography (SiO<sub>2</sub>, *n*-hexane/EtOAc 20:80). [Identification of intermediate via TLC-MS (ESI+): calcd. *m/z* 810.24 for C<sub>41</sub>H<sub>43</sub>ClN<sub>6</sub>O<sub>6</sub>SSi Found 833.0 [M+Na]<sup>+</sup>]. Deprotection in a 33% TFA/DCM mixture [Identification of intermediate via HRMS (ESI): exact mass calcd for C<sub>35</sub>H<sub>29</sub>ClN<sub>6</sub>O<sub>5</sub>S [M+Na]<sup>+</sup>: 703.15009. Found: 703.15078] and flash chromatographic purification (SiO<sub>2</sub>, *n*-hexane/(EtOAc/MeOH 5) 10:90), followed by deprotection under basic conditions and isolation of the product via extraction with EtOAc to obtain the product in 12% yield (25 mg, 0.04 mmol) as white solid. As mixture of tautomers: <sup>1</sup>H NMR (400 MHz, DMSO)  $\delta$  13.03 – 12.47 (m, 1H), 10.60 (s, 2H), 10.08 (s, 1H), 8.46 – 8.10 (m, 2H), 7.93 – 7.61 (m, 2H), 7.58 – 7.40 (m, 4H), 7.29 – 7.22 (m, 2H), 7.15 (s, 1H), 7.01 – 6.92 (m, 2H), 4.72 (s, 2H), 4.36 (s, 2H), 2.61 (s, 3H), 2.05

(s, 3H). HRMS (ESI): exact mass calcd for C<sub>33</sub>H<sub>27</sub>ClN<sub>6</sub>O<sub>4</sub>S [M+Na]<sup>+</sup>: 661.13952. Found: 661.14065.

***N*-(3-(5-(2-Acetamidopyridin-4-yl)-2-ethyl-1*H*-imidazol-4-yl)phenyl)-3-hydroxy-2-((1-oxoisindolin-2-yl)methyl)benzamide (9)**

The title compound was synthesized according to *general procedure B*) from 80 mg (0.18 mmol) **S40**, 69 mg (0.21 mmol) **S21**, 51 mg (0.27 mmol) EDC-HCl in toluene at 0 °C starting temperature. Flash chromatography (SiO<sub>2</sub>, *n*-hexane/EtOAc 5:95). [Identification of intermediate via TLC-MS (ESI+): calcd. *m/z* 758.32 for C<sub>42</sub>H<sub>46</sub>N<sub>6</sub>O<sub>6</sub>Si, found 780.9 [M+Na]<sup>+</sup>]. Deprotection in a 25% TFA/DCM mixture [Identification of intermediate via TLC-MS (ESI+): calcd. *m/z* 628.24 for C<sub>36</sub>H<sub>32</sub>N<sub>6</sub>O<sub>5</sub>, found 651.7 [M+Na]<sup>+</sup>] and flash chromatographic purification (SiO<sub>2</sub>, EtOAc/IPA 90:10), followed by deprotection under basic conditions afforded an off-white solid in 26% yield (27 mg, 0.05 mmol). <sup>1</sup>H NMR (400 MHz, DMSO) δ 12.55 (br s, 1H), 10.69 (s, 1H), 10.34 (s, 1H), 10.05 (s, 1H), 8.31 (s, 1H), 8.09 (d, *J* = 5.0 Hz, 1H), 7.85 (s, 1H), 7.72 (d, *J* = 8.0 Hz, 1H), 7.61 (d, *J* = 7.5 Hz, 1H), 7.58 – 7.50 (m, 2H), 7.47 – 7.40 (m, 1H), 7.35 (t, *J* = 7.8 Hz, 1H), 7.27 (t, *J* = 7.8 Hz, 1H), 7.15 (d, *J* = 7.6 Hz, 1H), 7.06 (d, *J* = 4.8 Hz, 1H), 7.02 – 6.93 (m, 2H), 4.76 (s, 2H), 4.38 (s, 2H), 2.72 (q, *J* = 7.5 Hz, 2H), 2.04 (s, 3H), 1.28 (t, *J* = 7.6 Hz, 3H). HRMS (ESI): exact mass calcd for C<sub>34</sub>H<sub>30</sub>N<sub>6</sub>O<sub>4</sub> [M+H]<sup>+</sup>: 587.24013. Found: 587.23726.

***N*-(3-(5-(2-Acetamidopyridin-4-yl)-2-ethoxy-1*H*-imidazol-4-yl)phenyl)-3-hydroxy-2-((1-oxoisindolin-2-yl)methyl)benzamide (10)**

The title compound was synthesized according to *general procedure B*) from 90 mg (0.19 mmol) **S7**, 75 mg (0.23 mmol) **S21**, 55 mg (0.29 mmol) EDC-HCl in toluene at 0 °C starting temperature. Flash chromatography (SiO<sub>2</sub>, *n*-hexane/EtOAc 5:95). [Identification of intermediate via TLC-MS (ESI+): calcd. *m/z* 774.32 for C<sub>42</sub>H<sub>46</sub>N<sub>6</sub>O<sub>7</sub>Si Found 796.9 [M+Na]<sup>+</sup>]. Deprotection in a 25% TFA/DCM mixture [Identification of intermediate via TLC-MS (ESI+): calcd. *m/z* 644.24 for C<sub>36</sub>H<sub>32</sub>N<sub>6</sub>O<sub>6</sub> Found 666.7 [M+Na]<sup>+</sup>] and flash chromatographic purification (SiO<sub>2</sub>, EtOAc/IPA 10%), followed by deprotection under basic conditions. The product was precipitated in cold demineralized water and filtration afforded the product in 45% yield (55 mg, 0.09 mmol) as off-white solid. As mixture of tautomers: <sup>1</sup>H NMR (400 MHz, DMSO) δ 11.95 (s, 1H), 10.67 (s, 1H), 10.32 (s, 1H), 10.03 (s, 1H), 8.36 – 8.17 (m, 1H), 8.05 (s, 1H), 7.92 – 7.80 (m, 1H), 7.72 (d, *J* = 6.6 Hz, 1H), 7.61 (d, *J* = 7.3 Hz, 1H), 7.58 – 7.50 (m, 2H), 7.47 – 7.41 (m, 1H), 7.35 (s, 1H), 7.27 (t, *J* = 7.8 Hz, 1H), 7.14 (d, *J* = 7.0 Hz, 1H), 7.06 (s, 1H), 7.02 – 6.94 (m, 2H), 4.76 (s, 2H), 4.47 – 4.33 (m, 4H), 2.03 (s, 3H), 1.36 (t, *J* = 6.9 Hz, 3H). HRMS (ESI): exact mass calcd for C<sub>34</sub>H<sub>30</sub>N<sub>6</sub>O<sub>5</sub> [M+H]<sup>+</sup>: 603.23504. Found: 603.23308.

**3-Hydroxy-*N*-(3-(2-(methylthio)-5-(2-(phenylamino)pyridin-4-yl)-1*H*-imidazol-4-yl)phenyl)-2-((1-oxoisindolin-2-yl)methyl)benzamide (11)**

The title compound was synthesized according to *general procedure B*) from 100 mg (0.20 mmol) **S38**, 65 mg (0.22 mmol) **S21**, 57 mg (0.30 mmol) EDC-HCl in toluene at 0 °C starting temperature. Flash chromatography (SiO<sub>2</sub>, *n*-hexane/EtOAc 30:70). [Identification of intermediate via TLC-MS (ESI+): calcd. *m/z* 810.30 for C<sub>45</sub>H<sub>46</sub>N<sub>6</sub>O<sub>5</sub>SSi Found 833.2 [M+Na]<sup>+</sup>]. Deprotection in a 25% TFA/DCM mixture [Identification of intermediate via TLC-MS (ESI+): calcd. *m/z* 680.22 for C<sub>39</sub>H<sub>32</sub>N<sub>6</sub>O<sub>4</sub>S Found 703.3 [M+Na]<sup>+</sup>] and flash chromatographic purification (SiO<sub>2</sub>,

DCM/MeOH 8%), followed by deprotection under basic conditions and purification via flash chromatography (SiO<sub>2</sub>, *n*-hexane/(EtOAc/MeOH 5%) 40:60) to obtain the product in 30% yield (40 mg, 0.06 mmol) as off-white solid. <sup>1</sup>H NMR (400 MHz, DMSO) δ 12.75 (s, 1H), 10.72 (s, 1H), 10.05 (s, 1H), 9.14 (s, 1H), 8.00 (s, 1H), 7.87 (s, 1H), 7.76 (d, *J* = 5.9 Hz, 1H), 7.60 (d, *J* = 6.8 Hz, 1H), 7.56 – 7.33 (m, 6H), 7.29 – 7.15 (m, 4H), 7.12 – 7.02 (m, 1H), 6.97 (t, *J* = 7.5 Hz, 2H), 6.91 – 6.85 (m, 1H), 6.85 – 6.76 (m, 1H), 4.76 (s, 2H), 4.36 (s, 2H), 2.62 (s, 3H). HRMS (ESI): exact mass calcd for C<sub>37</sub>H<sub>30</sub>N<sub>6</sub>O<sub>3</sub>S [M+H]<sup>+</sup>: 639.21729. Found: 639.22006.

***N*-(3-(2-Ethyl-5-(2-(phenylamino)pyridin-4-yl)-1*H*-imidazol-4-yl)phenyl)-3-hydroxy-2-((1-oxoisindolin-2-yl)methyl)benzamide (12)**

The title compound was synthesized according to *general procedure B*) from 70 mg (0.14 mmol) **S35**, 50 mg (0.17 mmol) **S21**, 41 mg (0.22 mmol) EDC-HCl in toluene at 0 °C starting temperature. Flash chromatography (SiO<sub>2</sub>, *n*-hexane/EtOAc 10:90). [Identification of intermediate via TLC-MS (ESI<sup>+</sup>): calcd. *m/z* 792.35 for C<sub>46</sub>H<sub>48</sub>N<sub>6</sub>O<sub>5</sub>Si Found 815.2 [M+Na]<sup>+</sup>]. Deprotection in a 33% TFA/DCM mixture [Identification of intermediate via TLC-MS (ESI<sup>+</sup>): calcd. *m/z* 662.26 for C<sub>40</sub>H<sub>34</sub>N<sub>6</sub>O<sub>4</sub> Found 685.1 [M+Na]<sup>+</sup>], followed by deprotection under basic conditions and purification via flash chromatography (SiO<sub>2</sub>, *n*-hexane/EtOAc/MeOH 5:85:10) to obtain the product in 23% yield (21 mg, 0.03 mmol) as off-white solid. As mixture of tautomers: <sup>1</sup>H NMR (400 MHz, DMSO) δ 12.21 (s, 1H), 10.76 – 10.61 (m, 1H), 10.07 – 9.98 (m, 1H), 9.02 – 8.92 (m, 1H), 8.10 – 7.84 (m, 2H), 7.77 – 7.66 (m, 1H), 7.61 (d, *J* = 6.9 Hz, 1H), 7.58 – 7.48 (m, 4H), 7.48 – 7.35 (m, 2H), 7.28 – 7.24 (m, 1H), 7.23 – 7.12 (m, 4H), 6.96 (d, *J* = 7.4 Hz, 2H), 6.88 – 6.77 (m, 2H), 4.76 (s, 2H), 4.35 (s, 2H), 2.73 – 2.65 (m, 2H), 1.28 (t, *J* = 7.5 Hz, 3H). HRMS (ESI): exact mass calcd for C<sub>38</sub>H<sub>32</sub>N<sub>6</sub>O<sub>3</sub> [M+H]<sup>+</sup>: 621.26087. Found: 621.26382.

***N*-(3-(2-Ethoxy-5-(2-(phenylamino)pyridin-4-yl)-1*H*-imidazol-4-yl)phenyl)-3-hydroxy-2-((1-oxoisindolin-2-yl)methyl)benzamide (13)**

The title compound was synthesized according to *general procedure B*) from 105 mg (0.21 mmol) **S10**, 72 mg (0.24 mmol) **S21**, 60 mg (0.31 mmol) EDC-HCl in toluene at 0 °C starting temperature. Flash chromatography (SiO<sub>2</sub>, *n*-hexane/EtOAc 20:80). [Identification of intermediate via TLC-MS (ESI<sup>+</sup>): calcd. *m/z* 808.34 for C<sub>46</sub>H<sub>48</sub>N<sub>6</sub>O<sub>6</sub>Si, found 831.2 [M+Na]<sup>+</sup>]. Deprotection in a 25% TFA/DCM mixture [Identification of intermediate via TLC-MS (ESI<sup>+</sup>): calcd. *m/z* 678.26 for C<sub>40</sub>H<sub>34</sub>N<sub>6</sub>O<sub>5</sub>, found 701.2 [M+Na]<sup>+</sup>] and flash chromatographic purification (SiO<sub>2</sub>, *n*-hexane/EtOAc/IPA 15:75:10), followed by deprotection under basic conditions and purification via flash chromatography (SiO<sub>2</sub>, DCM/MeOH 90:10) to obtain the product in 52% yield (45 mg, 0.11 mmol) as off-white solid. As mixture of tautomers: <sup>1</sup>H NMR (400 MHz, DMSO) δ 11.88 (s, 1H), 10.76 – 10.63 (m, 1H), 10.07 – 9.98 (m, 1H), 9.00 – 8.89 (m, 1H), 8.06 – 7.92 (m, 1H), 7.89 – 7.81 (m, 1H), 7.77 – 7.69 (m, 1H), 7.63 – 7.60 (m, 1H), 7.58 – 7.53 (m, 2H), 7.53 – 7.47 (m, 2H), 7.46 – 7.41 (m, 1H), 7.41 – 7.34 (m, 1H), 7.30 – 7.20 (m, 2H), 7.19 – 7.15 (m, 2H), 7.13 – 7.08 (m, 1H), 7.00 – 6.91 (m, 2H), 6.85 – 6.78 (m, 1H), 6.78 – 6.69 (m, 1H), 4.81 – 4.70 (m, 2H), 4.44 – 4.31 (m, 4H), 1.41 – 1.33 (m, 3H). HRMS (ESI): exact mass calcd for C<sub>38</sub>H<sub>32</sub>N<sub>6</sub>O<sub>4</sub> [M+H]<sup>+</sup>: 637.25578. Found: 637.25215.

**3-Hydroxy-*N*-(3-(2-(methylthio)-5-(2-((4-(piperazin-1-yl)phenyl)amino)pyridin-4-yl)-1*H*-imidazol-4-yl)phenyl)-2-((1-oxoisindolin-2-yl)methyl)benzamide (14)**



To begin, 85 mg (0.09 mmol) **S42** was dissolved 33% TFA/DCM mixture and stirred overnight at ambient temperature. After complete consumption of the starting material was indicated by TLC, solvents were removed in vacuo and the residue was dissolved in MeOH. Small amounts of a saturated, aqueous NaHCO<sub>3</sub> solution were added and the mixture was stirred at ambient temperature for 0.5 h. The aqueous layer was extracted several times with EtOAc, and the combined organic layers were dried over Na<sub>2</sub>SO<sub>4</sub>. After evaporation of the solvents, the crude product was purified via flash chromatography (SiO<sub>2</sub>, EtOAc/MeOH 20:80). The obtained solid was dissolved in EtOAc, filtered and the organic solvent was removed in vacuo to obtain an off-white solid in 58% yield (36 mg, 0.05 mmol). As mixture of tautomers: <sup>1</sup>H NMR (400 MHz, DMSO) δ 12.70 (br s, 1H), 10.75 (s, 1H), 10.37 (br s, 1H), 8.65 (s, 1H), 7.94 (s, 1H), 7.84 (s, 1H), 7.79 (d, *J* = 7.9 Hz, 1H), 7.61 (d, *J* = 7.5 Hz, 1H), 7.56 – 7.49 (m, 2H), 7.45 – 7.40 (m, 1H), 7.39 – 7.33 (m, 1H), 7.29 (d, *J* = 8.7 Hz, 2H), 7.24 (t, *J* = 7.9 Hz, 1H), 7.15 (d, *J* = 7.5 Hz, 1H), 7.03 (d, *J* = 8.0 Hz, 1H), 6.98 – 6.85 (m, 2H), 6.79 – 6.70 (m, 3H), 4.75 (s, 2H), 4.35 (s, 2H), 2.95 – 2.88 (m, 4H), 2.84 – 2.75 (m, 4H), 2.60 (s, 3H). With missing signal of piperazine ‘N-H’. HRMS (ESI): exact mass calcd for C<sub>41</sub>H<sub>38</sub>N<sub>8</sub>O<sub>3</sub>S [M+H]<sup>+</sup>: 723.28604. Found: 723.29059.

***N*-(3-(5-(2-((5-Acrylamido-2-methoxyphenyl)amino)pyridin-4-yl)-2-(methylthio)-1*H*-imidazol-4-yl)phenyl)-2-((1-oxoisindolin-2-yl)methyl)benzamide (15)**

The title compound was synthesized according to *general procedure A* from 60 mg (0.10 mmol) **S39**, 31 mg (0.11 mmol) 2-((1-oxoisindolin-2-yl)methyl)benzoic acid<sup>32</sup> 29 mg (0.15 mmol) EDC-HCl in toluene at 0 °C starting temperature. Flash chromatography (SiO<sub>2</sub>, *n*-hexane/EtOAc 20:80). [Identification of intermediate via TLC-MS (ESI+): calcd. *m/z* 851.33 for C<sub>47</sub>H<sub>49</sub>N<sub>7</sub>O<sub>5</sub>SSi Found 874.3 [M+Na]<sup>+</sup>]. Deprotection in a 25% TFA/DCM mixture and flash chromatographic purification (RP-18, H<sub>2</sub>O/ACN 90:10->35:65) to obtain the product in 25% yield (18 mg, 0.025 mmol) as off-white solid. As mixture of tautomers: <sup>1</sup>H NMR (400 MHz, DMSO) δ 12.88 – 12.55 (m, 1H), 10.65 – 10.50 (m, 1H), 10.06 – 9.89 (m, 1H), 8.41 – 8.31 (m, 1H), 8.11 – 8.04 (m, 1H), 8.00 – 7.93 (m, 1H), 7.88 – 7.66 (m, 3H), 7.58 – 7.51 (m, *J* = 6.7 Hz, 3H), 7.49 – 7.44 (m, 2H), 7.43 – 7.34 (m, 3H), 7.31 – 7.09 (m, 3H), 6.96 – 6.86 (m, 1H), 6.79 – 6.68 (m, 1H), 6.45 (dd, *J* = 16.4, 10.4 Hz, 1H), 6.20 (d, *J* = 17.2 Hz, 1H), 5.68 (d, *J* = 8.7 Hz, 1H), 4.88 (s, 2H), 4.38 (s, 2H), 3.76 (s, 3H), 2.63 (s, 3H). HRMS (ESI): exact mass calcd for C<sub>41</sub>H<sub>35</sub>N<sub>7</sub>O<sub>4</sub>S [M+H]<sup>+</sup>: 722.2544. Found: 722.24945.

***N*-(3-(5-(2-((5-Acrylamido-2-methoxyphenyl)amino)pyridin-4-yl)-2-(methylthio)-1*H*-imidazol-4-yl)phenyl)-3-hydroxy-2-((1-oxoisindolin-2-yl)methyl)benzamide (16)**

The title compound was synthesized according to *general procedure B* from 80 mg (0.13 mmol) **S39**, 46 mg (0.15 mmol) **S21**, and 38 mg (0.20 mmol) EDC-HCl in toluene at 0°C starting temperature. Flash chromatographic purification (SiO<sub>2</sub>, *n*-hexane/EtOAc 25:75). [Identification of intermediate via TLC-MS (ESI+): calcd. *m/z* 909.33 for C<sub>49</sub>H<sub>51</sub>N<sub>7</sub>O<sub>7</sub>SSi Found 932.5 [M+Na]<sup>+</sup>]. Basic deprotection in 3 mL of MeOH and few drops of 0.1 N aqueous NaOH at ambient temperature over 5 h until complete conversion was indicated via HPLC [Identification of intermediate via TLC-MS (ESI+): calcd. *m/z* 867.32 for C<sub>47</sub>H<sub>49</sub>N<sub>7</sub>O<sub>6</sub>SSi Found 890.1 [M+Na]<sup>+</sup>]. Neutralization with saturated aqueous NH<sub>4</sub>Cl solution and extraction of the aqueous layer with EtOAc. The combined organic layers were dried over Na<sub>2</sub>SO<sub>4</sub>, filtered and solvents were removed in vacuo. The residue was dissolved in a 25% mixture of TFA/DCM and the mixture was stirred at

ambient temperature until complete conversion was indicated via HPLC. The mixture was concentrated in vacuo and the pH of the mixture was adjusted to 7 with saturated aqueous NaHCO<sub>3</sub> solution under precipitation of a white solid, which was collected by filtration and washed with demineralized water to obtain the product in 39% yield (32 mg, 0.05 mmol) as a white solid. As mixture of tautomers: <sup>1</sup>H NMR (400 MHz, DMSO) δ 12.79 – 12.62 (m, 1H), 10.74 – 10.60 (m, 1H), 10.06 (s, 1H), 10.00 (s, 1H), 8.36 – 8.22 (m, 1H), 8.12 – 7.91 (m, 2H), 7.82 (s, 1H), 7.76 – 7.67 (m, 1H), 7.59 (d, *J* = 6.7 Hz, 1H), 7.55 – 7.48 (m, 2H), 7.45 – 7.37 (m, 2H), 7.35 – 7.30 (m, 1H), 7.28 – 7.24 (m, 1H), 7.21 – 7.09 (m, 2H), 7.06 – 6.99 (m, 1H), 6.98 – 6.92 (m, 2H), 6.81 – 6.69 (m, 1H), 6.45 (dd, *J* = 16.9, 10.2 Hz, 1H), 6.21 (dd, *J* = 16.8, 1.3 Hz, 1H), 5.69 (dd, *J* = 10.1, 1.5 Hz, 1H), 4.77 (s, 2H), 4.35 (s, 2H), 3.75 (s, 3H), 2.62 (s, 3H). HRMS (ESI): exact mass calcd for C<sub>41</sub>H<sub>35</sub>N<sub>7</sub>O<sub>5</sub>S [M+H]<sup>+</sup>: 738.24932. Found: 738.25099.

***N*-(3-(5-(2-((5-Acrylamido-2-methoxyphenyl)amino)pyridin-4-yl)-2-(methylthio)-1*H*-imidazol-4-yl)phenyl)-2-fluoro-6-((1-oxoisindolin-2-yl)methyl)benzamide (17)**

The title compound was synthesized according to *general procedure A*) from 60 mg (0.10 mmol) **S39**, 33 mg (0.11 mmol) **S15**, 29 mg (0.15 mmol) EDC-HCl in toluene at 0 °C starting temperature. Flash chromatography (SiO<sub>2</sub>, *n*-hexane/EtOAc 20:80). [Identification of intermediate via TLC-MS (ESI<sup>+</sup>): calcd. *m/z* 869.32 for C<sub>47</sub>H<sub>48</sub>FN<sub>7</sub>O<sub>5</sub>SSi Found 892.2 [M+Na]<sup>+</sup>]. Deprotection in a 25% TFA/DCM mixture and flash chromatographic purification (RP-18, H<sub>2</sub>O/ACN 90:10->35:65) to obtain the product in 50% yield (37 mg, 0.05 mmol) as off-white solid. As mixture of tautomers: <sup>1</sup>H NMR (400 MHz, DMSO) δ 12.69 (s, 1H), 10.84 – 10.72 (m, 1H), 9.95 (s, 1H), 8.35 (s, 1H), 8.07 (s, 1H), 8.00 – 7.90 (m, 1H), 7.80 – 7.69 (m, 1H), 7.69 – 7.59 (m, 2H), 7.58 – 7.52 (m, 2H), 7.52 – 7.47 (m, 1H), 7.47 – 7.39 (m, 3H), 7.35 – 7.29 (m, 1H), 7.27 (d, *J* = 8.7 Hz, 1H), 7.19 (d, *J* = 7.1 Hz, 1H), 7.12 (d, *J* = 7.5 Hz, 1H), 6.90 (d, *J* = 8.8 Hz, 1H), 6.72 (dd, *J* = 5.4, 1.1 Hz, 1H), 6.45 (dd, *J* = 16.9, 10.1 Hz, 1H), 6.21 (dd, *J* = 16.9, 1.3 Hz, 1H), 5.69 (dd, *J* = 10.1, 1.5 Hz, 1H), 4.79 (s, 2H), 4.38 (s, 2H), 3.76 (s, 3H), 2.63 (s, 3H). HRMS (ESI): exact mass calcd for C<sub>41</sub>H<sub>34</sub>FN<sub>7</sub>O<sub>4</sub>S [M+H]<sup>+</sup>: 740.24498. Found: 740.24148.

***N*-(3-(5-(2-((5-Acrylamido-2-methoxyphenyl)amino)pyridin-4-yl)-2-(methylthio)-1*H*-imidazol-4-yl)phenyl)-6-fluoro-3-hydroxy-2-((1-oxoisindolin-2-yl)methyl)benzamide (18)**

The title compound was synthesized according to *general procedure A*) from 60 mg (0.10 mmol) **S39**, 54 mg (0.13 mmol) 3-((*tert*-butyldimethylsilyl)oxy)-6-fluoro-2-((1-oxoisindolin-2-yl)methyl)benzoic acid<sup>32</sup>, 29 mg (0.15 mmol) EDC-HCl in 2 mL toluene at 0 °C starting temperature. Flash chromatography (SiO<sub>2</sub>, *n*-hexane/EtOAc 15:85). [Identification of intermediate via TLC-MS (ESI<sup>+</sup>): calcd. *m/z* 999.40 for C<sub>53</sub>H<sub>62</sub>FN<sub>7</sub>O<sub>6</sub>SSi<sub>2</sub> Found 1022.5 [M+Na]<sup>+</sup>]. Deprotection in a 25% TFA/DCM mixture at ambient temperature overnight and removal of the solvents in vacuo. Addition of an aqueous 25% sulfuric acid solution and vigorous stirring of the mixture for 0.5 h at ambient temperature, followed by neutralization with saturated aqueous NaHCO<sub>3</sub> and extraction of the aqueous layer with EtOAc. The combined organic layers were dried over Na<sub>2</sub>SO<sub>4</sub>, filtered and the solvents were removed in vacuo. The crude product was purified via flash chromatography (RP-18, H<sub>2</sub>O/ACN 90:10->35:65) to obtain the product in 57% yield (43 mg, 0.06 mmol) as off-white solid. As mixture of tautomers: <sup>1</sup>H NMR (400 MHz, DMSO) δ 13.08 (s, 1H), 10.78 (s, 1H), 10.20 (s, 1H), 10.18 – 9.97 (m, 2H), 7.83 – 7.75 (m, 3H), 7.60 – 7.57 (m, 1H), 7.56 (s, 1H), 7.54 – 7.48 (m, 3H), 7.40 – 7.33 (m, 3H), 7.21 – 7.13 (m, 3H), 7.00 – 6.94 (m,

2H), 6.42 (dd,  $J = 16.9, 10.1$  Hz, 1H), 6.24 (dd,  $J = 16.7, 1.1$  Hz, 1H), 5.75 (dd,  $J = 10.2, 1.3$  Hz, 1H), 4.72 (s, 2H), 4.31 (s, 2H), 3.74 (s, 3H), 2.65 (s, 3H). HRMS (ESI): exact mass calcd for  $C_{41}H_{34}FN_7O_5S$   $[M+H]^+$ : 756.23989. Found: 756.23682.

***N*-(3-(5-(2-((5-Acrylamido-2-methoxyphenyl)amino)pyridin-4-yl)-2-ethyl-1*H*-imidazol-4-yl)phenyl)-3-hydroxy-2-((1-oxoisindolin-2-yl)methyl)benzamide (19)**

The title compound was synthesized according to *general procedure B*) from 50 mg (0.09 mmol) **S41**, 36 mg (0.11 mmol) **S21**, 25 mg (0.13 mmol) EDC-HCl in toluene at 0 °C starting temperature. [Identification of intermediate via TLC-MS (ESI+): calcd.  $m/z$  891.38 for  $C_{50}H_{53}N_7O_7Si$  Found 915.1  $[M+Na]^+$ ]. Deprotection in 3 mL of MeOH and few drops of 0.1 N aqueous NaOH at ambient temperature over 5 h until complete conversion was indicated via HPLC [Identification of intermediate via TLC-MS (ESI+): calcd.  $m/z$  849.37 for  $C_{48}H_{51}N_7O_6Si$  Found 872.7  $[M+Na]^+$ ]. Neutralization with saturated aqueous  $NH_4Cl$  solution and extraction of the aqueous layer with EtOAc. The combined organic layers were dried over  $Na_2SO_4$ , filtered and solvents were removed in vacuo. The residue was dissolved in a 25% mixture of TFA/DCM and the mixture was stirred at ambient temperature until complete conversion. After evaporation of solvents, the residue was neutralized with saturated aqueous  $NHCO_3$  solution, and the aqueous layer was extracted with EtOAc. Organic layers were dried over  $Na_2SO_4$ , filtered and solvents were removed in vacuo. The crude product was purified via flash chromatography ( $SiO_2$ , *n*-hexane/ [EtOAc/IPA 10%] 40:60 to 0:100) to obtain 23% (14 mg, 0.02 mmol) yield of an off-white solid.  $^1H$  NMR (400 MHz, DMSO)  $\delta$  12.38 (s, 1H), 10.66 (s, 1H), 10.03 (s, 1H), 9.96 (s, 1H), 8.32 (s, 1H), 8.10 (s, 1H), 7.97 (d,  $J = 5.2$  Hz, 1H), 7.87 (s, 1H), 7.68 (d,  $J = 7.9$  Hz, 1H), 7.60 (d,  $J = 7.4$  Hz, 1H), 7.54 – 7.49 (m, 2H), 7.45 – 7.42 (m, 1H), 7.42 – 7.39 (m, 1H), 7.33 (t,  $J = 7.5$  Hz, 1H), 7.27 (t,  $J = 7.8$  Hz, 2H), 7.16 (d,  $J = 7.6$  Hz, 1H), 7.00 – 6.95 (m, 2H), 6.92 (d,  $J = 8.8$  Hz, 1H), 6.75 (dd,  $J = 5.6, 0.8$  Hz, 1H), 6.45 (dd,  $J = 16.9, 10.2$  Hz, 1H), 6.21 (dd,  $J = 17.0, 1.9$  Hz, 1H), 5.69 (dd,  $J = 10.2, 2.0$  Hz, 1H), 4.77 (s, 2H), 4.36 (s, 2H), 3.76 (s, 3H), 2.71 (q,  $J = 7.6$  Hz, 2H), 1.28 (t,  $J = 7.6$  Hz, 3H). HRMS (ESI): exact mass calcd for  $C_{42}H_{37}N_7O_5$   $[M+H]^+$ : 720.29289. Found: 720.29501.

**3-Hydroxy-*N*-(3-(5-(2-((2-methoxy-5-propionamidophenyl)amino)pyridin-4-yl)-2-(methylthio)-1*H*-imidazol-4-yl)phenyl)-2-((1-oxoisindolin-2-yl)methyl)benzamide (20)**

The title compound was synthesized according to *general procedure B*) from 50 mg (0.08 mmol) **S35**, 28 mg (0.10 mmol) **S21**, 24 mg (0.12 mmol) EDC-HCl in 3 mL toluene at 0 °C starting temperature. Flash chromatography ( $SiO_2$ , *n*-hexane/EtOAc 35:65). [Identification of intermediate via TLC-MS (ESI+): calcd.  $m/z$  911.35 for  $C_{49}H_{53}N_7O_7SSi$  Found 934.2  $[M+Na]^+$ ]. Deprotection in a 33% TFA/DCM mixture [Identification of intermediate via TLC-MS (ESI+): calcd.  $m/z$  781.27 for  $C_{43}H_{39}N_7O_6S$  Found 804.0  $[M+Na]^+$ ] followed by deprotection under basic conditions and purification via flash chromatography (RP-18,  $H_2O/ACN$  90:10->35:65) to obtain the product in 33% yield (20 mg, 0.03 mmol) as off-white solid.  $^1H$  NMR (400 MHz, DMSO)  $\delta$  12.64 (s, 1H), 10.67 (s, 1H), 10.11 (s, 1H), 9.64 (s, 1H), 8.22 (d,  $J = 2.3$  Hz, 1H), 7.99 (s, 1H), 7.98 – 7.79 (m, 2H), 7.71 – 7.64 (m, 1H), 7.60 (d,  $J = 7.5$  Hz, 1H), 7.55 – 7.48 (m, 2H), 7.46 – 7.22 (m, 5H), 7.15 (d,  $J = 7.7$  Hz, 1H), 6.96 (d,  $J = 7.8$  Hz, 2H), 6.87 (d,  $J = 8.8$  Hz, 1H), 6.71 (dd,  $J = 5.4, 0.8$  Hz, 1H), 4.76 (s, 2H), 4.36 (s, 2H), 3.74 (s, 3H), 2.62 (s, 3H), 2.28 (q,  $J = 7.5$  Hz, 2H), 1.06 (t,  $J = 7.6$  Hz, 3H). HRMS (ESI): exact mass calcd for  $C_{41}H_{37}N_7O_5S$   $[M+H]^+$ : 740.26497. Found: 740.2627.



## References

- (1) Lynch, T. J.; Bell, D. W.; Sordella, R.; Gurubhagavatula, S.; Okimoto, R. A.; Brannigan, B. W.; Harris, P. L.; Haserlat, S. M.; Supko, J. G.; Haluska, F. G.; Louis, D. N.; Christiani, D. C.; Settleman, J.; Haber, D. A. Activating Mutations in the Epidermal Growth Factor Receptor Underlying Responsiveness of Non-Small-Cell Lung Cancer to Gefitinib. *The New England journal of medicine* **2004**, *350* (21), 2129–2139. DOI: 10.1056/NEJMoa040938.
- (2) Paez, J. G.; Jänne, P. A.; Lee, J. C.; Tracy, S.; Greulich, H.; Gabriel, S.; Herman, P.; Kaye, F. J.; Lindeman, N.; Boggon, T. J.; Naoki, K.; Sasaki, H.; Fujii, Y.; Eck, M. J.; Sellers, W. R.; Johnson, B. E.; Meyerson, M. EGFR Mutations in Lung Cancer: Correlation with Clinical Response to Gefitinib Therapy. *Science (New York, N.Y.)* **2004**, *304* (5676), 1497–1500. DOI: 10.1126/science.1099314.
- (3) Cohen, P.; Cross, D.; Jänne, P. A. Kinase drug discovery 20 years after imatinib: progress and future directions. *Nat Rev Drug Discov* **2021**. DOI: 10.1038/s41573-021-00195-4.
- (4) David E. Heppner, Michael J. Eck. A structural perspective on targeting the RTK/Ras/MAP kinase pathway in cancer. *Protein Science* **2021** (30), 1535–1553.
- (5) Yun, C.-H.; Mengwasser, K. E.; Toms, A. V.; Woo, M. S.; Greulich, H.; Wong, K.-K.; Meyerson, M.; Eck, M. J. The T790M Mutation in EGFR Kinase Causes Drug Resistance by Increasing the Affinity for ATP. *Proceedings of the National Academy of Sciences of the United States of America* **2008**, *105* (6), 2070–2075. DOI: 10.1073/pnas.0709662105.
- (6) Gazdar, A. F. Activating and Resistance Mutations of EGFR in Non-Small-Cell Lung Cancer: Role in Clinical Response to EGFR Tyrosine Kinase Inhibitors. *Oncogene* **2009**, *28 Suppl 1*, S24-31. DOI: 10.1038/onc.2009.198.
- (7) Kobayashi, S.; Boggon, T. J.; Dayaram, T.; Jänne, P. A.; Kocher, O.; Meyerson, M.; Johnson, B. E.; Eck, M. J.; Tenen, D. G.; Halmos, B. EGFR Mutation and Resistance of Non-Small-Cell Lung Cancer to Gefitinib. *The New England journal of medicine* **2005**, *352* (8), 786–792. DOI: 10.1056/NEJMoa044238.
- (8) Edgar R. Wood; Anne T. Truesdale; Octerloney B. McDonald; Derek Yuan; Anne Hassell; Scott H. Dickerson; Byron Ellis; Christopher Pennisi; Earnest Horne; Karen Lackey; Krystal J. Alligood; David W. Rusnak; Tona M. Gilmer; Lisa Shewchuk. A Unique Structure for Epidermal Growth Factor Receptor Bound to GW572016 (Lapatinib): Relationships among Protein Conformation, Inhibitor Off-Rate, and Receptor Activity in Tumor Cells. *Cancer research* **2004**, *64* (18), 6652–6659.
- (9) Tsou, H.-R.; Overbeek-Klumpers, E. G.; Hallett, W. A.; Reich, M. F.; Floyd, M. B.; Johnson, B. D.; Michalak, R. S.; Nilakantan, R.; Discafani, C.; Golas, J.; Rabindran, S. K.; Shen, R.; Shi, X.; Wang, Y.-F.; Upeslaci, J.; Wissner, A. Optimization of 6,7-disubstituted-4-(arylamino)quinoline-3-carbonitriles as orally active, irreversible inhibitors of human epidermal growth factor receptor-2 kinase activity. *Journal of medicinal chemistry* **2005**, *48* (4), 1107–1131. DOI: 10.1021/jm040159c.
- (10) Cross, D. A. E.; Ashton, S. E.; Giorghiu, S.; Eberlein, C.; Nebhan, C. A.; Spitzler, P. J.; Orme, J. P.; Finlay, M. R. V.; Ward, R. A.; Mellor, M. J.; Hughes, G.; Rahi, A.; Jacobs, V. N.; Red Brewer, M.; Ichihara, E.; Sun, J.; Jin, H.; Ballard, P.; Al-Kadhimi, K.; Rowlinson, R.; Klinowska, T.; Richmond, G. H. P.; Cantarini, M.; Kim, D.-W.; Ranson, M. R.; Pao, W. AZD9291, an Irreversible EGFR TKI, Overcomes T790M-Mediated Resistance to EGFR Inhibitors in Lung Cancer. *Cancer discovery* **2014**, *4* (9), 1046–1061. DOI: 10.1158/2159-8290.CD-14-0337.
- (11) Zhou, W.; Ercan, D.; Chen, L.; Yun, C.-H.; Li, D.; Capelletti, M.; Cortot, A. B.; Chirieac, L.; Iacob, R. E.; Padera, R.; Engen, J. R.; Wong, K.-K.; Eck, M. J.; Gray, N. S.; Jänne, P. A. Novel mutant-selective EGFR kinase inhibitors against EGFR T790M. *Nature* **2009**, *462* (7276), 1070–1074. DOI: 10.1038/nature08622.
- (12) Heppner, D. E.; Wittlinger, F.; Beyett, T. S.; Shaurova, T.; Urul, D. A.; Buckley, B.; Pham, C. D.; Schaeffner, I. K.; Yang, B.; Ogboo, B. C.; May, E. W.; Schaefer, E. M.; Eck, M. J.; Laufer, S. A.; Hershberger,

- P. A. Structural Basis for Inhibition of Mutant EGFR with Lazertinib (YH25448). *ACS medicinal chemistry letters* **2022**, *13* (12), 1856–1863. DOI: 10.1021/acsmchemlett.2c00213. Published Online: Nov. 10, 2022.
- (13) Wittlinger, F.; Laufer, S. A. The pre-clinical discovery and development of osimertinib used to treat non-small cell lung cancer. *Expert opinion on drug discovery* **2021**, *16* (10), 1091–1103. DOI: 10.1080/17460441.2021.1936496.
- (14) Thress, K. S.; Paweletz, C. P.; Felip, E.; Cho, B. C.; Stetson, D.; Dougherty, B.; Lai, Z.; Markovets, A.; Vivancos, A.; Kuang, Y.; Ercan, D.; Matthews, S. E.; Cantarini, M.; Barrett, J. C.; Jänne, P. A.; Oxnard, G. R. Acquired EGFR C797S Mutation Mediates Resistance to AZD9291 in Non-Small Cell Lung Cancer Harboring EGFR T790M. *Nature medicine* **2015**, *21* (6), 560–562. DOI: 10.1038/nm.3854.
- (15) Niederst, M. J.; Hu, H.; Mulvey, H. E.; Lockerman, E. L.; Garcia, A. R.; Piotrowska, Z.; Sequist, L. V.; Engelman, J. A. The Allelic Context of the C797S Mutation Acquired upon Treatment with Third-Generation EGFR Inhibitors Impacts Sensitivity to Subsequent Treatment Strategies. *Clinical cancer research : an official journal of the American Association for Cancer Research* **2015**, *21* (17), 3924–3933. DOI: 10.1158/1078-0432.CCR-15-0560. Published Online: May. 11, 2015.
- (16) To, C.; Jang, J.; Chen, T.; Park, E.; Mushajiang, M.; Clercq, D. J. H. de; Xu, M.; Wang, S.; Cameron, M. D.; Heppner, D. E.; Shin, B. H.; Gero, T. W.; Yang, A.; Dahlberg, S. E.; Wong, K.-K.; Eck, M. J.; Gray, N. S.; Jänne, P. A. Single and Dual Targeting of Mutant EGFR with an Allosteric Inhibitor. *Cancer discovery* **2019**, *9* (7), 926–943. DOI: 10.1158/2159-8290.CD-18-0903.
- (17) To, C.; Beyett, T. S.; Jang, J.; Feng, W. W.; Bahcall, M.; Haikala, H. M.; Shin, B. H.; Heppner, D. E.; Rana, J. K.; Leeper, B. A.; Soroko, K. M.; Poitras, M. J.; Gokhale, P. C.; Kobayashi, Y.; Wahid, K.; Kurppa, K. J.; Gero, T. W.; Cameron, M. D.; Ogino, A.; Mushajiang, M.; Xu, C.; Zhang, Y.; Scott, D. A.; Eck, M. J.; Gray, N. S.; Jänne, P. A. An allosteric inhibitor against the therapy-resistant mutant forms of EGFR in non-small cell lung cancer. *Nature cancer* **2022**. DOI: 10.1038/s43018-022-00351-8. Published Online: Apr. 14, 2022.
- (18) Jia, Y.; Yun, C.-H.; Park, E.; Ercan, D.; Manuia, M.; Juarez, J.; Xu, C.; Rhee, K.; Chen, T.; Zhang, H.; Palakurthi, S.; Jang, J.; Lelais, G.; DiDonato, M.; Bursulaya, B.; Michellys, P.-Y.; Epple, R.; Marsilje, T. H.; McNeill, M.; Lu, W.; Harris, J.; Bender, S.; Wong, K.-K.; Jänne, P. A.; Eck, M. J. Overcoming EGFR(T790M) and EGFR(C797S) resistance with mutant-selective allosteric inhibitors. *Nature* **2016**, *534* (7605), 129–132. DOI: 10.1038/nature17960.
- (19) Beyett, T. S.; To, C.; Heppner, D. E.; Rana, J. K.; Schmoker, A. M.; Jang, J.; Clercq, D. J. H. de; Gomez, G.; Scott, D. A.; Gray, N. S.; Jänne, P. A.; Eck, M. J. Molecular basis for cooperative binding and synergy of ATP-site and allosteric EGFR inhibitors. *Nature communications* **2022**, *13* (1), 2530. DOI: 10.1038/s41467-022-30258-y. Published Online: May. 9, 2022.
- (20) Niggenaber, J.; Heyden, L.; Grabe, T.; Müller, M. P.; Lategahn, J.; Rauh, D. Complex Crystal Structures of EGFR with Third-Generation Kinase Inhibitors and Simultaneously Bound Allosteric Ligands. *ACS Med. Chem. Lett.* **2020**. DOI: 10.1021/acsmchemlett.0c00472.
- (21) Damghani, T.; Wittlinger, F.; Beyett, T. S.; Eck, M. J.; Laufer, S. A.; Heppner, D. E. Structural elements that enable specificity for mutant EGFR kinase domains with next-generation small-molecule inhibitors. *Methods in Enzymology* **2023**, ISSN 0076-6879. DOI: 10.1016/bs.mie.2023.03.013.
- (22) Günther, M.; Juchum, M.; Kelter, G.; Fiebig, H.; Laufer, S. Lung Cancer:EGFR Inhibitors with Low Nanomolar Activity against a Therapy-Resistant L858R/T790M/C797S Mutant. *Angewandte Chemie (International ed. in English)* **2016**, *55* (36), 10890–10894. DOI: 10.1002/anie.201603736.
- (23) Günther, M.; Lategahn, J.; Juchum, M.; Döring, E.; Keul, M.; Engel, J.; Tumbrink, H. L.; Rauh, D.; Laufer, S. Trisubstituted Pyridinylimidazoles as Potent Inhibitors of the Clinically Resistant

- L858R/T790M/C797S EGFR Mutant: Targeting of Both Hydrophobic Regions and the Phosphate Binding Site. *Journal of medicinal chemistry* **2017**, *60* (13), 5613–5637. DOI: 10.1021/acs.jmedchem.7b00316.
- (24) Juchum, M.; Günther, M.; Döring, E.; Sievers-Engler, A.; Lämmerhofer, M.; Laufer, S. Trisubstituted Imidazoles with a Rigidized Hinge Binding Motif Act As Single Digit nM Inhibitors of Clinically Relevant EGFR L858R/T790M and L858R/T790M/C797S Mutants: An Example of Target Hopping. *Journal of medicinal chemistry* **2017**, *60* (11), 4636–4656. DOI: 10.1021/acs.jmedchem.7b00178.
- (25) Heppner, D. E.; Günther, M.; Wittlinger, F.; Laufer, S. A.; Eck, M. J. Structural Basis for EGFR Mutant Inhibition by Trisubstituted Imidazole Inhibitors. *Journal of medicinal chemistry* **2020**. DOI: 10.1021/acs.jmedchem.0c00200.
- (26) Beyett, T. S.; Rana, J. K.; Schaeffner, I. K.; Heppner, D. E.; Eck, M. J. Structural analysis of the macrocyclic inhibitor BI-4020 binding to EGFR kinase **2022**. DOI: 10.1101/2022.08.27.505540.
- (27) Uchibori, K.; Inase, N.; Araki, M.; Kamada, M.; Sato, S.; Okuno, Y.; Fujita, N.; Katayama, R. Brigatinib combined with anti-EGFR antibody overcomes osimertinib resistance in EGFR-mutated non-small-cell lung cancer. *Nature communications* **2017**, *8*, 14768. DOI: 10.1038/ncomms14768. Published Online: Mar. 13, 2017.
- (28) Kashima, K.; Kawauchi, H.; Tanimura, H.; Tachibana, Y.; Chiba, T.; Torizawa, T.; Sakamoto, H. CH7233163 overcomes osimertinib resistant EGFR-Del19/T790M/C797S mutation. *Molecular cancer therapeutics* **2020**. DOI: 10.1158/1535-7163.MCT-20-0229.
- (29) Engelhardt, H.; Böse, D.; Petronczki, M.; Scharn, D.; Bader, G.; Baum, A.; Bergner, A.; Chong, E.; Döbel, S.; Egger, G.; Engelhardt, C.; Etmayer, P.; Fuchs, J. E.; Gerstberger, T.; Gonnella, N.; Grimm, A.; Grondal, E.; Haddad, N.; Hopfgartner, B.; Kousek, R.; Krawiec, M.; Kriz, M.; Lamarre, L.; Leung, J.; Mayer, M.; Patel, N. D.; Simov, B. P.; Reeves, J. T.; Schnitzer, R.; Schrenk, A.; Sharps, B.; Solca, F.; Stadtmüller, H.; Tan, Z.; Wunberg, T.; Zoephel, A.; McConnell, D. B. Start Selective and Rigidify: The Discovery Path toward a Next Generation of EGFR Tyrosine Kinase Inhibitors. *Journal of medicinal chemistry* **2019**, *62* (22), 10272–10293. DOI: 10.1021/acs.jmedchem.9b01169.
- (30) Eno, M. S.; Brubaker, J. D.; Campbell, J. E.; Savi, C. de; Guzi, T. J.; Williams, B. D.; Wilson, D.; Wilson, K.; Brooijmans, N.; Kim, J.; Özen, A.; Perola, E.; Hsieh, J.; Brown, V.; Fetalvero, K.; Garner, A.; Zhang, Z.; Stevison, F.; Woessner, R.; Singh, J.; Timsit, Y.; Kinkema, C.; Medendorp, C.; Lee, C.; Albayya, F.; Zalutskaya, A.; Schalm, S.; Dineen, T. A. Discovery of BLU-945, a Reversible, Potent, and Wild-Type-Sparing Next-Generation EGFR Mutant Inhibitor for Treatment-Resistant Non-Small-Cell Lung Cancer. *Journal of medicinal chemistry* **2022**, *65* (14), 9662–9677. DOI: 10.1021/acs.jmedchem.2c00704. Published Online: Jul. 15, 2022.
- (31) Elamin, Y. Y.; Rouskin-Faust, T.; Zhang, N.; Green, T.; Dhande, A.; Mar, B. G.; Heymach, J. V.; Conti, C. Abstract LB123: Poorer outcomes in EGFR L858R-driven NSCLC treated with osimertinib may be addressed with novel combination of BLU-945 and osimertinib. *Cancer research* **2023**, *83* (8\_Supplement), LB123-LB123. DOI: 10.1158/1538-7445.AM2023-LB123.
- (32) Wittlinger, F.; Heppner, D. E.; To, C.; Günther, M.; Shin, B. H.; Rana, J. K.; Schmoker, A. M.; Beyett, T. S.; Berger, L. M.; Berger, B.-T.; Bauer, N.; Vasta, J. D.; Corona, C. R.; Robers, M. B.; Knapp, S.; Jänne, P. A.; Eck, M. J.; Laufer, S. A. Design of a “Two-in-One” Mutant-Selective Epidermal Growth Factor Receptor Inhibitor That Spans the Orthosteric and Allosteric Sites. *J. Med. Chem.* **2021**. DOI: 10.1021/acs.jmedchem.1c00848.
- (33) Li, Q.; Zhang, T.; Li, S.; Tong, L.; Li, J.; Su, Z.; Feng, F.; Sun, D.; Tong, Y.; Wang, X.; Zhao, Z.; Zhu, L.; Ding, J.; Li, H.; Xie, H.; Xu, Y. Discovery of Potent and Noncovalent Reversible EGFR Kinase Inhibitors of EGFR L858R/T790M/C797S. *ACS medicinal chemistry letters* **2019**, *10* (6), 869–873. DOI: 10.1021/acsmchemlett.8b00564.

- (34) Wittlinger F, Ogboo BC, Pham CD, Schaeffner IK, Chitnis SP, Damghani T, et al. Examining molecular factors of inactive versus active bivalent EGFR inhibitors: A missing link in fragment-based drug design. ChemRxiv. Cambridge: Cambridge Open Engage; This content is a preprint and has not been peer-reviewed. **2023**.
- (35) Gilmer, T. M.; Cable, L.; Alligood, K.; Rusnak, D.; Spehar, G.; Gallagher, K. T.; Woldu, E.; Carter, H. L.; Truesdale, A. T.; Shewchuk, L.; Wood, E. R. Impact of common epidermal growth factor receptor and HER2 variants on receptor activity and inhibition by lapatinib. *Cancer research* **2008**, *68* (2), 571–579. DOI: 10.1158/0008-5472.CAN-07-2404.
- (36) Zhou, W.; Ercan, D.; Chen, L.; Yun, C.-H.; Li, D.; Capelletti, M.; Cortot, A. B.; Chirieac, L.; Iacob, R. E.; Padera, R.; Engen, J. R.; Wong, K.-K.; Eck, M. J.; Gray, N. S.; Jänne, P. A. Novel mutant-selective EGFR kinase inhibitors against EGFR T790M. *Nature* **2009**, *462* (7276), 1070–1074. DOI: 10.1038/nature08622.
- (37) Huang, W.-S.; Li, F.; Gong, Y.; Zhang, Y.; Youngsaye, W.; Xu, Y.; Zhu, X.; Greenfield, M. T.; Kohlmann, A.; Taslimi, P. M.; Toms, A.; Zech, S. G.; Zhou, T.; Das, B.; Jang, H. G.; Tugnait, M.; Ye, Y. E.; Gonzalez, F.; Baker, T. E.; Nadworny, S.; Ning, Y.; Wardwell, S. D.; Zhang, S.; Gould, A. E.; Hu, Y.; Lane, W.; Skene, R. J.; Zou, H.; Clackson, T.; Narasimhan, N. I.; Rivera, V. M.; Dalgarno, D. C.; Shakespeare, W. C. Discovery of mobocertinib, a potent, oral inhibitor of EGFR exon 20 insertion mutations in non-small cell lung cancer. *Bioorganic & medicinal chemistry letters* **2023**, *80*, 129084. DOI: 10.1016/j.bmcl.2022.129084. Published Online: Nov. 21, 2022.
- (38) Wissner, A.; Mansour, T. S. The Development of HKI-272 and Related Compounds for the Treatment of Cancer. *Arch. Pharm. Pharm. Med. Chem.* **2008**, *341* (8), 465–477. DOI: 10.1002/ardp.200800009.
- (39) Chen, H.; Hu, S.; Patterson, A. V.; Smail, J. B.; Ding, K.; Lu, X. Structural Mechanism and Inhibitors Targeting EGFR Exon 20 Insertion (Ex20ins) Mutations. *Journal of medicinal chemistry* **2023**. DOI: 10.1021/acs.jmedchem.3c00875. Published Online: Sep. 5, 2023.
- (40) Tinworth, C. P.; Young, R. J. Facts, Patterns, and Principles in Drug Discovery: Appraising the Rule of 5 with Measured Physicochemical Data. *Journal of medicinal chemistry* **2020**, *63* (18), 10091–10108. DOI: 10.1021/acs.jmedchem.9b01596. Published Online: May. 11, 2020.
- (41) O' Donovan, D. H.; Fusco, C. de; Kuhnke, L.; Reichel, A. Trends in Molecular Properties, Bioavailability, and Permeability across the Bayer Compound Collection. *Journal of medicinal chemistry* **2023**, *66* (4), 2347–2360. DOI: 10.1021/acs.jmedchem.2c01577. Published Online: Feb. 8, 2023.
- (42) Clercq, D. J. H. de; Heppner, D. E.; To, C.; Jang, J.; Park, E.; Yun, C.-H.; Mushajiang, M.; Shin, B. H.; Gero, T. W.; Scott, D. A.; Jänne, P. A.; Eck, M. J.; Gray, N. S. Discovery and Optimization of Dibenzodiazepinones as Allosteric Mutant-Selective EGFR Inhibitors. *ACS medicinal chemistry letters* **2019**, *10* (11), 1549–1553. DOI: 10.1021/acsmchemlett.9b00381.
- (43) Gehringer, M.; Laufer, S. A. Emerging and Re-Emerging Warheads for Targeted Covalent Inhibitors: Applications in Medicinal Chemistry and Chemical Biology. *Journal of medicinal chemistry* **2019**, *62* (12), 5673–5724. DOI: 10.1021/acs.jmedchem.8b01153. Published Online: Jan. 25, 2019.
- (44) Harris, C. M.; Foley, S. E.; Goedken, E. R.; Michalak, M.; Murdock, S.; Wilson, N. S. Merits and Pitfalls in the Characterization of Covalent Inhibitors of Bruton's Tyrosine Kinase. *SLAS discovery : advancing life sciences R & D* **2018**, *23* (10), 1040–1050. DOI: 10.1177/2472555218787445. Published Online: Jul. 10, 2018.
- (45) Reynders, M.; Chaikuad, A.; Berger, B.-T.; Bauer, K.; Koch, P.; Laufer, S.; Knapp, S.; Trauner, D. Controlling the Covalent Reactivity of a Kinase Inhibitor with Light. *Angewandte Chemie (International ed. in English)* **2021**, *60* (37), 20178–20183. DOI: 10.1002/anie.202103767. Published Online: Aug. 11, 2021.

- (46) Thress, K. S.; Paweletz, C. P.; Felip, E.; Cho, B. C.; Stetson, D.; Dougherty, B.; Lai, Z.; Markovets, A.; Vivancos, A.; Kuang, Y.; Ercan, D.; Matthews, S. E.; Cantarini, M.; Barrett, J. C.; Jänne, P. A.; Oxnard, G. R. Acquired EGFR C797S mutation mediates resistance to AZD9291 in non-small cell lung cancer harboring EGFR T790M. *Nature medicine* **2015**, *21* (6), 560–562. DOI: 10.1038/nm.3854.
- (47) Vivanco, I.; Robins, H. I.; Rohle, D.; Campos, C.; Grommes, C.; Nghiemphu, P. L.; Kubek, S.; Oldrini, B.; Chheda, M. G.; Yannuzzi, N.; Tao, H.; Zhu, S.; Iwanami, A.; Kuga, D.; Dang, J.; Pedraza, A.; Brennan, C. W.; Heguy, A.; Liaw, L. M.; Lieberman, F.; Yung, W. K. A.; Gilbert, M. R.; Reardon, D. A.; Drappatz, J.; Wen, P. Y.; Lamborn, K. R.; Chang, S. M.; Prados, M. D.; Fine, H. A.; Horvath, S.; Wu, N.; Lassman, A. B.; DeAngelis, L. M.; Yong, W. H.; Kuhn, J. G.; Mischel, P. S.; Mehta, M. P.; Cloughesy, T. F.; Mellinger, I. K. Differential sensitivity of glioma- versus lung cancer-specific EGFR mutations to EGFR kinase inhibitors. *Cancer discovery* **2012**, *2* (5), 458–471. DOI: 10.1158/2159-8290.CD-11-0284. Published Online: Mar. 31, 2012.
- (48) An, Z.; Aksoy, O.; Zheng, T.; Fan, Q.-W.; Weiss, W. A. Epidermal growth factor receptor and EGFRvIII in glioblastoma: signaling pathways and targeted therapies. *Oncogene* **2018**, *37* (12), 1561–1575. DOI: 10.1038/s41388-017-0045-7. Published Online: Jan. 11, 2018.
- (49) Chaikuad, A.; Koch, P.; Laufer, S. A.; Knapp, S. The Cysteineome of Protein Kinases as a Target in Drug Development. *Angewandte Chemie (International ed. in English)* **2018**, *57* (16), 4372–4385. DOI: 10.1002/anie.201707875. Published Online: Feb. 2, 2018.
- (50) Heider, F.; Haun, U.; Döring, E.; Kudolo, M.; Sessler, C.; Albrecht, W.; Laufer, S.; Koch, P. From 2-Alkylsulfanylimidazoles to 2-Alkylimidazoles: An Approach towards Metabolically More Stable p38 $\alpha$  MAP Kinase Inhibitors. *Molecules (Basel, Switzerland)* **2017**, *22* (10). DOI: 10.3390/molecules22101729. Published Online: Oct. 14, 2017.
- (51) van Alderwerelt Rosenburgh, I. K.; Lu, D. M.; Grant, M. J.; Stayrook, S. E.; Phadke, M.; Walther, Z.; Goldberg, S. B.; Politi, K.; Lemmon, M. A.; Ashtekar, K. D.; Tsutsui, Y. Biochemical and structural basis for differential inhibitor sensitivity of EGFR with distinct exon 19 mutations. *Nature communications* **2022**, *13* (1), 6791. DOI: 10.1038/s41467-022-34398-z. Published Online: Nov. 10, 2022.
- (52) Brown, B. P.; Zhang, Y.-K.; Kim, S.; Finneran, P.; Yan, Y.; Du, Z.; Kim, J.; Hartzler, A. L.; LeNoue-Newton, M. L.; Smith, A. W.; Meiler, J.; Lovly, C. M. Allele-specific activation, enzyme kinetics, and inhibitor sensitivities of EGFR exon 19 deletion mutations in lung cancer. *Proceedings of the National Academy of Sciences of the United States of America* **2022**, *119* (30), e2206588119. DOI: 10.1073/pnas.2206588119. Published Online: Jul. 22, 2022.
- (53) Liu, C.; Dai, R.; Yao, G.; Deng, Y. Selective Bromination of Pyrrole Derivatives, Carbazole and Aromatic Amines with DMSO/HBr under Mild Conditions. *Journal of Chemical Research* **2014**, *38* (10), 593–596. DOI: 10.3184/174751914X14114780483352.
- (54) Xie, D.; Lu, J.; Xie, J.; Cui, J.; Li, T.-F.; Wang, Y.-C.; Chen, Y.; Gong, N.; Li, X.-Y.; Fu, L.; Wang, Y.-X. Discovery and analgesic evaluation of 8-chloro-1,4-dihydropyrido2,3-bpyrazine-2,3-dione as a novel potent d-amino acid oxidase inhibitor. *European journal of medicinal chemistry* **2016**, *117*, 19–32. DOI: 10.1016/j.ejmech.2016.04.017. Published Online: Apr. 9, 2016.
- (55) Marcel Günther. Design, Synthese und Optimierung neuer mutationsspezifischer EGFR Inhibitoren. Dissertation, Eberhard Karls Universität, Tübingen, 2017.